A THERMOGRAVIMETRIC STUDY OF THE PYROLYTIC BEHAVIOUR OF SOUTH WALES COALS

ANGELA ISABEL PORTER

ABSTRACT

The major aim of this research was to provide quantitative data about the pyrolytic behaviour of a series of coals from the South Wales Coalfield using thermogravimetry as the major experimental technique. It is hoped that this data will (1) provide information of value to the development of coal conversion technologies, (2) provide information about the kinetics of coal pyrolysis, (3) provide information about the effect upon the kinetic results by the addition of some transition metal elements to two of the coal samples.

An extensive literature survey revealed that work of this nature had not been done previously. It was also revealed that a computer interfaced to the thermogravimetric apparatus to collect and manipulate data would aid the research. An extra aim of the research was added: to interface a Model B BBC Microcomputer to the apparatus and to develop the necessary programs. This aim was successfully realised.

Hot-Stage Microscopy was used to provide qualitative information about the physical changes the samples underwent during pyrolysis. This information was used to aid the interpretation of the thermogravimetric results.

Thermogravimetric studies of the coals at three heating rates revealed distinct trends in behaviour with rank. The computerised data recording system also revealed more information about the pyrolysis of coals and allowed the tentative suggestion of a system of fingerprinting the pyrolytic behaviour of the coals. One avenue of further research could be the expansion and validation of this system.

The kinetic analysis of the thermogravimetric results revealed that for each sample there are a series of temperature regions with their own activation energy. These regions and activation energies vary with the heating rate. It is suggested that each activation energy relates to a different kind of pyrolysis reaction, and although some suggestions have been made, further research incorporating other techniques is necessary to identify these reactions.

The effect of the addition of some transition metal elements upon the activation energies for two of the samples was then investigated. It was found that most of the metals affected the activation energies in some way - either inhibiting or promoting the reactions. No general trends in behaviour were observed. Another possible avenue of further research is apparent here - to find out the ways in which these metals affect the production of the products of pyrolysis, particularly the gaseous products.

A THERMOGRAVIMETRIC STUDY OF THE PYROLYTIC BEHAVIOUR
OF SOUTH WALES COALS

BY

ANGELA ISABEL PORTER

Thesis submitted to the C.N.A.A. in partial fulfillment of
candidature for the degree of Doctor of Philosophy.

Department of Chemical Engineering,

Polytechnic of Wales,

Treforest, Pontypridd,

Mid Glamorgan.

MAY 1988.

CONTENTS

Acknowledgements

Declaration

Certificate of Research

Abstract

ACKNOWLEDGEMENTS

DECLARATION

This is to certify that neither this thesis nor
any part of it has been presented or is being concurrently
submitted in candidature for any other degrees.

Angela I Power
Candidate

Dated: 5th May 1988

CERTIFICATE OF RESEARCH

This is to certify that, except where specific reference
is made, the work in this thesis is the result of the
investigation carried out by the candidate.

Angela J Ponyer

Candidate

G.J.Rees

Director of Studies

Dated 5ᵗ May 1988

A THERMOGRAVIMETRIC STUDY OF THE PYROLYTIC BEHAVIOUR OF SOUTH WALES COALS

ANGELA ISABEL PORTER

ABSTRACT

The major aim of this research was to provide quantitative data about the pyrolytic behaviour of a series of coals from the South Wales Coalfield using thermogravimetry as the major experimental technique. It is hoped that this data will (1) provide information of value to the development of coal conversion technologies, (2) provide information about the kinetics of coal pyrolysis, (3) provide information about the effect upon the kinetic results by the addition of some transition metal elements to two of the coal samples.

An extensive literature survey revealed that work of this nature had not been done previously. It was also revealed that a computer interfaced to the thermogravimetric apparatus to collect and manipulate data would aid the research. An extra aim of the research was added: to interface a Model B BBC Microcomputer to the apparatus and to develop the necessary programs. This aim was successfully realised.

Hot-Stage Microscopy was used to provide qualitative information about the physical changes the samples underwent during pyrolysis. This information was used to aid the interpretation of the thermogravimetric results.

Thermogravimetric studies of the coals at three heating rates revealed distinct trends in behaviour with rank. The computerised data recording system also revealed more information about the pyrolysis of coals and allowed the tentative suggestion of a system of fingerprinting the pyrolytic behaviour of the coals. One avenue of further research could be the expansion and validation of this system.

The kinetic analysis of the thermogravimetric results revealed that for each sample there are a series of temperature regions with their own activation energy. These regions and activation energies vary with the heating rate. It is suggested that each activation energy relates to a different kind of pyrolysis reaction, and although some suggestions have been made, further research incorporating other techniques is necessary to identify these reactions.

The effect of the addition of some transition metal elements upon the activation energies for two of the samples was then investigated. It was found that most of the metals affected the activation energies in some way - either inhibiting or promoting the reactions. No general trends in behaviour were observed. Another possible avenue of further research is apparent here - to find out the ways in which these metals affect the production of the products of pyrolysis, particularly the gaseous products.

CHAPTER 1.

INTRODUCTION AND AIMS.

With the rapid depletion of oil and natural gas reserves it is likely that coal will become a far more useful and valuable resource than it is at present. A new raw material for the chemical industry will be needed to supply the chemicals once obtained from the distillation of oil. It is likely that coal will no longer be wastefully burned, with its consequent pollution of the environment. Also, it is probable that coal deposits that are no longer considered economically workable will be mined. During the course of this research, a number of collieries from which the coal samples were obtained have closed, and although this work has in a large part become academic , in the future it may be of value as a piece of groundwork into the pyrolysis behaviour of a cross-section of the coals found in the South Wales coalfield. It is also the author's belief that now is the time for research to begin in order to develop efficient and economically viable processes for the utilization of coal as a chemical feedstock in order that the knowledge and the means are available when mankind will need it. This

should also be the case for research into alternative energy sources.

The fundamental raison d'etre of this research is to provide a valuable piece of groundwork for future research into the subject, to provide guidelines and suggestion for this, and to investigate the effect of the addition of various transition metal elements, which are common catalysts in industry, upon the pyrolysis reaction. The interfacing of a computer to the experimental apparatus and the development of the programs necessary to replace the functions of a chart recorder and to complete all the necessary data processing, was not one of the original aims, but rapidly became an integral part of the research.

The experimental work which was to be completed involved

1. the thermogravimetric investigation of the pyrolytic behaviour of a series of coals from the South Wales coalfield in a nitrogen atmosphere at various linear heating rates, viz. 20, 40, and $80^{\circ}Cmin^{-1}$,

2. a kinetic analysis of the thermogravimetric results obtained in (1),

3. an investigation into the effect of the addition of some transition metal elements on two coal samples in two different proportions, and the effect upon the kinetic results,

4. hot-stage microscopy to visually observe the physical changes which the coal samples undergo during pyrolysis,

5. The interfacing of a computer and the development of appropriate computer programs to replace the chart recorder in the thermogravimetric apparatus and the more normal subsequent manual analysis of the data.

CHAPTER 2.

LITERATURE SURVEY.

In the past, a considerable amount of research has been done concerning the thermal decomposition of coal. Much of the earliest work was performed to provide an insight into the nature and properties of coal. Nowadays, most of the work is undertaken to provide information to aid coal conversion technologies, as well as to give more information about the constitution and behaviour of coal.

Many techniques are used in the attempt to quantify coal. Chemical analysis can be carried out using techniques such as solvent extraction, with subsequent analysis either by classical methods or by techniques such as gas chromatography, infra-red spectroscopy, and nuclear magnetic resonance. The analysis of physical properties can be performed by the use of techniques such as thermogravimetry, dilatometry, and differential scanning calorimetry.

Because of the quantity of work that has been published, it
has been considered prudent to limit this literature survey
to articles of particular relevance to the research
presented in this thesis.

Research into the decomposition of coal began as early as
1857 when Delesse, as reported by Evans and Phelps[1], noted
that peat decomposed under the action of heat at
approximately 250°C, lignite at 300°C, and coal at 400°C.
The first signs of "odeurs empyrematique" and liquid
products were used as the criteria of decomposition.

Burgess and Wheeler[2-4], using 200g charges of a coal with
a carbon content of 80%, examined the products obtained in a
stepwise vacuum distillation of the sample at 100, 200, 300,
400 and 450°C. They found that:

(a) occluded gases were evolved in small quantities upto
    200°C

(b) some simplification of the coal molecule, accompanied by
    the copious evolution of water, began at 200°C and
    continued upto 450°C

(c) at 270-300°C hydrogen sulphide was freely evolved

(d)   liquid products other than water began to distil at
        310°C, but the appearance of oil was not marked by any
        large gas evolution

(e)   a critical point occured at 350°C, marked by the rapid
        increase in the gas yield and by the appearance of much
        viscous oil.

Holroyd and Wheeler[8] described a detailed study of the
decomposition of English coals using a stepwise vacuum
distillation at a number of temperatures and supplemented by
an examination of the products of distillation. They
plotted the total gas yields and the yields of gaseous
alkanes, alkenes and oxides of carbon against temperature
and found well defined breaks in the curves which varied
with the coal under examination. The temperature at which
the first extensive disruption of the ulmic material occurs,
called the "active decomposition point", is accompanied by a
rapid evolution of gaseous and other products and by a
profound change in the nature of the residue. This point
also appeared to be definitive for any one coal.   At and
above this temperature, the composition of the gas evolved
also changed rapidly, the alkanes increasing and the oxides
decreasing in importance. At this temperature it was found
that the rate of tar evolution also accelerated considerably

and quantities of water and phenolic compounds appeared among the products of distillation. It was also observed that the decomposition point was not appreciably affected by variation of the experimental conditions.

Evans and Phelps[1] investigated the effect of heat on coals from the South Wales coalfield with carbon content varying between 84 and 93% and volatile matter content in the range 7-35%. 4g samples of the coals were gradually heated at rates not more than $1^{\circ}Cmin^{-1}$ under vacuum conditions. The rate of pressure change caused by evolution of gases was plotted against temperature with sharp inflexion points occuring which indicated a sudden acceleration of the rate of gas evolution. By heating the coals at a uniform rate a slightly higher decomposition point for each sample occurred than for a stepwise series of isothermal reactions. It was found that the temperature of decomposition of South Wales coals increased progressively with increasing carbon content and carbon to hydrogen ratio. At around 91%C a change in curvature occurs on the %C versus decompositon temperature diagram which had also been noted by other workers[1] and corresponds to a change in coal properties. The curves that were plotted indicate the essential continuity of the coal series as found in the South Wales coalfield. This, together with the gradual changes observed in the

decomposition point and other physical and chemical properties point to, they suggested, a definite similarity in the chemical constitution of the coals. They also suggested that any differences in properties must be of degree rather than type and can be explained as being due to progressive polymerisation of the same original materials forming all coals.

In 1926 Audibert[6] reported using a technique for accurately studying the thermal decomposition of coal. By heating a coal preparation in an electric oven, with the temperature of the oven being raised at a constant rate, he obtained a curve of weight loss against temperature by measuring the weight of the sample. This is one of the first instances of the use of the technique called thermogravimetry to study coal. Thermogravimetry (TG) was developed by Honda[7] in 1915 and gives a graph of sample weight against temperature which is known as a thermogravimetric or TG curve. A graph of rate of weight loss or derivative TG (DTG) against temperature can also be obtained by differentiating the TG curve.

With the advent of automated control, renewed interest was shown in the use of TG for coal analysis by Thevenin in 1950[5]. But it was Van Krevelen et.al.[7] who really pioneered the use of TG in coal research. They studied the formation of coke by the pyrolysis of coal using apparatus similar to that described by Audibert[6] but with the modification of automated heating rate control and sample weighing. It was found that the conversion of coal into coke depended upon the intrinsic properties of the coal and the additional properties which the material has acquried by pretreatment of the sample. Although the thermal decomposition of coal is a very complicated gross process yielding a multitude of final reaction products, the essential elementary mechanism must be simple, e.g.

```
                     slow disintegration
coal + complex --------------------->primary decomposition
                                                product + residue
                          rapidly
primary decomposition product--------->final decomposition
                                                products
residue---------->semi-coke
semi-coke-------->coke
```

It was found that for a bituminous coal a marked decomposition occured at about $350^{\circ}C$ with the rate of decomposition passing through a maximum at $465^{\circ}C$. At $550^{\circ}C$ primary decomposition started with mainly hydrogen evolved from bond cleavage. Van Krevelen et.al. used a kinetic model, based upon the following equation, to obtain kinetic data for the coal and a series of related compounds such as cellulose and dibenzanthrone:

$$-\frac{dF}{dt} = Ae^{-E/RT} \cdot F^n$$

where

   $-dF/dt$ is the rate of weight loss

   F is the fraction of non-decomposed coal

   A is the frequency factor

   E is the activation energy

   n is the rate constant

   R is the ideal gas constant

and T is the absolute temperature

From the kinetic analysis the authors concluded that extensive aromatic structures do not appear in the coalification series before the anthracite stage, and the structures in the bituminous coal are mainly of a non-cyclic character.

Boyer[10] used TG to study the decomposition of French coals and found that a coal of low rank had a maximum rate of weight loss at a lower temperature than a high rank coal, and that the maximum rate of weight loss was greater for the lower ranked coal. Work of a similar nature was performed by Tanno[11] and Bracia Goyanes[12].

Van Krevelen et.al.[13] found, by using a thermobalance both isothermally and dynamically at a heating rate $3^{\circ}Cmin^{-1}$ under conditions of pyrolysis, that

(a) when the coal is heated at a constant temperature, the loss in weight eventually reaches a limit; this limit value rises with an increase in temperature.

(b) at a   constant   rate of   heating the decomposition (i.e. weight loss) curve adopts a sigmoidal shape and the curve for the decomposition rate (i.e. the rate of weight loss) forms a bell shape.

(c) at an increased heating rate the curve showing the rate of decomposition is shifted to higher temperatures and there is an increase in the rate of weight loss.

(d) the rate of decomposition decreases as rank increases, increases in the range of coking coals, and finally decreases again; the maximum in the DTG curve is gradually shifted to higher temperatures with increasing rank.

By comparing the results obtained from TG and other thermal amalysis methods (Geisler plastometer and Audibert-Arnu dilatometer), Van Krevelen et.al. maintain that the results point to a direct relation between the pyrolysis phenomena observed by the different methods. But, since the characteristic temperatures vary with the apparatus used, this suggests that the data are not related to the physiscal properties of the coal substance but are the result of kinetic phenomena.

For a coal to coke, the softening, degassing, and condensation processes must all occur in the same temperature range. The following mechanisms are ascribed to these three processes in coal pyrolysis[13] :

(a) the softening process is a kind of depolymerisation with rupture of bonds between the coal units and this gives the primary pyrolysis product or "meta-plast". This meta-plast is ascribed as being responsible for the plastic behaviour of the mass as a whole and it is believed to act as a plasticiser.

(b) the meta-plast is rather unstable and is subject to further conversions which result in an increase in aromaticity with liberation of non-aromatic groups. This accounts for the mechanisms of both condensation and degassing: the radicals formed by the decomposition of the meta-plast will rapidly react with each other and condense to form semi-coke, the liberated groups escaping into the gaseous phase. This semi-coke will be further decomposed as heating is continued and secondary degassing occurs, particularly demethanation and dehydrogenation with the aromatic clusters growing together.

This mechanism can be summarized in the following equations:

$$P \xrightarrow{\quad k_1 \quad} M$$

$$M \xrightarrow{\quad k_2 \quad} R + G_1$$

$$R \xrightarrow{\quad k_3 \quad} S + G_2$$
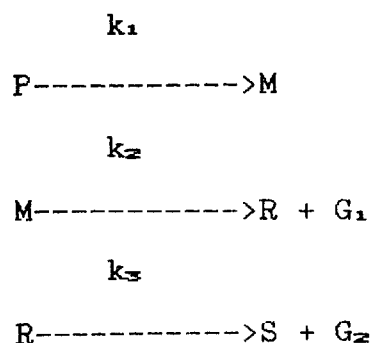
where

P is the original coal

M is the meta-plast

R is the solid residue or semi-coke

S is the coke

G_1 is the primary gas

G_2 is the secondary gas

k_{1-3} are reaction rate constants

This is a highly simplified reaction rate scheme amd is an elaboration on a scheme presented in an earlier paper[7].

Chermin and Van Krevelen[14] presented a mathematical model, also presented by Van Krevelen and Schuyer[15], based upon the above mechanism[13]. The conversion of coal to

meta-plast, which can be considered as a kind of depolymerisation reaction, and the conversion of meta-plast to semi-coke and primary gas, which is a kind of cracking process, have often been shown to be first-order cracking reactions[16,17]. By plotting the log of the heating rate against the reciprocal of the temperature of the maximum rate of degasification for various percentage volatile matter contents a series of straight lines were obtained which had slopes equal to

$$\frac{E + 2RT_1}{2.3R}$$

where T_1 = 720K

      E is the activation energy

      R is the ideal gas constant

The activation energies calculated using this model varied from 217 to 247 $kJmol^{-1}$ for coals whose volatile matter content ranged between 17.9 and 38.8%.

From these studies, Chermin and Van Krevelen postulated that the meta-plast can only form in sufficient concentration if the reaction rate constant, and hence the activation energies of the primary depolymerization, E_1, and the subsequent decomposition of the meta-plast, E_2, are approximately equal. The activation energies of these

reactions vary over the coalification series.   It can be supposed that during the primary decomposition of low rank coals with very high oxygen contents and relatively small aromatic clusters, highly reactive radicals have a very short lifetime and that only a small amount of liquid product is formed and, under normal heating rates, there is no measurable plasticity.   In the case of low volatile coals, which have retained their polymeric character, stable radicals are produced, but due to the large dimensions of the aromatic clusters the intramolecular forces[18] will now be so great that no mobility, and hence no plasticity, can be expected.

$E_1 \simeq E_2$ is indicative of a coking coal and, as a result, the lifetime of the meta-plast allows the formation of extensive recondensation cycles. The aromatic clusters are still small enough i.e. possess a sufficiently low cohesion energy to allow the formation of a liquid structure and yet still possess the resonance possibilities that are needed to make the radicals stable enough.

Brown[17], using the same equipment as Waters[20,21], published the DTG curves of Australian coals heated under pyrolysis conditions.   At a heating rate of $3^{\circ}Cmin^{-1}$, the maximum in the DTG curve for coking coals appeared at

temperatures above 440°C, and below this temperature for the lower ranked coals. The lower ranked coals were also characterized by a much broader temperature range over which decomposition occured.

Dryden[22] obtained the rate of weight loss curves for samples of coal under several conditions of constant temperature and found that the rate gradually decreases. The suggestion was made that this was due to a range of bond strengths on a molecular scale where those of lowest strength break first, whilst those of a stronger nature need a longer period of time before enough energy is accumulated in order that cleavage can occur.

Berkowitz[23] recorded the weight loss curves of coals heated in an inert atmosphere at constant temperature. The conclusion was reached that these curves do not represent a protracted thermal decomposition of coal and it was suggested that the curves are governed by a rate determining diffusion process, and that the decomposition reactions at any one temperature must be relatively fast. The time periods required for an isothermally heated sample to attain a zero rate of weight loss appeared to bear no systematic relationship to the nature of the reactions presumed to take place over different tmeperature regions. This resulted in

an objection to the interpretation of isothermal weight loss curves as a measure of the rates of thermal decomposition. Berkowitz stated that there was a general agreement that the chemical changes in coal at temperatures below 300-350°C are confined to relatively simple condensation and disproportionation reactions with the possibility of limited depolymerization whilst intensive chemical reorganisation can only occur at higher temperatures. Despite this, a low rank coal of 40% volatile matter content does not reach equilibrium (i.e. zero rate of weight loss) significantly faster at 250°C (with the total weight loss not exceeding 3%) than at 600°C (with the total weight loss greater than 30%). It was also found that the kinetics of weight loss curves did not allow the interpretation of such curves in terms of chemical change alone.

More recently there has been an upsurge in the quantity of literature published concerning the themal behaviour of coal. This has been caused by an expected, but not fully realized, need for replacement fuels and chemical feedstocks to fill the gaps that will be left by dwindling oil and natural gas reserves. Much research has also been done to formulate kinetic mechanisms to explain the process of the thermal decomposition of coal in various atmospheres, with and without the addition of possible catalysts.

Veraa and Bell[24] studied the effect of alkali metal chlorides, hydroxides, and carbonates upon the gasification rate to fixed carbon relationship. It has been known for a long time[28-33] that alkali metal salts are the most effective catalysts for steam gasification of coal char and that for a given cation, the associated anion plays an important role. It was concluded that oxides, hydroxides, bicarbonates, and carbonates are more active than other alkali metal salts. Veera and Bell's results showed that aqueously impregnated K_2CO_3 is a more active catalyst than the other salts studied.

Rai and Tran[34] performed a kinetic analysis of TG data obtained for both catalysed and non-catalysed samples of a bituminous coal and its char under conditions of pyrolysis and hydrogasification. Heating rates of 10, 20, 50 and $100^{\circ}Cmin^{-1}$ were used with the temperature of the furnace being raised from room temperature to $850^{\circ}C$ and $950^{\circ}C$ for the pyrolysis and hydrogasification studies respectively. Nitrogen and hydrogen atmospheres at atmospheric pressure and flow rate of $150cm^3min^{-1}$ were used for the pyrolysis and hydrogasification studies respectively. The catalysts used were K_2CO_3 and K_2CO_3/Ni.

The kinetic model of coal pyrolysis used by Rai and Tran is based on an Arrhenius relationship. For a series of degrees of conversion, the maximum amount of pyrolysable coal, the rate of weight loss, the weight of the sample at a time t, and the temperature are used to calculate the kinetic parameters. The activation energy for pyrolysis was found to vary from 121 to 311kJmol^{-1} as the non-catalysed coal conversion increased from 0 to 88%, whilst the catalysed activation energy increased only from 121 to 230kJmol^{-1}. The orders of reaction were found to be 0.24 and 0.32 with corresponding reaction rate constants of 2.03x10^{13}min^{-1} and 1.47x10^{13}min^{-1} for non-catalysed and catalysed coal respectively. It was found that if the degree of conversion was defined using weights of coal on a dry-ash-free basis, the orders of reaction would be 0.95 and 0.94 for non-catalysed and catalysed coal respectively.

Ciuryla et.al.[39] used TG to characterize the pyrolysis behaviour and reactivity of four coals and their chars in helium and air atmospheres at ambient pressure. Heating rates of 40 and 160°Cmin^{-1} were used with the temperature of the furnace being raised from 125 to 1000°C. The samples were first heated to 125°C and held at this temperature until no more weight loss was observed, i.e. until all the

moisture had been driven off. Sample masses of 2 and 4mg were used with particle sizes of 40x80 and 200x230 U.S. standard mesh. Helium and air were the purge gases used for the pyrolysis and reactivity measurements respectively; the purge gas flow rates used were 10 and $40cm^3min^{-1}$. The results were found to show that the heating rate was the only variable which has a significant effect upon the maximum rate of weight loss for the pyrolysis experiments. The results indicated that the maximum rate of weight loss increased with increasing heating rate. Changing the heating rate had no effect upon the total yield of volatiles upto $1000^{\circ}C$.

Ciuryla et.al. used a first order kinetic model which used the weight loss and temperature data from the pyrolysis experiments to calculate the required kinetic parameters. The calculated activation energy for pyrolysis of bituminous coals was $218kJmol^{-1}$, and for lignites was $225kJmol^{-1}$. These results, together with other calculated kinetic parameters, are consistent with the view that coal pyrolysis involves numerous parallel first-order organic decomposition reactions.

Smith et.al.[36] studied the combustion of coal samples by TG. The samples analysed varied in rank from lignites (69%C on a dry-mineral-matter-free basis) to low volatile bituminous (91%C$_{dmmf}$). A heating rate of 15°Cmin^{-1} was used with a temperature range of 25-900°C. Sample masses of 300mg were used with the particle size of the coal being <0.149mm. The purge gas was air at atmospheric pressure and with a flow rate of 800cm^{3}min^{-1}. The weight loss data thus obtained were used in a first order Arrhenius equation to yield kinetic results. The authors found four distict regions of combustion with activation energies ranging from 4kJmol^{-1} in the high temperature, diffusion controlled, region to 290kJmol^{-1} in the chemical reaction controlled, low temperature region. It was also found that the temperature at which half of a coal sample has been combusted is rectilinearly related to carbon content.

Rosenvold et.al.[37] examined a series of Ohio bituminous coals using both TG and differential scanning calorimetry (DSC). For the TG experiments, a 10-25mg sample was heated at either 2 ,5 ,10 or 20°Cmin^{-1} in a nitrogen atmosphere at ambient pressure and with a flow rate of 500cm^{3}min^{-1}. A temperature range of 20-1100°C was used. A plot of the fractional weight loss vs. temperature was recorded with heating rate as the variable parameter. The fractional

weight loss is given by

$$f = \frac{W_o - W_t}{W_o - W_f}$$

where f = fractional weight loss

W_o = initial mass of dry sample

W_t = mass of sample at temperature T

W_f = final mass after loss of volatile matter

A systematic shift in df/dT peaks to higher temperatures with increasing heating rate was noted and this is attributed to a thermal lag induced by limitations in the rate of supply of heat to the pyrolysing samples. Also, lower heating rates are able to resolve multiple, overlapping processes in the overall pyrolysis reaction.

Cumming and McLaughlin[38] investigated the TG behaviour of coal in order to

(a) perform a proximate analysis using TG

(b) establish a burning profile test in which the DTG curve is recorded for a 20mg sample heated in air. The DTG curve gives a measure of the combustibility of the fuel. This test was originally developed by Wagoner and Duzy[39] and enhanced by Wagoner and Weingarter[40] and

Vecci et.al.[41].

(c) develop a volatile release profile test, which is similar to the burning profile except that an inert atmosphere is used so that combustion does not occur. The resultant DTG curve gives information about the way in which the organic substance of the coal breaks down as the sample is heated.

The conditions used for the burning profile test were as follows:

    heating rate = $15^\circ C min^{-1}$

    sample weight = $20\pm0.5mg$

    atmosphere = air flowing at $75cm^3 min^{-1}$

    temperature range = ambient $- 900^\circ C$

For the volatile release profile the conditions used were as follows:

    heating rate = $23^\circ C min^{-1}$

    sample weight = $40\pm0.5mg$

    atmosphere = nitrogen flowing at $50cm^3 min^{-1}$

    temperature range = ambient $- 960^\circ C$

To characterise the burning profile a series of four temperatures were used:

(1) the initiation temperature where weight loss first begins after the moisture has been driven off

(2) the fixed carbon initiation temperature which is an inflexion point between the end of volatile loss and the start of combustion

(3) the peak temperature where the maximum rate of weight loss occurs

(4) the burn out temperature, which is the point at which the rate of weight loss becomes zero once combustion is complete

The volatile release profile is of relevance to carbonisation studies. The DTG curve represents the progressive thermal degradation of the organic species present in the coal substance and the loss of gaseous products. Volatile loss take place throughout the bulk of the sample and is not critically dependent upon the prticle-gas interface, as is the case for combustion. It was found that coals of similar composition gave very different volatile release profiles, and this led to the suggestion that this test is much more specific to

individual coal and could lead to a system of
"fingerprinting" coals.

In a later paper, Cumming[42] again utilized the burning
profile together with it's four datum tempertures and a
weighted mean activation energy to assess coal reactivity.

To obtain activation energies, Cumming used the same
equation as Smith et.al.[34], which is based on a first
order Arrhenius equation. The resulting Arrhenius graphs
showed several regions of Arrhenius linearity, each with its
own associated apparent activation energy.

A correlation was found between the burning profile peak
temperature and the weighted mean activation energy, E_m. It
was suggested that E_m is a more reliable, accurate, and
concise indicator of reactivity since it covers the whole
combustion process. The calculated activtion energies
varied between 50 and $180kJmol^{-1}$.

Serageldin and Pan[43] performed kinetic analyses upon TG
data from a bituminous coal heated in a nitrogen atmosphere
at atmospheric pressure. A heating rate of $20^{\circ}Cmin^{-1}$ was
used and the purge flow rate was $50cm^3min^{-1}$. The
temperature range studied was $20-950^{\circ}C$. The results

obtained were then used to compare various methods of kinetic analysis in order to ascertain the most suitable method. They recommended the following equation:

$$\left[\log \left[\frac{-dm/dt}{m_i - m_f} \right] \right]_{\cdot} \frac{m_i - m_f}{m - m_f} = \log A - \frac{E}{2.3RT}$$

where dm/dt = rate of weight loss

m_i = initial sample mass

m_f = final sample mass

m = mass at temperature T

A = pre-exponential factor

E = activation energy

R = ideal gas constant

T = absolute temperature

The value of E was found to vary between 20 and 70kJmol^{-1} along the thermogram (i.e. the TG and DTG curves recorded together).

In a later paper, Serageldin and Pan[44] used TG and the above method of kinetic analysis to investigate the catalytic effect of alkali metal carbonates and chlorides on the decomposition of a sub-bituminous coal in atmospheres of air, nitrogen, and carbon dioxide. A 15mg sample was heated at a rate of $20^{\circ}Cmin^{-1}$ over a temperature range of 20-950°C. The particle size of the sample was -270 and +325 U.S. mesh. The gas flow rate at s.t.p. was $50cm^3min^{-1}$. Infra-red spectroscopy was used to detect the evolution of methane, carbon monoxide, and carbon dioxide from the sample by monitoring the effluent gas stream.

The DTG pyrolysis curve exhibits three distinct zones. The first represents the evolution of water and occurs below 250°C. The second covers the temperature range 250-665°C where compounds containing C,H and O are released as a result of reactions of the fuctional groups, and this region is termed the primary devolatilization zone. The third region contains the secondary decomposition zone in which mostly methane and hydrogen are evolved. These results are in agreement with those of Van Krevelen[45] and Juntgen and Van Heek[46].

In an atmosphere of carbon dioxide, these three zones are observed but there is an increase in the rate of reaction in the third zone where $C + CO_2$ reactions are important.

In air, coal decomposition was much more rapid, and due to the high rate of the $C + O_2$ reaction, resulting in much sharper DTG peaks, zones 2 and 3 merged. Also, the reaction completed in a much shorter time.

In a nitrogen atmosphere, it was found that the added salts first reduced and then promoted the decomposition of the coal. A decrease in mass loss of coal occured in zone 2 and was accompanied by a decrease in activation energy. Therefore, a lowering of activation energy does not reflect an increase in coal reactivity.

It has been found that the activation energy, pre-exponential factor and order of reaction change with operating parameters which suggests that the mechanism of reaction is changing and hence the activation energies are not intrinsic values. It was also reported that the catalysts decreased both the activation energy and the heat of reaction but the reduction in activation energy is not always related to coal conversion. As the heat of reaction increases, the activation energy decreases, which indicates

that the heat of reaction influences the chemical change and is typical of elementary reactions[47]. Such evidence reinforced the assumption that coal decomposition is a first order process[48].

Merrick[48,49,50], in a series of papers, developed mathematical models to describe the thermal decomposition of coal with the aim to aid studies of the coking process. Models of the physical properties of coal during decomposition to coke were constructed in terms of the changes in chemical composition and structure. It was suggested that a model of volatile matter release should satisfy the following criteria:

(1) the model should describe the kinetics of volatile matter release

(2) the model should be defined solely in terms of identifiable chemical species

(3) all of the major components of the volatile matter should be included so that changes in the mass and composition of the solid residue can be related to the release of volatile matter by element balances

(4) correlations between the parameters of the model and commonly available measurements of coal rank should be included in order for predictions to be made.

For simplicity, the composition of volatile matter in the model was defined in terms of CH_4, C_2H_6, CO, tar, H_2, H_2O, and NH_3, and these were considered to be the minimum number of species required to provide a sufficiently detailed description of the volatile matter in order to allow reasonably accurate element balances to be constructed.

The predictions made by the model reproduced the main trends in volatile matter evolution rate with varying heating rates and coal types and noted in previous studies[14].

In the two later papers, Merrick derives models based along similar lines which allow the prediction of specific heats, heats of reaction, density, porosity, and contraction behaviour of coals in a coke oven.

Juntgen[51] utilised TG to provide data for the kinetic analysis of the pyrolysis reactions of coal. The rate of weight loss of a German coal heated at a rate of $3^\circ Cmin^{-1}$ was recorded as a function of temperature. The volatile products were purged from the reaction chamber by nitrogen into a gas chromatograph which analysed the effluent for H_2, CH_4, C_2H_6, CO_x, and H_2O. From these results, a mechanism

for coal pyrolysis was proposed by the author. The main reaction steps are (without diffusion of trapped molecules):

(a) cracking of the bridges between ring systems, with formation of radical groups

(b) partial saturation of the radicals by H_2 with the formation of CH_4, other aliphatics, and H_2O, which diffuse out of the coal particles

(c) simultaneous saturation of the radicals of the larger molecules to yield tar products (of medium molecular weight); diffusion from the coal particles

(d) condensation of the substances of higher molecular weight to yield coke, with the elimination of H_2, which is released as a gas from the coal particle.

This mechanism also applies at higher heating rates and pressures.

Elder and Harris[82] performed a detailed investigation into the thermal characteristics of a series of six Kentucky bituminous coals undergoing pyrolysis in an inert atmosphere. Three heating rates (20, 50, and $100^{\circ}Cmin^{-1}$) were used. The data obtained from the resultant TG and DTG curves were used to calculate kinetic results using a model of pyrolysis based on a first order Arrhenius equation.

These investigators found that the temperature of the maximum rate of weight loss increased with increasing heating rate. In the region 200-350°C, the coals started to lose small amounts of pyrolysis water from decomposing phenolic structures, and oxides of carbon from carboxylic and carbonyl groups. At 350°C, primary carbonisation begins with the release of CO_2 and H_2. As the temperature increased, CH_4 and other lower aliphatics were evolved together with H_2, CO and alkyl aromatics. The heat from the

furnace provided the energy for the competing endothermic devolatilization of condensable oils and tars. The loss of volatile matter occurred mainly in the region 300-600°C. Global activation energies were found to be in the range 198-220kJmol^{-1}.

Ghetti et.al.[53] characterized a series of coals of different rank by measuring their surface areas. The samples were then heated in air and quenched at a series of temperatures and their surface areas measured again. The results gave information about the way in which the surface areas of the coals changed during combustion of the samples. Burning profiles were then obtained for each of the samples by heating a 18mg sample from room temperature to 1000°C at

a rate of $15^\circ Cmin^{-1}$ and with air flowing at a purge rate of $70cm^3min^{-1}$ in a thermobalance. The maximum rate of weight loss and the temperature at which it occurs were then used to test for correlations with the surface area measurements. The authors found that a close relationship could be established between the surface areas and the TG behaviour of the samples, and this confirms the strict connection between combustion kinetics and the available gas-solid interface.

Ghetti[84] used Proximate and Ultimate analysis data to rank and characterise 22 samples of coal. The samples were then analysed by TG. The sample weight used was chosen so that the amount of reactive material in the sample was equal to 18mg; this allowed a direct comparison of results. For the burning profile test, both the volatile matter (VM) and fixed carbon (FC) contents were taken into account for calculating the required mass, whilst for the volatile release profile test, only the VM was required. The samples were then heated in a platinum crucible from room temperature to $1000^\circ C$ at a heating rate of $15^\circ Cmin^{1-}$ with the purge gas flowing at $70cm^3min^{-1}$. Air was the purge gas used for the burning profile, and nitrogen for the volatile release profile.

Using the resultant TG and DTG curves for the burning and volatile release profiles, the initiation and peak temperatures and the peak heights were found using the methods described by previous workers[38,42,53]. Correlations were found between the Proximate and ultimate analyses by plotting C/H and (C+H)/O against VM/FC. The VM/FC ratio is indicative of rank, C/H is related to aromaticity, and (C+H)/O gives an indication of the extent of oxidation of the fuel. The curves obtained confirmed the knowledge that as rank decreases, the aromaticity also decreases, and the extent of oxidation increases[45,15].

For the burning profiles, a plot of the combustion initiation temperature vs. VM/FC ratio was constructed. A decrease in the initiation temperature, a decrease in the peak temperature, and an increase in the rate of combustion were observed with an increase in the VM/FC ratio.

In the case of the volatile release profiles, the initiation temperature of devolatilization and the peak temperature decreased with increasing VM/FC ratio. No trend was observed between the maximum rate of devolatilization and the VM/FC ratio.

From these results, Ghetti deduced that low rank coals react at lower temperatures and show faster rates of weight loss during both combustion and pyrolysis than higher rank coals. It was thus asserted that as rank decreases, the organic part of the coal becomes increasingly more reactive towards combustion and pyrolysis.

Vargas and Perlmutter[55] presented and interpretation of coal pyrolysis kinetics which showed that dynamic programmed pyrolysis can be considered to proceed via a series of successive isothermal steps, each of which corresponds to the breakdown of a pseudo-component of the coal.

A series of decomposition reactions were carried out upon three coal samples of bituminous coals using various heating rates and temperature ranges. 5-100mg sample weights of a coal with a particle size of $<460 \mu m$ were examined. The changes in weight and rate of weight change with temperature were recorded. The resultant TG data were kinetically analysed using a model based upon first order kinetics for a series of coal components.

The activation energies thus calculated range from 96 to 522 kJmol^{-1} for the three coals studied. These results compare favourably with the results of Suubert et.al.[54] who found activation energies for the reactions producing the gaseous products of decomposition of a lignite to be in the range 150-371kJmol^{-1}. The highest activation energies are intermediate between those needed for single bond scission (368kJmol^{-1} for ethane) and double bond scission (720kJmol^{-1} for ethene)[57]. Both Vargas and Perlmutter and Suubert et.al. found pre-exponential factors to be in the range 10^{8}-10^{22}s^{-1}.

CHAPTER 3

THEORY

3.1 THE ORIGIN OF COAL.

Francis[36] defined coal as "a compact stratified mass of mummified plants which have been altered by degrees and interspersed with varying amounts of inorganic matter". Other authors have given definitions of coal which place emphasis on other aspects of coal constitution. Van Krevelen and Schuyer[15] described coal simply as "fossilised plant remains", whilst Pitt and Milward[57] gave the following more detailed definition: "coal is a complex mixture of organic substances which contain C, H, and O in chemical combination, together with smaller amounts of N and S". Harker and Backhurst[40] defined it as "an organic rock formed from the remains of decaying trees and vegetation".

As can be seen from the above definitions, coal is derived from vegetable matter. Hence, coal formation has been possible from the time plants first began to appear in profusion on the Earth's surface. Geologically, some coals

are over 250 million years old, whilst some are mere youngsters at 25 million years old[40]. Coals are also widely distributed geographically and occur in the most diverse types of strata. This suggests that the processes necessary for coal formation were commonplace througout much of geological history, and that particular types of plant debris were not necessary.

3.1.1 The Coal Series[15,58,60,62]

Before discussing the mechanism of coal formation, certain aspects of the nature of coal need to be discussed in order to explain the terms used in the following discussion.

Coal is formed from plant matter, and differences in the degree of departure from the structure of the original plant matter are described as changes in rank. These changes allow coals to be grouped according to these changes into a series of ranks known as the coal series:

Peat -> Lignite -> Subbituminous -> Bituminous -> Anthracite

Increasing Rank ->

The conceptual end-point of this series is graphite, but this is rarely reached due to the immense energy required to

transform even extensively aromatised carbon into graphitic carbon.

It should not be thought, however, that this series implies a close genetic relationship between its members, and while it is consistent with the idea that lignites in time become sub-bituminous coals and the latter in time become bituminous coals, this progression is not inevitable.

With increasing rank there are a number of changes which occur in the mass of vegetable matter.

(1) the carbon content increases progressively and uniformly

(2) the hydrogen content decreases first gradually and then more rapidly once the carbon content has reached 89%

(3) the amount of volatile matter evolved on destructive distillation decreases

(4) the calorific value of the substance increases until the hydrogen content has decreased to 4.5%

(5) the moisture content, particularly the inherent moisture, at first decreases and then increases towards the anthracites

(6) the absolute density of the substance increases

(7) coking properties develop over a certain rank range

It is these changes which are utilised in systems of coal classification by rank. The most common method of assessing the rank of a coal is by the technique of Proximate analysis. In this method, the moisture, volatile matter, fixed carbon, and ash content of the coal sample are determined. From these results, the rank of a coal can be determined. The methods for Proximate analysis are strictly laid down in BS1016 (1957).

The moisture contained within a coal can be of three types:

(1) surface water acquired during washing/cleaning and storage

(2) inherent moisture, which is absorbed and adsorbed within the capillaries in the coal structure

(3) combined moisture, which is held in loose chemical combination within the coal matrix.

The volatile matter component of the coal is composed of the substances which are evolved on heating the sample. These substances derive from small molecules trapped within the coal matrix and from small molecules produced as the result of the decomposition of the coal substance itself.

The ash is basically the non-combustible, inorganic portion of the coal matrix.

The fixed carbon component of the sample is the carbonaceous matter left behind once all the moisture and volatile matter have been driven off, excluding the ash content.

3.1.2 The Accumulation of Plant Debris[15,58]

The first stage in the formation of coal is the extensive accumulation of plant debris in a waterlogged area of land subsidence known as a geosyncline. When the rate of subsidence is exceeded by the rate of sedimentation, shallow lagoons are formed. This allows aquatic plants to grow in the lagoon. In time, the further accumulation of sediments and plant debris from the aquatic plants result in the formation of a weak, boggy soil, and the lagoon is transformed into a swamp. The soil allows the growth of larger plants such as shrubs and even trees. The water in the swamp becomes stagnant, except, that is, for a few fresh water rivers traversing it. These rivers transport nutrients into the swamp, as well as plant debris such as leaves, twigs, and logs from sources external to the swamp. This transported matter is known as allochthonous material. The material deposited by plants growing within the swamp is

known as _autochthonous_ matter.   Major coal deposits are
mainly   autochthonous   in   nature,   although allochthonous
material is almost invariably present.   The flooding of the
swamp by the rivers, which carry extraneous vegetable and
mineral matter, movement of fine plant debris in any free
patches of water, and the concentration of plankton, spores,
pollen, leaves, and twigs in shallow pools of lakes, all
have an important bearing upon the composition and variation
in composition of mainly autochthonous deposits   of coal.
The   allochthonous   portions   of   a   deposit differ from the
autochthonous parts in the nature of the organic components
and   the   proportions   of the   inorganic components present.
Allochthonous material forms bands or pockets of material of
high ash content, and these have properties widely different
from the more massive portions of the plant debris, which is
substantially free from extraneous matter.

The   mode   of   accumulation and the subsequent environment of
the coal forming materials modifies the character of the
products.   Figure 3.1, as formulated by Stopes and
Wheeler[43] , shows the principal ways in which the coal
forming plant debris accumulated. This table is presented below.

Fig. 3.1 [63]

A. IN SEA WATER.

(1) Drifted land material, which may travel far, settling waterlogged beyond the reach of mineral detritus. This would principally be (a) tree trunks and logs which may accumulate in large quantities, (b) "floating islands" of various plants growing entangled together and generally very local.

(2) Fucoid algae forming a shore accumulation.

B. IN BRACKISH WATER.

(1) In situ material, the droppings of coastal forests or mangrove-like swamps.

(2) In situ lowly swamp or bog plants.

(3) Partly in situ and partly drifted from short distances in swamps.

(4) B(1), (2), (3) and A(1)(a) and (b) mingled in any proportion.

C. IN FRESH WATER.

(1) In undisturbed lakes (a) from the grass debris drifted in from neighbouring forests, (b) the pure plankton of the lake, (c) b mixed only with the spores, pollen and finer ultimate debris of higher plants, (d) plants growing in situ, reeds, etc., (e) a, b, and c layered or mingled in any proportion,

may be layered with d as the water level changes.

(2) In estuaries, river bends, and deltas (a) drift material which may have travelled far, nearly all trees and branches, (b) drift material from near at hand - includes soft leaves and spores as well as trees and branches, (c) floating islands, (d) swamp or bog plants, in situ growths, (e) a, b, c and d mingled in all possible proportions.

D. ON LAND.

(1) High land moors of various types, moss and moor peats.

(2) Moorland peat and forest, mingled or alternating.

(3) Swamp peats - these merge with (2)

(4) Forest floor accumulations.

Fig. 3.1: Mode of Accumulation of Plant Debris.[63]

This accumulation of plant matter continues until the balance between the rate of subsidence and the accumulation of plant debris is disturbed. If the rate of subsidence is increased relative to the rate of debris accumulation, the area sinks below the level of the water, sedimentation occurs and the plant debris is preserved. If the flooding water is fron the sea, the sediments will be composed of

sand and calcareous mud; if the water is fresh, the deposit is covered by soil or clay. If the rate of subsidence is decreased relative to the rate of debris accumulation, the land level rises and accumulation of plant debris eventually ceases due to rapid decay by microbial agencies and erosional forces. In time, the plant debris will be completely destroyed.

3.1.3 The Transformation of Plant Debris into Peat[15,58,62]

The next stage in the formation of coal is the formation of peat from the accumulated plant debris. This is accomplished by microbial agencies, i.e. bacteria, fungi and enzymes. Information about this <u>biochemical</u> or <u>diagenetic</u> stage comes mainly from studies of plant remains which can be identified in thin sections of coal viewed microscopically, but also it is inferred from studies of contemporary accumulations of plant debris. As the modes of accumulation and types of plant debris were diverse, individual diagenetic histories also varied widely, and the following account is a broad outline of the diagenetic processes.

All multicelled plants, regardless of their origin, are ultimately composed of:

(1) Carbohydrates: mono-, di-, and poly-saccharides, the latter mainly represented by starches, celluloses and compound celluloses.

(2) Glycosides: complexes of mono-saccharides and hydroxylated aromatic or aliphatic compounds.

(3) Proteins: high molecular weight polypeptides, each with a specific sequence of amino acids.

(4) Fats, waxes, and resins: principally derived fron terpenes or primary oxidation products of terpenes.

(5) A broad array of alkaloids, purines, chitins, enzymes, and pigments, the most important of the latter being chlorophyll and the carotenoids.

The structure of some possible coal precursors is given in figure 3.2 below.

Woody tissues also contain lignin, which is closely related to hemicellulose, and is diffused throughout the cell walls of these tissues. Lignin is a non-crystalline, three-dimensional, cross-linked polymer built up of various hydroxy/methoxy/phenyl propane units having a very characteristic distribution of substituents around the benzene ring (1,4-, 1,3,4- or 1,3,4,5-); the propane side chain is also oxygenated.
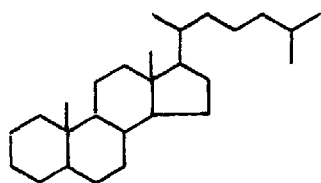
Sterols
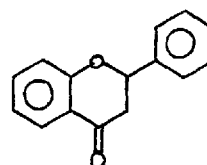
Flavonoids
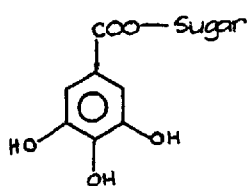
Tannins
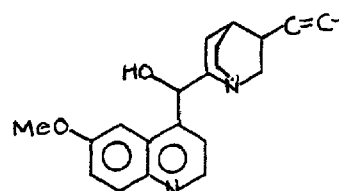
Alkaloids
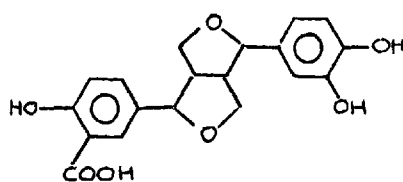
Lignins
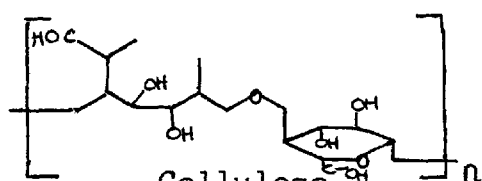
Cellulose

Protein

$$C_{23}H_{47}-\overset{\overset{\displaystyle O}{\parallel}}{C}-O-C_{23}H_{65}$$
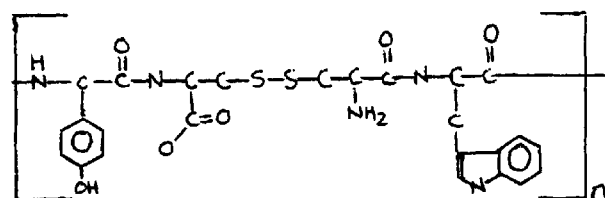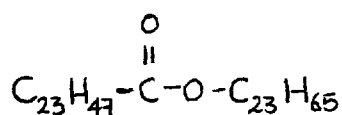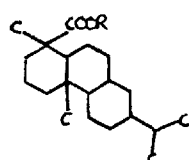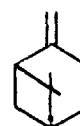
Waxes

Resins

Terpenes

(100)
Fig. 3.2: Coal Precursors.

The response of dead plant matter to microbial and/or abiotic attack depends upon its composition. Plant fats, waxes and resins generally resist microbial degradation, even in strongly aerobic environments they only undergo oxygen-promoted polymerisation. Some pigments also survive for long periods without far-reaching alteration, e.g. chlorophyll intramolecularly rearranges to form a stable porphyrin. However, except in completely stagnant media, where all plant components are substantially preserved, cellulosic material is quickly broken down into simple sugars; lignins are progressively oxidised to complex, variously structured "humic acids" and then to water-soluble benzenoid derivatives; glycosides are hydrolysed to sugars and a variety of aglycons, notably sapogenins and derivatives of hydroquinone; proteins are denatured by random scission of the polypeptide chain and yield ill-defined slimes as well as free amino acids. If the processes are not prematurely interrupted, the plant material is gradually converted to an undifferentiated humus where many of the degradation products have interacted with one another to further alter the residue.

The rate of decay, the mechanisms which operated, and the kinds of residue created depended upon environmental factors. Provided that temperature fluctuations were not so

great as to impede microbial activity, the rates of decay generally increased with temperature. Where the geological environment could neutralize acid decay products by an infusion of dissolved alkaline mineral matter, a higher level of bacterial activity could be maintained than was otherwise the case. Bacterial activity is markedly slowed when the pH falls below 5, and generally ceases altogether at a pH of 3. Fungal activity usually ceases at a pH of 2. Decay mechanisms, however, are principally determined by the accessibility of the debris to oxygen. In substantially dry and fully exposed (i.e. aerobic accumulations) decay proceeds almost entirely by "dry rotting" (i.e. abiotic oxidation) and fungal hydrolysis of the debris; cellulosic material is preferentially destroyed and little true humus is formed. The surviving residue consists mainly of humic acids and their oxidation products, and of woody fragments whose texture resembles that of charcoal. In strongly anaerobic environments, the dominant decay processes are bacterial hydrolysis and reduction of plant matter, the bacteria using the oxygen in the plant matter for their own life processes, and the resultant slimes and gels penetrate and thus preserve other plant entities. Between these two archetypal extremes is a whole spectrum of humid environments in which fungal and bacterial attack on the

plant matter, together with some abiotic attack by enzymes from the plant matter itself, form a whole variety of humic masses.

The humic mass is a good trap for both mineral grains in suspension e.g. clays, quartz, rutile, and cations in solution e.g. Ca^{2+}, Na^+, Mg^{2+}, K^+, and a variety of minor and trace elements. Functional groups in the organic matter fix cations on the carboxyl groups by ion exchange or a chelate coordination complexes with pairs of adjacent functional groups. The organic matter not only fixes minerals but it can change them e.g. organic acids leach potassium fron illite and thus convert it to kaolinite, and iron from ilmenite leaving the TiO_2 mineral anatase. The respiration by roots of living plants rooted in the humus and aerobic bacteria generates CO_2 which can lead to the formation of carbonates which precipitate out of solution. If the water is saline, anaerobic bacteria will reduce the abundant sulphate ion to H_2S, a process that leads to the accumulation of both pyrites and organic sulphur compounds.

Thus while all diagenetic processes tend to homogenise the organic mass, the composition of the mixtures produced depends upon site-specific factors and on the time interval between the onset and termination of decay. The only common

feature of different situations is that increasingly aromatic and acidic residues are produced as time elapses. By the time decay is arrested, carbon contents, based on dry weights, usually increase from 40-45% in fresh debris to >60% in the humus.

The nature of the decay processes also defines the mechanisms that eventually terminate decay and bring about the end of diagenesis. Microbial activity can be assumed to end either when the decaying mass becomes too acidic for bacteria and fungi, or when the mass becomes inundated to depths at which it becomes wholly stagnant. But since the termination of microbial degradation by excessive acidity would not terminate abiotic oxidation, which would continue as long as the residue remains open to the air, complete arrest of decay can only be achieved by flooding to stagnancy levels and subsequent siltation.

If siltation continues so that an appreciable · burden of inorganic sediments is built up over the residue, then the next stage of coal formation, viz. coalification, is initiated.

3.1.4 The Processes of Coalification[15,62]

Once the peat has been buried and microbial agencies have ceased decomposing the plant matter, other processes act upon it to transform it into coal. These agencies are those of heat and pressure. This stage of coal formation is known as <u>metamorphism</u>, and this is the means by which the humic mass matures.

Pressure is caused by the weight of the overbearing strata and also by orogenic earth movements. Pressure alone only modifies certain physical properties e.g. porosity, but it may facilitate certain chemical reactions by maintaining the coal mass under compression. The role pressure plays depends upon the way in which it affects the surrounding strata. If it renders the strata less permeable to the passage of gaseous maturation products, thus making it difficult for them to escape, then metamorphism is retarded. If extensive brecciation of fracturing of the surrounding strata is the result of the action of pressure, the release of gaseous products is facilitated and metamorphism is thus accelerated.

Heat is imparted to the coal mass from at least three different sources:

(1) There is a heat flow from the interior of the Earth to the surface. This causes _geothermal gradients_: as depth increases, the temperature of the strata also increases. These gradients vary from one location to another and range from $<10^\circ Ckm^{-1}$ to $>30^\circ Ckm^{-1}$, and this variation is a direct result of the heterogeneity of the srtucture of the Earths' surface. Rates of chemical reactions are known to be sensitive to changes in temperature, and generally the rates of reaction increase with increasing temperature. A general rule is that for every $10^\circ C$ rise in temperature, the reaction rate doubles. Geological studies have shown that burial of the debris to depths of 1000-2000m is sufficient to raise carbon contents from <60% to as much as 80-85%. This is the basis of Hilts' Rule which states that "in a given borehole, the volatile matter decreases at increasing depth". Thus the lower seams of coal are more mature than those of higher seams and this can be directly related to the geothermal gradients of the Earths' crust. The variation in the gradient from one locale to the next is the cause of the differences in maturation of comparble

coal masses geographiclly separated. This is the most common form of metamorphism and is thus termed <u>normal metamorphism</u>.

(2) The second form of heat input to the metamorphic process comes from localised heat sources such as incursions of magma. This form of metamorphism is described as being <u>regional</u>. The heat from these sources superimposes itself on the geothermal gradient and thus can mature the coals to levels beyond those possible by normal metamorphism. Also to be included in this form of heat imput is the rarer occurrence of metamorphism caused by radioactive emissions rather than by heat. The changes caused by radiation are very different fron those caused by normal or regional metamorphism.

(3) Tectonic forces associated with orogeny cause localized heat sources from frictional or shear stress. These forces have played an important role in coal maturation as very mature coals with carbon contents >85% are rarely found anywhere else except in heavily folded and/or faulted regions

The chemical changes brought about by these metamorphic forces are the stripping of functional groups and condensation reactions. These involve the removal of peripheral substituent groups e.g. -OH, -COOH, -OMe, and

-Me, and, concurrently, the production of condensation products of increasing molecular weight. These processes continue until the coal is mined and, if not interrupted, will continue until anthracites are formed. These processes further homogenise the coal mass, the carbon content increases, first at the expense of its oxygen content and then by abstraction of hydrogen, mainly in the form of methane.

3.1.5 Mineral Matter in Coal[18,61,62]

There is no universally accepted definition of the term "mineral matter"[63]. Some workers restrict the definition to include only discrete mineral grains contained within the coal matrix, others also include all elements except organically bound or organically derived C, H, O, N and S[66].

Most of the mineral matter found in coal is fine-grained. The average diameter for most of the discrete mineral grains is 20μm; few mineral grains exceed 100μm, except for massive deposits of pyrite or marcasite in cleats or fractures.

Coal minerals may be classified according to (1) origin and (2) time of emplacement. Classification may also be made in terms of major, minor and trace relative abundancies of minerals.

1. Origin.

(a) Detrital. These minerals are derived from a source
    external to the peat swamp and are transported to the
    swamp as particulates carried by water or wind. The
    most abundant minerals in coal - clay minerals and
    quartz - are detrital in nature and are introduced into
    the swamp as over-bank deposits of streams in times of
    flood. Thus mineral matter of detrital origin occurs in
    coals which formed close to stream channels. Except in
    exceptional circumstances, detrital matter carried by
    the wind is not a major source of detrital mineral
    matter.

(b) Vegetal. These are minerals formed from the inorganic
    constituents of swamp plants. The inorganics contained
    within the plant depend upon the plant type, the type of
    plant tissue, the climate, and the soil and bedrock
    geology of the site where the plant grew.

    All plants need certain inorganic compounds for
    effective growth and these are preferentially adsorbed
    from the media in which the plant is rooted. Compounds
    of Ca, Mg, Fe, Al, Na, K, Mn, Ti, S, Cl, and P are the

most common inorganic elements found in plants and usually these inorganics make up <2% of the plant substance, although this varies from species to species and between different parts of the same plant. Fe is principally concentrated in the leaves, while the structural components of the plant are rich in Ca, Si and Al. The products of hydrolysis of the proteins, which are found in the plant cells and contain much of the nitrogen and sulphur found in the plant, the amino acids, condense with the products of decay of the compound celluloses and form humic acids. Part of the N and S compounds produced during the decay of the proteins also form inorganic constituents of coal by combining with inorganic acidic or basic constituents of the plants or mingled inorganic matter. During hydrolysis, the P present in the nucleic acids becomes phosphoric acid, which subsequently forms phosphates with any basic constituents of the organic mass. The sap of the plant contains solutions of inorganic compounds, particularly salts of K, Na, Mg, Fe, and Ca, Ca particularly as its oxalte or pectate. The outer bark of trees is rich in Ca, Fe and Si. Mg is a constituent of chlorophyll and the carotenoids.

Most of these inorganic plant constituents remain in the
peat, often in an altered form, after the decay of the
plant material. The only inorganic constituents that do
not appear in the resultant coal are those which are
removed by solution in water, as may be the case with
NaCl, KCl or $MgCl_2$, N from proteins as NH_3, or volatile
S compounds such as H_2S. The fixation of Ca, Mg, Fe and
Al as insoluble salts of humic acids under near neutral
conditions is one of the most important modes of
survival of inorganic constituents. Calcium pectate,
due to its close resemblance to oxycellulose, may form
part of the larger units of the Ca salts of humic acids.
Under alkaline, near neutral or slightly acidic
conditions, Ca can also appear as calcium humate after
decomposition of the pectate. When the pH is <4.5, then
the humic acid is precipitated and Ca appears as the
salt of the stronger acid. Similarly, the appearance of
the humic acid or of its Mg, Al or Fe salts depends upon
the pH of the system and the availability of these
elements as soluble salts. As an altermative, at a pH
>4.5, colloidal complexes of solutions of Fe or Al
hydroxides with solutions of humic acids may form.

The availability of metallic oxides is far too small in plants to allow, appreciable proportions of humic acid salts to be formed without an external input. When soluble salts of bases such as Ca and Mg bicarbonates or basic oxides of Al or Fe are washed into the deposit, the insoluble gels of humic acid, polyglucuronic or polygalacturonic acids are precipitated.

The behaviour of N and S compounds during decay is important in the study of coal formation. N and S are constituents of certain plant proteins that are rapidly hydrolysed by microbial agencies during wet decay. The primary products of hydrolysis of the products are complex amino acids, some of which combine with the degradation products of the compound celluloses to form humic acids, whilst others are decomposed still further to NH_3, H_2S, CO_2, and H_2O. The final behaviour of these compounds depends upon the immediate environmental conditions of the deposit. NH_3 may combine with any acids in the system and thus ultimately appears as part of either the organic or the inorganic constituents of the coal. If the deposit is shallow and well aerated with frequent changes of water, NH_3 may escape and be washed away in the ground-water. H_2S reacts with suitable metallic salts according to the conditions; in

almost neutral conditions it reacts with Fe to produce iron sulphides, which may, in time, be transformed into nodules or lenses of pyrite or marcasite.

(c) Chemical. These are minerals formed by direct chemical precipitation from solution or from chemical reactions between the solutions and the organic or inorganic materials already present in the plant debris. A range of sources exists for the dissolved ions. One source is external to the swamp: the weathering of rocks in the surrounding land and the subsequent transportation to the swamp by water movement. A second source is the release of inorganics from decaying plant matter the ions come from plant mineral matter, or water-soluble compounds within the plant tissue, or from the breaking of organometallic bonds during decomposition. Dissolved ions are also released from the plant matter during coalification as fundamental changes in the organic structure take place.

2. Time of Emplacement.

(a) Syngenetic stage[67]. This includes minerals incorporated into the coal from the very earliest peat formation to the earliest metamorphic stage, just before the formation of lignite. Thus, most minerals in coal are syngenetic.

(b) Epigenetic stage. The development of major fractures throughout the coal during coalification allows the movement of ground-water solutions of ions through the coal bed. Minerals may then be precipitated out of solution and into the coal. The most common epigenetic minerals are carbonates, pyrite and kaolinite. Calcite is the dominant carbonate, although dolomite is not uncommon.

Figure 3.3 shows the common types of minerals found in coal.

The following table shows the minerals found in coal:-

Mineral	Formula
kaolinite	$Al_2Si_2O_5(OH)_4$
illite	–
mixed layer	–
chlorite	$(MgFeAl)_6(SiAl)_4O_{10}(OH)_8$
quartz	SiO_2
calcite	$CaCO_3$
dolomite	$CaMg(CO_3)_2$
ankerite	$Ca(FeMg)CO_3$
siderite	$FeCO_3$
pyrite	FeS_2 cubic
marcasite	FeS_2 orthothambic
coquimbite	$Fe_2(SO_4)_3 \cdot 9H_2O$
szmokite	$FeSO_4 \cdot H_2O$
gypsum	$CaSO_4 \cdot 2H_2O$
bassamite	$CaSO_4 \cdot \frac{1}{2}H_2O$
anhydrite	$CaSO_4$
jarosite	$KFe_3(SO_4)_2(OH)_6$
plagiodase	$(NaCa)Al(AlSi)Si_2O_8$
orthodase	$KAlSi_3O_8$
sphalerite	ZnS
galena	PbS
pyrrhotite	FeS

Groupings (right side of table): clay minerals, silicates, carbonates, disulphides, sulphates, feldspars, sulphides — classified as Major, Minor, Trace.

Fig. 3.3: Minerals Found in Coal. [67]

3.2 THE GEOLOGY OF THE SOUTH WALES COALFIELD[68]

3.2.1 Geologic History.

The coals found in South Wales date to the Carboniferous period of geologic history. The strata below the coal seams are formed of Carboniferous Limestone, which were formed from relatively pure, shallow-water marine sediments and are richly fossiliferous. In Upper Carboniferous times, these limestones diminished in importance and were replaced by terrigenous grits, sandstones and shales, and these sediments were deposited under mainly marine conditions and formed the Millstone Grit series of strata. The Coal Measures, however, are almost without marine fossils and show every sign of being the deposits of fresh or brackish water in deltas or swamps, in which peats, formed from the debris of forest growths, were recurrent and were eventually lithified to form coal seams.

Before the end of Palaeozioc times, the region was affected by the powerful earth movements of the Hercynnian Orogeny and was uplifted and intensely folded to form corrugated mountain ranges. When these movements died down, a cycle of erosion, submergence, and sedimentation occurred.

Fig. 3.4: Simplified Geology Map of South Wales. (68)
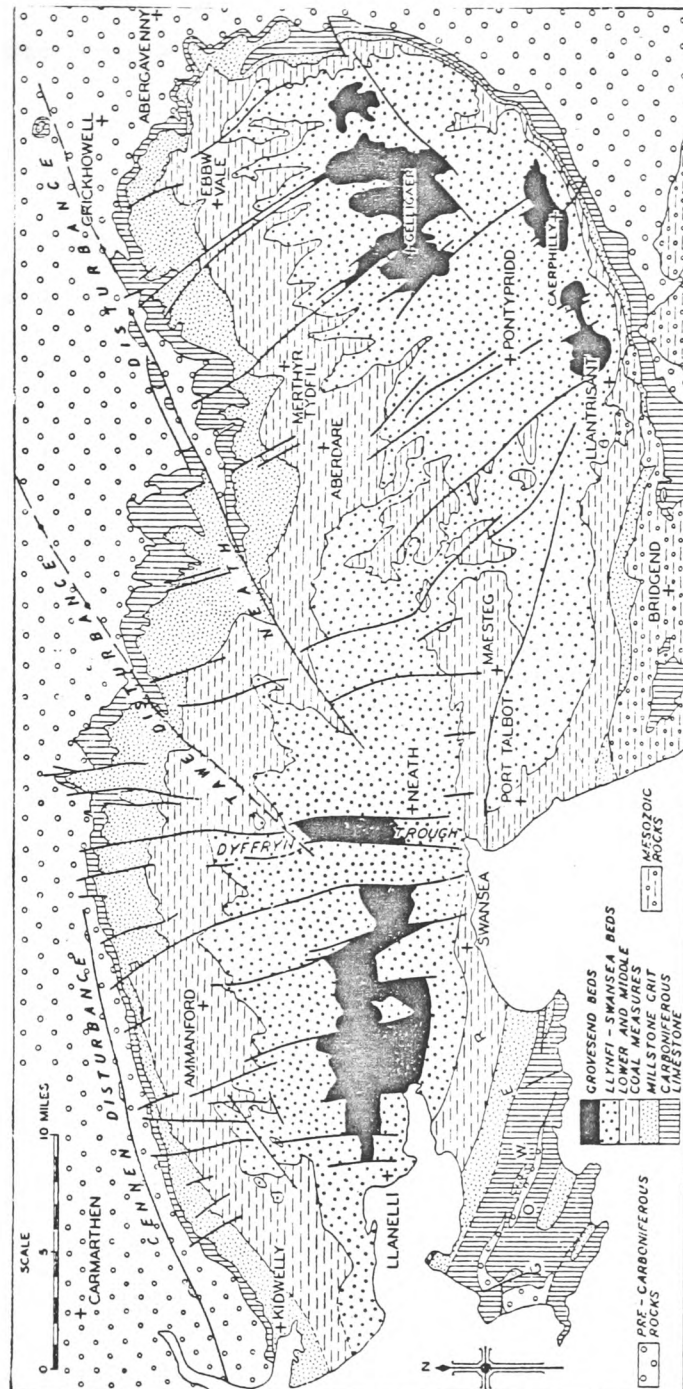
Fig. 3.5: The Geology of the South Wales Coalfield.[68]

3.2.2 The Structure of the Coal Measures.

As a result of repeated regional compression, all the solid rocks in South Wales are folded into anticlines and synclines which are broken by thrusts and faults. The oldest rocks display the greatest deformation, both in the sharpness of folding and the magnitude of fracture.

(a) Lithology.

The South Wales coal measures consist almost entirely of terrigenous detritus derived from nearby sources and carried into a shallow subsiding trough of sedimentation by rivers from a land mass lying mainly to the north of the coalfield. The deposits appear to have been laid down under estuarine or fresh-water conditions as alluvial muds or sands, swamp clays, and delta fans/aprons; the coarser layers are often cross-bedded in lenticular units; channeled washouts are common. Marine beds are few and thin and are restricted to the lower part of the sequence. The region throughout the period of accumulation of the local measures appears to never have been at any great height above sea-level, or to have been isolated as a land-locked basin, and the sediments are paralic in nature. The recurrent coal seams were formed as thick beds of water-logged peaty humus in swamps and

marshes supporting luxuriant vegetation, through which tributaries and distributaries of large rivers meandered.

Sedimentation of the Coal Measures occurred in rhythmic cycles called cyclotherms. In each typical cyclotherm, a coal seam, formed very near the water level as a thick and dense peat, is succeeded by a fine grained shale or an impure limestone with fossils, as a sign of sharp subsidence and of a marine incursion of the influence of one. There follow shales of increasingly shallow-water and non-marine character, with a fauna of mussels, and these gradually pass upwards into sandy shales, sandstones, and sometimes grits and conglomerates. The close of the cycle is marked by very shallow muds, now converted to underclays and rootlet beds by the growth of forests on them. These are overlain by a coal seam which marks the begining of the next cyclotherm. Usually, the full cyclotherm is not represented, with one or more elements omitted. Also, there is not a constant regularity in the thickness of the elements.

It is found that the coal measures can be grouped as follows:

(3) The Upper Coal Series or Supra-Pennant Series - predominantly shales

(2) The Pennant Series - predominantly sandstones of which the massive Pennant sandstone is the main formation

(1) The Lower Coal Series - predominantly shales.

(b) The Lower and Middle Coal Measures.

The shales of the lower part of the coal measures outcrop at the foot of the "Pennant" escarpment around the coalfield. They also emerge in the core of the Maesteg anticline, and appear in the floors of some of the deeply entrenched valleys of the Rhondda. They consist for the most part of a monotonous series of grey, blue and black pyritous and micaceous shales which are often imperfectly laminated. Some of the beds are highly carbonaceous and pass into a cannel shale or coal. Usually there is only minor development of sandstones. These measures contain the greatest number, the thickest, and the most important coal seams in South Wales.

A feature of the measures, particularly of the lower part, is the abundance of iron ore occuring in ironstone bands. There is an increase in the quantity but a decrease in the quality of the ore as the ironstone bands are followed westwards and south-westwards.

At maximum, the thickness of the Lower and Middle Coal Measures reaches some 3000ft in the Swansea district, but it diminishes as the group is traced towards the north-east and north. In the Maesteg district it is about 2100ft, near Merthyr Tydfil and in the south-east near Cardiff it is 1400ft. In the Pontypool district around Abertillery, the thickness is less than 800ft.

(c) The Upper Coal Measures.

Over most of the coal field there is a clear line division, both lithological and topographical, between the soft shales of the Middle Coal Measures and the massive sandstones of the Upper Measures.

Typically, the Pennant measures include thick, massive sandstones and grits. When un weathered, the sandstones are bluish-grey, but rapidly become rusty brown on exposure. Many bands are strongly cross-bedded, which indicates that

they were deposited close to a land mass which was being eroded by fast and powerful streams. Some of the beds are coarse grained and may be conglomeratic.

The Pennant Measures exceed 5000ft in thickness in the western part of the coalfield about Swansea. They are reduced to about 3500ft in the Duffryn Trough near Neath, and to about 2000ft in the Llantwit Syncline.

3.2.3 The Coals of South Wales.

Although coal seams account for <2% of the total thickness of the measures, they are economically the most important beds. The coals vary considerably in their properties and potential uses, generally they fall into three main types: bituminous coals, steam coals, and anthracites. Though these kinds are readily distingiushed in typical samples, they grade into one another and precise definition rests on fine chemical differences.

There is a two-fold systematic lithological variation in the development of coal rank across the South Wales Coalfield. On the one hand, in accordance with Hilt's Law, the lower seams in the sequence at any one locality tend to be of higher rank than the other seams, anthracites are rare in the Upper Measures. On the other hand, any one coal seam tends to become progressively higher in rank as it is followed towards the north, north-west and west. Thus bituminous coals are usually found along the southern and eastern outcrops, the steam coals in the central part of the coalfield between the Taff and Neath valleys, and the anthracites along the north crop westwards from the Neath valley.

These changes are not due to changes in the composition of the plants which made up the original peat. Trotter[69,70,71] argued that the increase in rank is due to shearing stresses correlated with the thrust plane which outcrops as the Careg Cennen disturbance on the north crop and which is believed to sink to depths southwards underneath the coal field. Thus, the rank of a coal is dependent upon its distance from the thrust plane.

3.3 Coal Structure.

The structure of coal is still only guessed at, although generalizations can be made and models can be constructed which are consistent with various aspects of coal behaviour. This vagueness is due to coal being an extremely complex substance: coal began its existence as a complex mass of plant matter which experienced an enormous number of chemical and physical changes. Some general aspects of coal structure are useful in aiding the understanding the nature of coal reactivity, but much more information must be obtained about both the physical and chemical structure before any realistic structure-reactivity relationships can be formulated.

3.3.1 Physical Structure.

Coal is a high surface area, extremely porous material, which can act as a molecular sieve[81]. Coal surface areas may be measured by gas adsorption, mercury porosimetry, or pyonometry[72].

Pyonometry measures the pore volume by first outgassing the sample in a vacuum and then measuring the volume of liquid required to fill all the pores greater than a known minimum pore diameter. By using a range of fluids, such as He, Hg, MeOH, and C_6H_{14}, a rough pore size distribution can be estimated.

Mercury porosimetry allows the determination of the total pore volume and the pore volume distribution. Mercury is forced into the coal pores at high pressures. By varying these pressures(1-1000atm.), the pore size in the range 10^1-10^4 nm can be examined. A hazard of this and the previous method is that molecular sieve effects may cause blind pores to be incorrectly measured.

The determination of adsorption isotherms allows the direct measurement of surface areas and surface area distribution. The amount of gas physically adsorbed upon a surface can be related to the pressure at a given temperature by the use of the BET[73] or the Dubinin-Polayni[74] adsorption isotherms. By calculating the amount of gas adsorbed in the first monolayer, the surface area can be determined. Kinetic theory predicts that higher temperatures will allow

penetration to smaller pores; thus, by varying both temperature and pressure, pores in the size range 1-40nm can be investigated.

Adsorption techniques can also be used to investigate the molecular sieve effect[77-80]. Both polar and non-polar gases are used; CO_2 at 298K and N_2 at 78K are most commonly used. Usually non-polar gases give significantly lower surface areas than polar gases: the surface area given by N_2 is lower than that given by CO_2 and this is a result of the molecular sieve effect. N_2 cannot penetrate capillaries with a diameter less than 0.5nm. This is due partly to the low temperatures necessary for the use of N_2 which results in the diffusion rate of the gas being so slow that in the course of experimental measurements not enough time is available for it to fill the blind pores. In the case of CO_2, polar interactions between the gas molecules and the coal substance allow the gas to migrate through the capillaries[77,80]. Figures 3.6 and 3.7 illustrate the porous nature of coal.
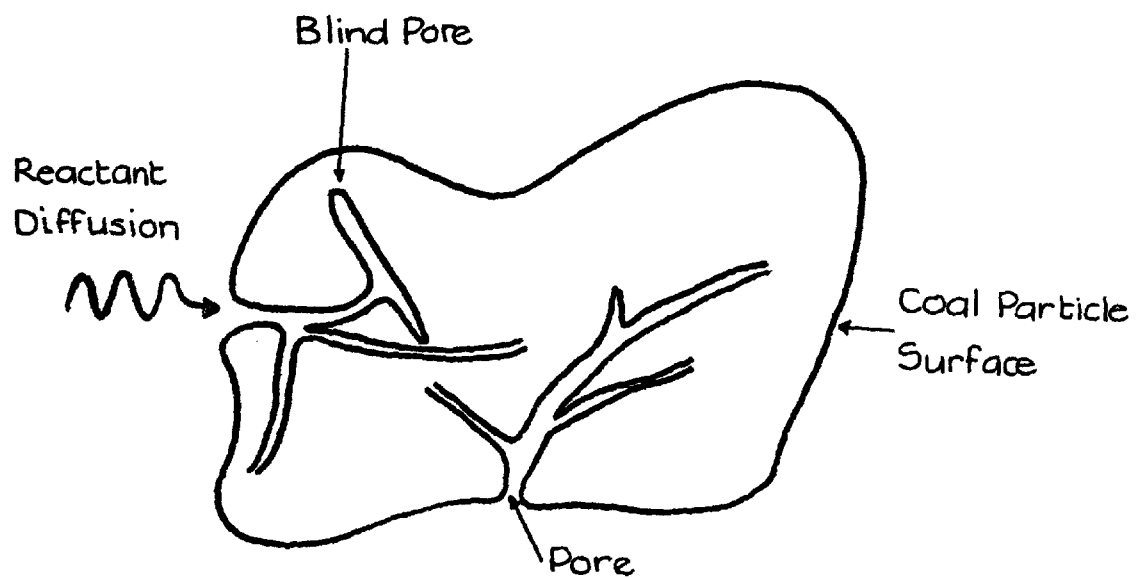
Fig. 3.6: The Physical Structure of a Coal Particle[72]
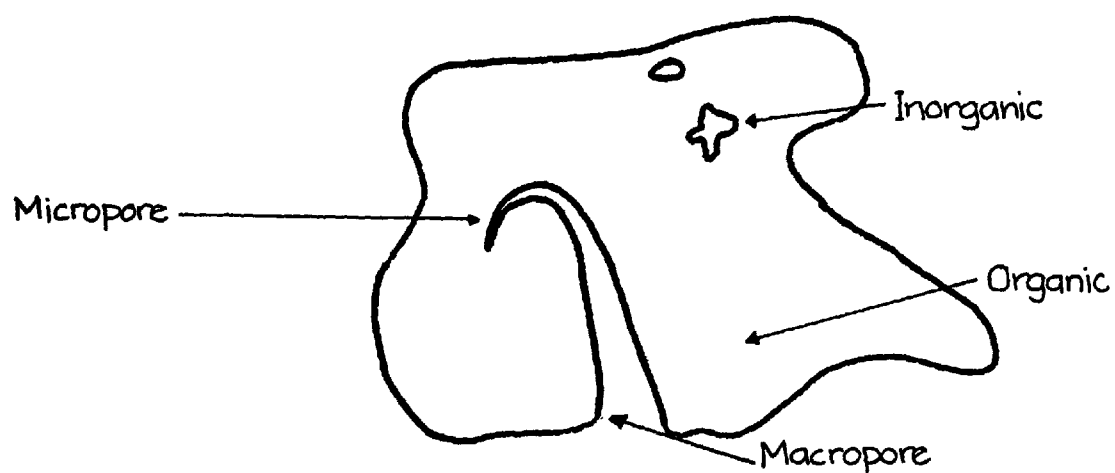
Fig. 3.7: Coal Structure[81]

The coal pore structure is usually classified by considering three broad size ranges[74]:

(1) micropores of diameter <2nm

(2) mesopores of diameter 2-50nm

(3) macropores of diameter >50nm

This classification suggests cylindrical pores, but X-ray studies[82] have shown that pores can be cylindrical, conical, flat, or a combination of these three qualities, especially in small interstices, in shape. Thus the concept of pore diameter only approximates the overall pore structure. It was found by Gan et.al.[83] that macropores are dominant in the lower rank coals, high rank coals contain mainly micropores, and in the case of middle rank coals mesopores predominate. Zweitering and Van Krevelen[84] believed the porous structure of coal to consist of a wide distribution of macropores which were believed to be due to cracks in the coal material. The surface area of these cracks was thought to be in the range $1-2m^2g^{-1}$. They also believed that coal had a system of very fine micropores with a surface area of $100m^2g^{-1}$.

The porous nature of coal arises from cross-links that exist between the aromatic and hydroaromatic "lamellae" and the heteroatom functional groups at their periphery. Hirsch[85,86], from an exhaustive X-ray study, developed a model of coal porosity which consisted of three different types of structure that could be found in a wide range of coals. These are shown in figure 3.8.

This porous structure causes coal to act as a molecular sieve and this greatly influences coal behaviour during the mining, preparation, and utilization of coals[87]. During mining, the pore size distribution determines the ease of diffusion of methane out of the pores. In the liquefaction and gasification conversion processes and in the use of metallurgical coke, chemical reactions occur between gases (or liquids) and coal surfaces, much of which is located within the pore system. Product molecules must be able to escape quickly enough from the pores to allow access of fresh reactants.

Cross Links (1) OPEN STRUCTURE. Characteristic of low rank coals in the range upto 85% carbon. Coals in this range are highly porous; the lamellae are connected by cross-links and are more or less randomly orientated in all directions.

Pores

layers

Amorphous Material

Group of layers

(2) LIQUID STRUCTURE. This structure is typical of bituminous coals in the range 85-91%C. The number of cross-links has decreased considerably and the lamellae show some orientation with the formation of crystallites consisting of two or more of these lamellae. Almost no pores are present.

Single layer and amorphous material

(3) ANTHRACITIC STRUCTURE. This structure is common in higher rank coals with a carbon content >91%. In this structure the degree of orientation of the lamellae with regard to one another has increased greatly and the cross-links have disappeared. As a result, high porosity is observed.

Pores

Fig. 3.8: Coal Structure According to Hirsch[85]

3.3.2 Chemical Structure.

In the search to gain insight into the chemical structure of coal, past reasearchers have attempted to break coal down into recognisable units which are then identified and then pieced back together again[12]. The most common technique used is that of oxidative degradation, with the use of oxidants such as HNO_3, $K_2Cr_2O_7/HNO_3$, $KMnO_4/OH^-$, $BuOOH/AlBN$, and peracetic acid. Using these methods, various researchers have concluded that coal is predominantly aromatic, and contains many condensed rings[65,66,67]. Other workers, by using $NaOCl/OH^-$, have reached a different conclusion and maintain that coal contains a large amount of quaternary aliphatic carbon, in other words, is diamond like in structure and contains 50% aromatic carbon or less[70].
All the above methods selectively oxidise the aliphatic portion of the coal molecule, but by using trifluoroacetic acid/hydrogen peroxide, the aromatic portions may be selectively oxidised. Little work has been done using this method, and conclusive results have not yet been drawn.

Because of the difficulties in piecing together the fragmented products of coal, a number of workers have attempted direct characterization of coal structure. The opacity of coal and its insolubility present major problems

in the use of direct methods. In the past, techniques such as X-ray scattering have been used and conflicting interpretations of the dominant structure of coal have resulted. Hirsch[69] first reported that coal was from 50-80% aromatic with primarily 89% ordered structure. Later, Ergun and Tiensuu[71,72], also using X-ray scattering, concluded that coal could not be polyaromatic and contained large amounts of amorphous regions. Friedel and Quiesler[73], using UV techniques, interpreted their results as showing that coal could not be polyaromatic and contained large amounts of aliphatic structures. Given and Peover[74], who characterized coal extracts by polarographic reduction, concluded that low rank coals contain >20% and high coals >50% aromatic structures, with polycyclic rings prevailing.

Thus polycyclic [58,68,81] aromatic structures are the fundamental structures of coal and form the backbone of the coal substance; they can be assumed to be represented as naphthalene units. Hydroaromatic and aliphatic structures account for much of the hydrogen in coal. The predominant functional groups are those containing oxygen. Specifically these include phenols, alcohols, carboxylic acids, carbonyls; lower ranked coals may also contain ethers, quinones, methoxy, and heterocyclic oxygen. Correlations

between the dry-ash-free carbon content of coals and the content of various functional groups have been noted[75-77].

The following table (fig. 3.9) shows the fundamental functional group distribution for different ranks of coal:

Coal	no. 10C aromatic rings	mol. wt.	Empirical Formula				No. of Functional Grps.				
			C	H	O	N	-COOH	-OH	-O-	>=O	-OMe
Lignite	1.7	513	30	28	7.4	.5	1.5	2.8	.8	.5	.2
Sub-bit.	2.0	461	30	24	4.4	.5	.6	1.8	1.1	.3	.1
Bituminous	2.3	419	30	22	1.9	.4	0	.9	.9	.1	0

Note: The ether contents were calculated by difference and thus include any undetermined oxugen functionality.   The figures in fig. 3.9 refer to the average number of aromatic rings and functional groups per average molecular unit of 30 carbon atoms.

Fig. 3.9 [95-99]

Note: No. 10C Aromatic Rings refers to the number of 10 carbon aromatic groups ie, naphthalene groups.

It can be seen that methoxyl and carboxyl carbon functionalities are of little importance in coals with >80% carbon content.

Sulphur and nitrogen occur as substituted aromatics or heterocyclics. Sulphur may appear in organic or inorganic structures within the coal. The major inorganic form is pyrite. The predominant organic sulphur functional groups are thiols, sulphides, and heterocyclic rings such as pyridine or pyrrole derivatives.

Since coal rank is a measure of the approach of coal to pure graphitic structure, increasing rank implies a loss of aliphatic and hydroaromatic forms. Hirsch's[93,94] X-ray scattering work has shown that the number of carbon atoms or aromatic rings per ordered cluster increases with rank. The implication here is that higher ranks are associated with lamellae orientation and hence reduced porosity.

Mazumdar et.al.[105,106] have shown that carbon atoms in most coals are destributed approximately as follows:

    75% aromatic

    17% hydroaromatic

    8% aliphatic

During carbonization, it is believed, aromatic carbon is primarily responsible for char formation, hydroaromatic carbon for tar formation, and aliphatic carbon for CH_4, CO_2, and CO.

Hayatsu et.al.[107] isolated the organic constituents of a lignite, a bituminous and an anthracite coal by vacuum distillation and solvent extraction. From the results, the authors demonstrated that as coalification progresses the aromatic charactier of the coal increases with rings fusing and becoming cross-linked. They also found that sulphur had not yet been incorporated into stable aromatics in lignites.

Below are given some of the structures that have been found in coal extracts.

polynuclear aromatic   arenes   substitued aromatics

hydroaromatics   methylene bridge   heterocyclics
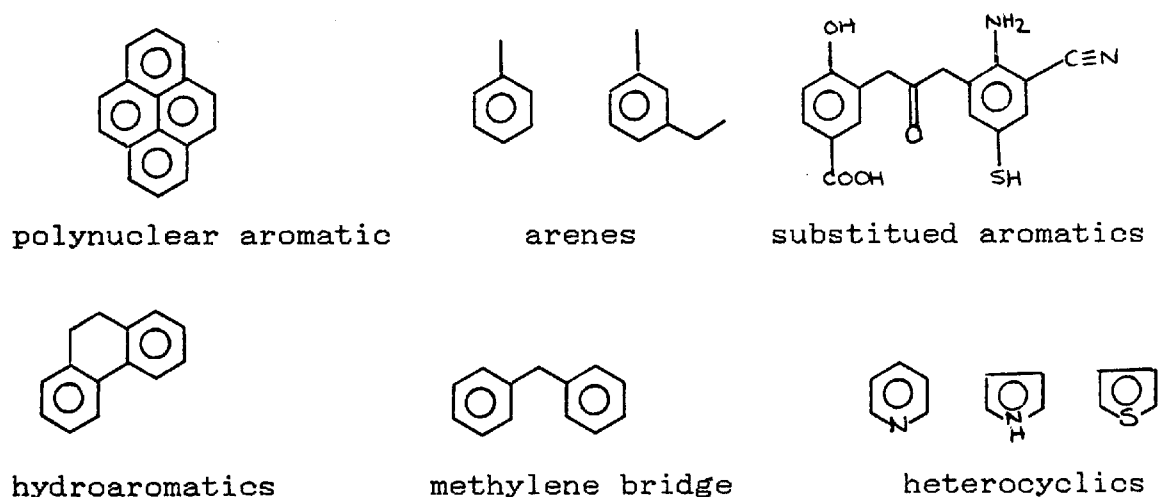
Fig. 3.10: Structures of Some Coal Extracts.[62]

Models of coal structure have been based upon these structures.

Fuchs and Sandhoff[103] pictured the molecular frame-work of coal as shown in fig. 3.11. Their structure was based upon Lowry's[103] view that coal could be envisaged as a "chicken-wire" type of 3-dimensional network with the atoms held together by covalent forces over very large atomic areas.
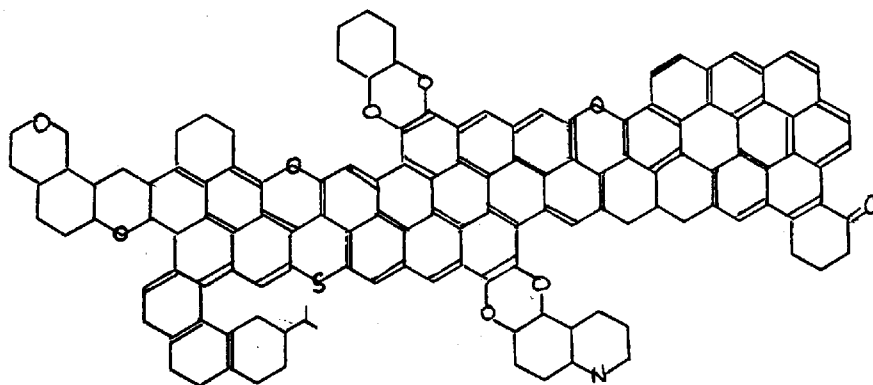
Fig. 3.11: Coal Structure Model According to Fuchs and Sandhoff[103]

Given's structure[101] was one of the first models to be formulated and, for many years, it was the major model. It illustrates the types of structures that a bituminous coal could be constructed from.
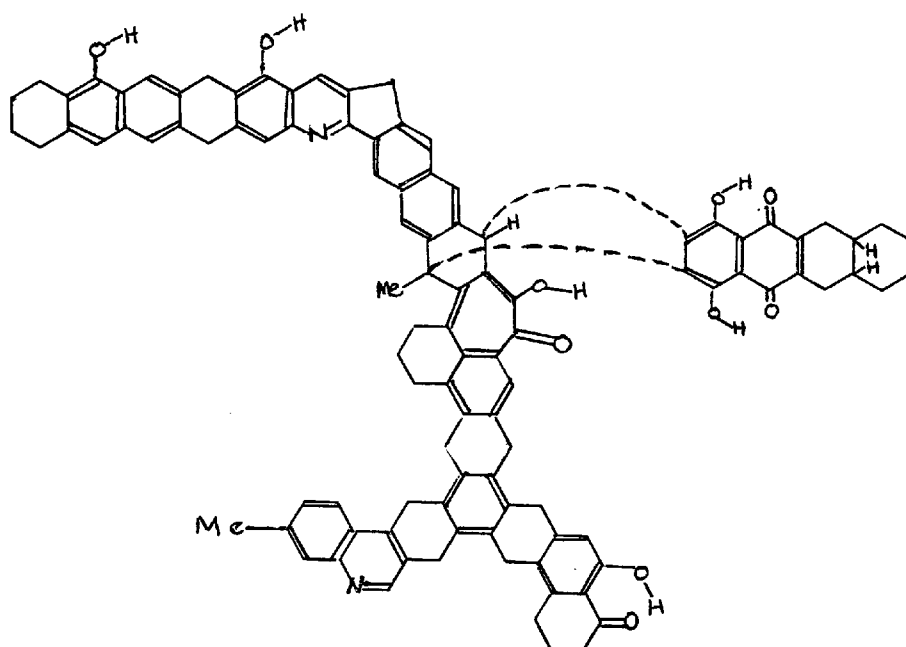
Fig. 3.12: Model of Coal Structure According to Given[101]

This model is consistent with coal's elemental composition, its highly subsituted, but not highly condensed, aromatics, and with the functionalities known to be present in coal.

Given's model has now been superceded by a model presented by Wiser[104] which illustrates the structures believed to be present in a typical bituminous coal. The model consists of a series of hydroaromatic clusters containing an average of 2-5 rings per cluster and joined by methylene , ether, and sulphide linkages which are 1-3 carbon atoms in length[45,101,104]. This arrangement promotes a complex, interlocking molecular structure, similar to many organic polymers. Since the clusters are only loosely connected by aliphatic linkages, clusters will appear on various planes and thus cross-linking and developments of an extensive pore structure are favoured. Aliphatic, hydroaromatic, and heterocyclic bonds are more susceptible to bond cleavage[101] and thus during any heat treatment these structures bear the heaviest responsisbility for devolatilization. Wiser's structure (as shown in fig. 4.13) gives a comprehensive overall picture, but it does contain flaws, e.g. the spatial distribution of any functional group is not known. There are a number of weak bonds which can account for the breakup of coal into smaller fragments by the action of heat.
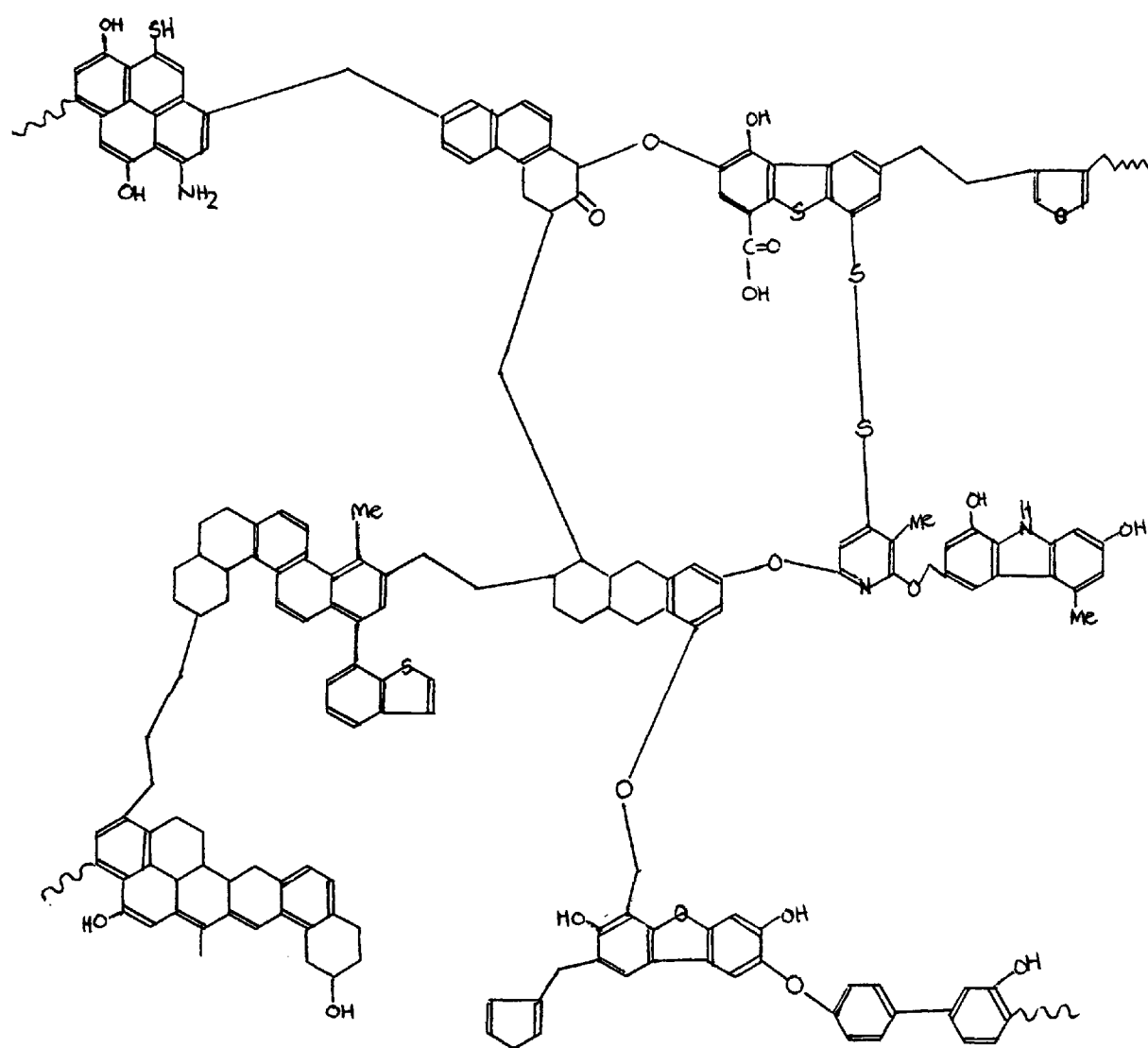
Fig. 3.13: Wiser's Structural Model of Coal.

Wender et.al.[108] proposed a model of the chemical srtucture of coal. The basic unit of the structure is $CH_{0.77}O_{0.07}N_{0.01}S_{0.01}$ and is based upon a high volatile bituminous coal with 83%C by weight.
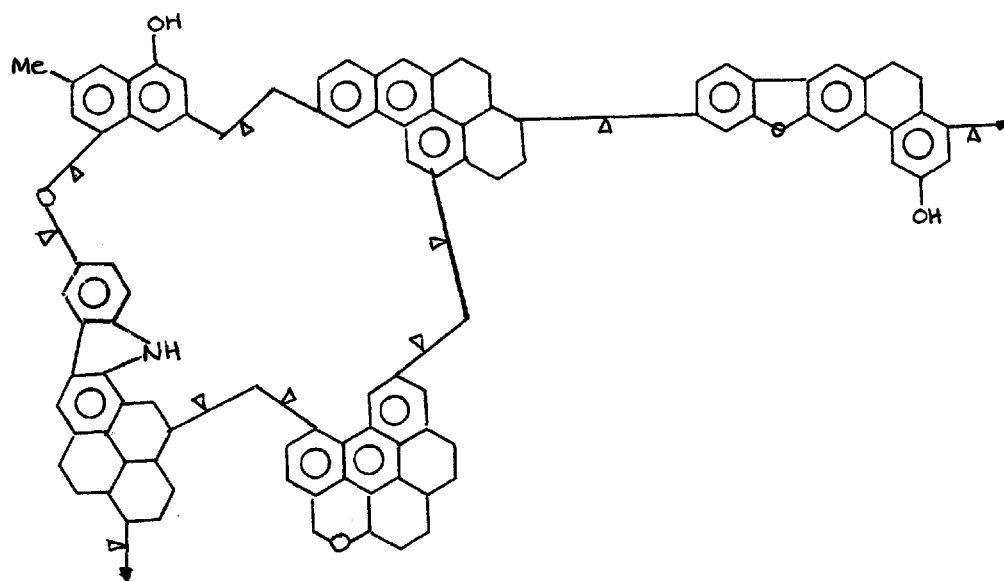
⟶ linkage of the molecular model to the rest of the coal structure

▷ weak chemical bond

Fig. 3.14: Structural Model of Coal According to Wender[108]

3.4 COAL PYROLYSIS[18,62,107,110].

The chemical and physical changes that take place when coal
is subjected to the action of heat in an inert atmosphere
are of great importance in studies of coal behaviour and in
coal technologies. Coals, due to their metamorphic mode of
genesis, would be expected to be resistant to thermal change
and there is very little evidence to indicate the occurence
of structural changes below temperatures at which pyrolytic
breakdown occurs[107]. During pyrolytic breakdown, samples
of some, but by no means all, coals melt, and this melting
is accompanied by rapid evolution of volatile organic
degradation products. Water, tar, and various gases diffuse
out of the sample particles and the melted sample
resolidifies to leave a solid residue known as a coke. If
the sample does not melt, then the residue is called a char.
The composition and properties of this residue vary in
direct relation to the heat treatment temperature if the
decomposition is carried out isothermally[62]. If the
temperature is increased to around 2200°C, the residue
becomes almost pure carbon with all the essential
characteristics of microcrystalline graphite.

Despite devolatilization being a continuous process, distinctions can be made between volatile matter lost during the softening stage - primary gases - and those lost after this stage - secondary gases. Primary degasification occurs in the temperature range 350-500°C, and secondary degasification begins around 700°C.

Lack of knowledge about the structure of coal means that any mechanism of thermal decomposition is highly speculative. Nevertheless, such mechanisms are worthwhile as they provide numerous suggestions for futher research. One common characteristic of all mild, degradative reactions upon coal is the production of a series of fragments differing significantly in molecular size, but usually showing closely related chemical properties.

3.4.1 Physical Changes.

When heated in an inert atmosphere to about 350-450°C, particles of certain coals soften and become deformable. These are characteristics attributable to thermoplastic substances. Coals exhibiting this property are termed plastic coals, and occur in the rank range of 85-92%C. The lack of softening characteristics in coals of a lower rank results in the formation of an incoherent char; in higher rank coals, few gaseous products are produced and the residue is little different from the original sample. When a caking coal is heated at a constant rate, the rate of devolatilization and the fluidity of the sample both reach their maximum at about the same temperature. This is the reason for the formation of a coke. For lower ranked coals, these two maxima do not occur close enough together and if caking does occur only a weakly coherent mass is formed.

Pyrolytic decomposition of the coal sample in the 350-450°C range of temperature results in the formation of volatile gases within the plastic particles, which leads to vacuole development and swelling. Because the particles of such coals are essentially viscous liquids in their plastic state, they can coalesce or agglomerate to form an

indivisible mass or "cake", thus plastic coals are commonly referred to as caking coals. As a result of successive chemical reactions and loss of volatile compounds, the plastic state is a transient phenomenon even under isothermal conditions.

Chermin and Van Krevelen[114] proposed a mechanism to explain the phenomenon for coal plasticity. They proceed from a supposition that coal decomposition can be separated into 3 stages:

1. formation fo an unstable intermediate phase that is partly responsible for plasticization, the intermediate being termed metaplast
2. the transformation of metaplast into semi-coke
3. the formation of coke from semi-coke.

The reaction of the metaplast to give semi-coke describes the resolidification of the plastic system and the evolution of gas causes the sample to swell.

Another theory to explain plasticity, known as the Partial Melting Theory[114-116], involves the concept of coal iso-colloids. It assumes that the smallest molecules in the coal substance become mobile on heating and act as plasticizers for the whole substance. Closely related to

this is the view that softening is due to the plasticizing of colloidal particles by surface films[117,118]. Great importance is placed on the physical structure of coal in this hypothesis and the swelling of the sample should be ascribed to the internal pore structure of the original coal.

The Thermobitumen Theory[117] postulates that the plastic behaviour of coal is due only to the fomation of a liquid primary product of pyrolysis.

All of these theories propose that the softening of coal is due to the plasticizing of the coal macromolecule (the colloidal system) and the plasticizing agent is formed either from the coal fragments of low molecular weight, or from primary decomposition products.

Orechkin[111] visualized the transformation of coal into a liqud phase by pyrolysis as being based on reducing polymerization i.e. the degradation of the macromolecules of humic matter by the cleavage of weak C-O bonds which join the carbon complexes composing the structural elements of coal. It was suggested that the primary stages of thermal decomposition can be represented by two interrelated processes:

1. reducing depolymerization which results in the isolation of complexes, a decrease in average molecular weight, and transformation into liquid or low-melting material

2. a reverse process which consists of the remaining oxygen
   being liberated
   in the form of water with a simultaneous condensation of the carbon complexes. A growth of the carbon skeletons and a loss of fusibility results.

For an ideal case, Neavel[110] gave the following description of coal plasticization:

1. General mobility of micellar units (packets of aligned aromatic lamellae) begins around 350-450°C as weak Van der Waals forces and hydrogen bonds become weakened. This process is described as physical melting. Some cleavage of covalent bonds, especially etheric bonds, may be involved.

2. Viscosity progressively decreases as the mean molecular size is reduced at a rate which reflects the thermal rupture of covalent bonds which bridge stable molecular units, but only as long as the free radicals thus produced are stabalized by donatable hydroaromatic hydrogen.

3. As the limited donor hydrogen inventory becomes consumed through the transfer of hydrogen and the loss of volatile, hydrogen-rich species, free radicals, which continue to be formed, are stabilized by repolymerization. Viscosity, having reached a minimum, progressively increases as the molecular weight of the redidual materials increases.

4. Repolymerization becomes the dominant fate of free radicals and resolidification occurs.

Three properties of coal seem to be necessary for plastic development:

1. lamellae bridging systems that can be thermally cleaved

2. an indigenous supply of hydroaromatic hydrogen

3. an intrinsic capability of micelles and lamellae to become mobile independently of significant bond rupture.

Changes also take place in the pore structure of the coal on heating. Hays et.al.[135] found that coke pre structure is determined largely during the plastic range and that the process could be divided into four stages.:

1. pore nucleation within larger particles

2. intraparticulate pore growth, the consequent swelling leading to the coalescence of particles when the interparticulate voids are completely filled

3. post-coalescence pore growth to maximum size

4. a decrease in pore size resulting in compaction of the structure near the resolidification temperature

If the mass of gas formed within a particle is greater than that able to escape by diffusion, the resulting internal pressure is capable of pore formation provided that the particle is sufficiently plastic.

Complete coalescence occurs when pore growth causes the swelling of individual particles to completely fill the interparticulate voids. This does not imply that swelling rather than softening is the principal force for coalescence since pore growth is dependent upon both the amount of volatile matter within the pores and the surface tension which might be expected to decrease as fluidity increases. For coalescence to occur the new pore volume must exceed the original pore volume.

After coalescence has occurred, the pore volume rises to a maximum value. This then decreases during resolidification as the highly porous zone is converted to a denser solid.

3.4.2 Chemical Changes.[62]

Generally, the decomposition of coal can be divided into 3 stages. The first stage starts well below 200°C and the decomposition is fairly slow with the release of small quantities of "chemically combined" water from the coal matrix, oxides of carbon, and dihydrogen sulphide. These products result from the detachment of substituent functional groups e.g.
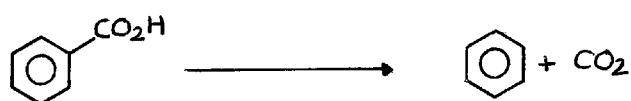
and from limited condensation reactions e.g.
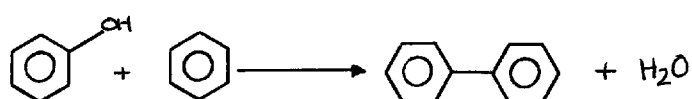
Above 200°C some benzylic carbon begins to isomerise to form methylphenyl derivatives and traces of alkylbenzenes are evolved. These low temperature processes alter the original structure of the coal enough to influence its subsequent thermal behaviour. Preheating[62] at about 200°C tends to destroy any caking properties the coal might possess.

The second stage, sometimes termed active decomposition, begins between 350 and 400°C and ends around 550°C. The maximum rate of weight loss occurs within this region and the temperature at which it occurs is closely related to the rank of the coal. Generally, about 75% of the total volatile yield, including tar and all lighter, condensable hydrocarbons, is evolved in this temperature region. The actual product composition, including that of the solid residue, is dependent upon the ambient conditions caused by factors such as pressure and heating rate. This is attributable to the fact that active decomposition involves extensive fragmentation of the coal molecule and concurrent random recombination of the free radicals thus formed. This stage also contains the region of plasticity found in coking coals.

The final stage of decomposition is termed secondary degasification and is characterized by the gradual elimination of heteroatoms, principally H and O, and ends only when the char is transformed into a graphitic solid. In practice, the composition and quantity of volatile matter released above 800-850°C is of such little interest that pyrolytic studies are not usually carried beyond 900-1000°C. The principal products of this decomposition stage are water, oxides of carbon, hydrogen, methane, and traces of

C$_2$-hydrocarbons. Its most important feature is the progressive aromatization of the char.
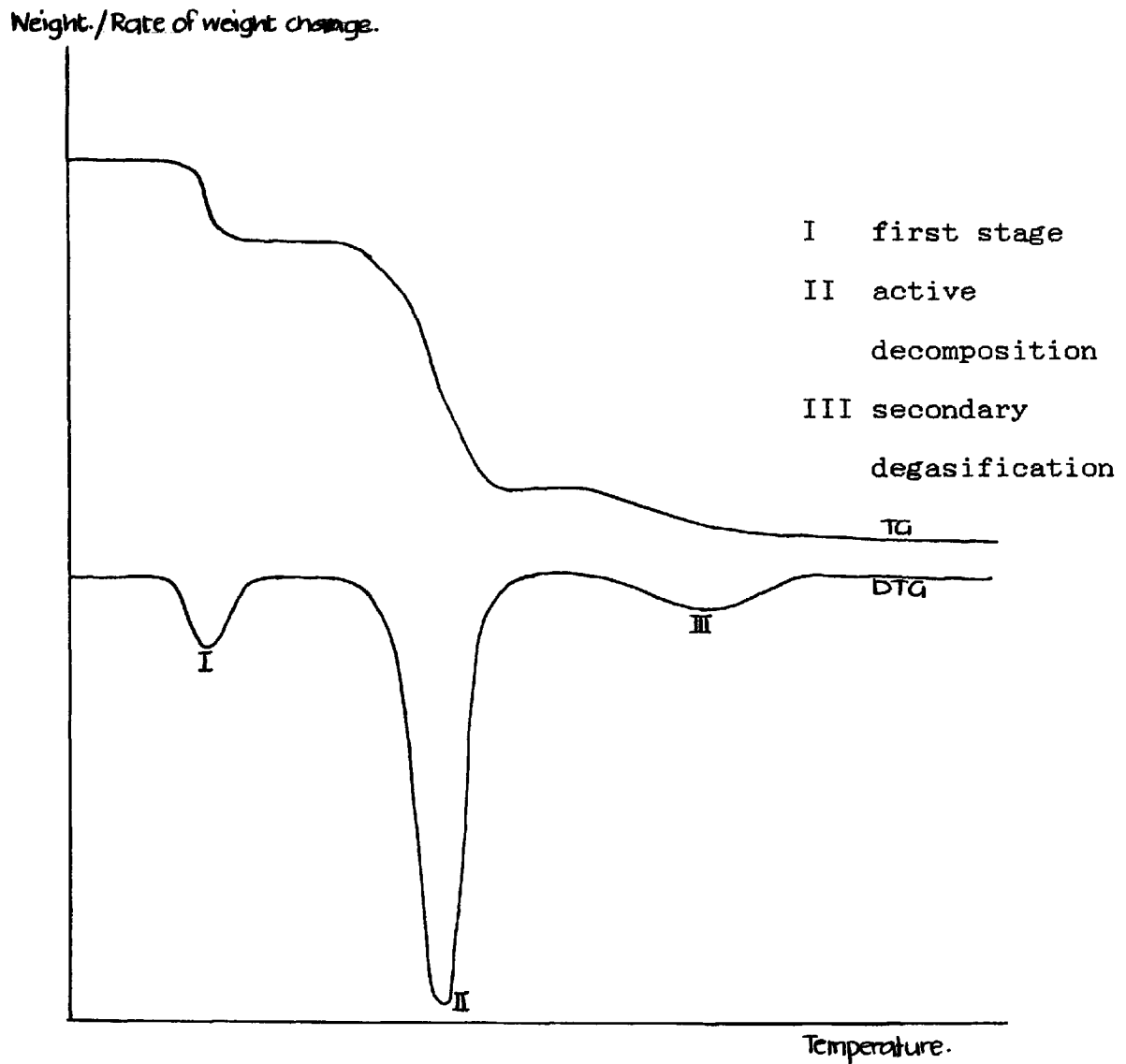
Fig. 3.15: Ideal TG Curve For Coal Pyrolysis[62]

Fuchs and Sandhoff[102] pictured the pyrolytic breakdown of coal as shown below in fig. 3.16, where rupture of the network and formation of tar and gas molecules are initiated by the splitting of rings containing heteroatoms
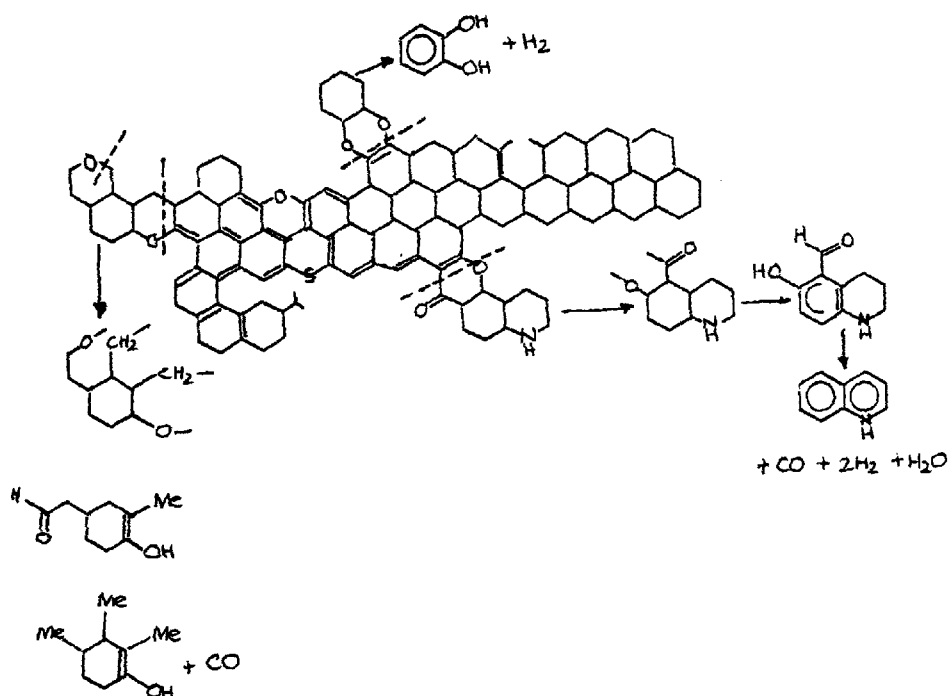
Fig. 3.16: Pyrolytic Breakdown of Coal Structure[102]

These researchers thought it was not probable that the variety of compounds making up gas and tar originate simultaneously, but that it was more probable that these compounds originate from slightly larger units which, within a certain temperature range, give low temperature tar and gas. They also found that the solid residues first lose their oxygen and then hydrogen as the temperature rises.

Lowry[112] concluded that the devolatilization process is primarily a function of temperature and is relatively unaffected by time, and thus the temperature of devolatilization could be estimated from the volatile matter content of the sample. The same conclusions were also reached by Nadziakiewicz[113].

Juntgen[46] proposed a mechanism for pyrolysis based upon results of thermogravimetric studies and consequent kinetic analysis. The molecular structure of coal used by Juntgen to deduce the reactions operating was that proposed by Wender et.al.[108]. The reaction pathway of pyrolysis depends upon the type and particle size of the coal, the type and pressure of the gaseous atmosphere, and the temperature/time history of the solids. The experimental conditions were selected so that the primary products of

pyrolysis are removed from the reaction chamber before any secondary reactions can take place.

Below about 350°C the major cause of weight loss is the evolution of capillary condensed moisture and the discharge of gases, such as CH_4 and CO_2, which are trapped within the pore system of the coal matrix.

The onset of tar formation at about 350°C can be assumed to be the distillation and diffusion of other smaller organic molecules (molecular weight <200) which are also trapped in the narrow pore structure of the coal. As this diffusion is an activated process throught the narrow pores, there is an exponential increase in the rates of diffusion with temperature and at 350°C the rates are high enough to allow diffusion of these molecules out of the coal solid.

Thermal degradation of the coal molecule begins to take place at about 400°C, and occurs in parallel with the gaseous diffusion. It is assumed that during thermal reactions, an equilibrium exists between the coal molecules and some activated forms of them in which the vibration energies of the bonds are concentrated around some of the bonds. The bridging carbons have their bonds cracked first because they have the lowest bonding energies and this is

followed by dissociation of the aromatic ring units, whereby radials are formed, particularly $:CH_2$ from C-C bridges, and $:O$ from ether bridges and larger ring systems containing one or two fre radicals. Due to the rapid recombining reactions among the smaller radicals and their reaction with hydrogen, small aliphatic gas molecules are formed, particularly CH_4 and H_2O, and these diffuse unhindered from the interior of the particles into the gas space. Also, larger ring fragments become hydrogen saturated and distil from the solid to the gaseous phase as a tar of medium molecular weight. This mechanism explains the simultaneous occurence of tar, CH_4, C_2-/C_3- hydrocarbons, and H_2O at temperatures $>400^{\circ}C$.

Because polynuclear systems of high molecular weight cannot diffuse fast enough within the solid at still higher temperatures, the formation of coke commences via condensation of these ring systems with elimination of hydrogen, which appears for the first time in gaseous form at about $420^{\circ}C$. At still higher temperatures, CO will also be produced by the cracking of heterocyclic oxygen groups.

The above mechanism for pyrolysis can be summarised in the following reaction steps, which exclude the diffusion of trapped molecules:

1. Cracking of the bridges between ring systems with the formation of radical groups.

2. Partial saturation of the radicals by hydrogen with the fromation of CH_4, other aliphatics, and H_2O which diffuse out of the coal particles.

3. Simultaneous saturation of the radicals of the larger molecules to yield tar products (of medium molecular weight); diffusion from the coal particles.

4. Condensation of the substances of higher molecular weight to yield coke, with elimination of hydrogen which is also released as a gas from the coal particles.

The above mechanism basically applies at high pressures and temperatures. High pressure results in the shifting of tar formation towards higher temperatures due to a shift in the boiling range; as a consequence, there is an intensification of coke generation at the expense of the tar yield. At high pressures, the elementary hydrogen liberated will, at temperatures >700°C, lead to an increased CH_4 yield due to a partial hydrogasification of carbon. High heating rates result in a faster evolution of tar and thus reduce the proportion of condensation reactions.

Solomon and Colket[120] investigated the release of nitrogen from coals undergoing pyrolysis. They concluded that during the initial stage of devolatilization, nitrogen exists in tightly bound compounds which are among the most thermally stable structures in the coal during devolatilization. During the initial stage of devolatilization, these nitrogen compounds are released without rupture as part of the tar. Subsequent release of nitrogen occurs when the nitrogen compounds decompose at high temperatures.

In the case of oxygen in coal, it has been found that the number of -OH groups in coking coals increase in the temperature range 500-600°C after first decreasing in abundance[121,122]. This is explained as being in connection with the formation of a plastic layer. In other coals, the -OH content steadily decreases with increasing temperature. An interesting result is that the residual -OH content increases with decreasing rank. This is explained by the greater ability of reactive oxygen structures in lower rank coals to be transformed into less reactive oxygen containing ggroups. This is interpreted as an indication that pyrolysis imitates and continues the processes of geochemical metamorphosis. Carboxyl group content decreases with increasing rank. Upon pyrolysis, carboxyl content decreases rapidly, and by 500°C all detectable carboxyl

groups have been decomposed. Similarly, methoxy group content decreases upon pyrolysis, but a small quantity of methoxy groups are still detectable above 800°C. In some caking coals, an increase in methoxy groups occurs concurrent to the increase in hydroxyl groups.

3.5 THEMOGRAVIMETRY[123-126]

3.5.1 Introduction.

Thermogravimetry (TG) is the technique used to measure the change in mass (w) of a sample as a function of temperature (T) as T is raised or lowered at a linearly programmed heating rate. TG is a dynamic, non-isothermal thermal analysis technique. The resultant graph of sample mass vs. temperature (or time, t) is known as a thermogravimetric (TG) curve. Another curve is usually recorded with the TG curve, that of the rate of change of sample weight (dw/dt), or the derivative thermogravimetric curve (DTG). An ideal, single-stage TG/DTG graph is shown in figure 3.17.
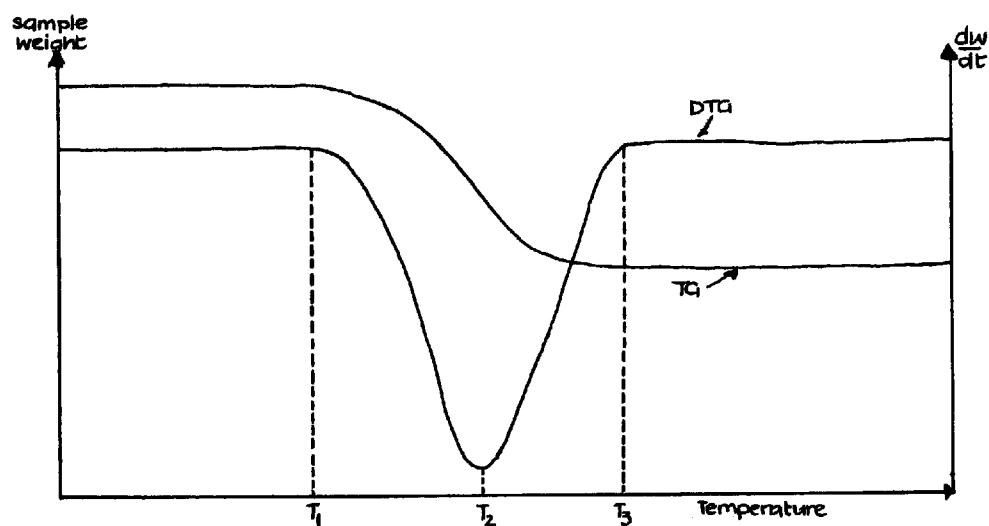
Fig. 3.17: A Simple TG/DTG Graph.

Except for the changes in sample mass and the rate of weight change, the information obtained from the TG and DTG curves is of an empirical nature as the transition temperatures observed are dependent upon instrumental and sample parameters. Information is gained about the sample composition, its thermal stability, its mode of decomposition/reaction, and the products formed on heating.

3.5.1 Instrumentation

Figure 3.18 shows a block diagram of a simple thermogravimetric balance.
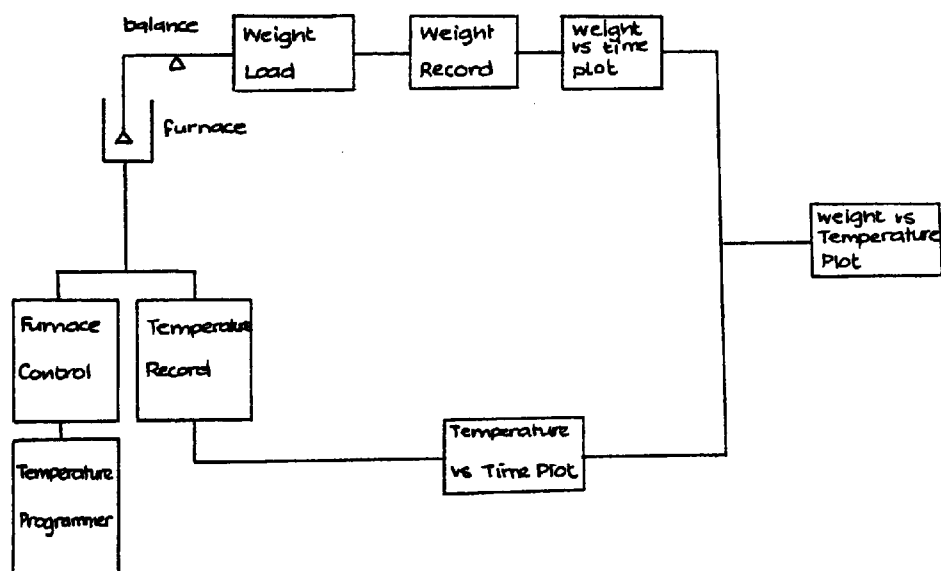
Fig. 3.18: The Components of a Contemporary TG Balance.

The weight of the sample is continuously recorded and plotted on a graph against time. The temperature of the sample in the furnace is recorded by a termocouple located close to, but not touching the sample holder; this may also be recorded against time, or, if the temperature is being increased/decreased at a linear rate then the time axis may be used as a measure of temperature.

3.5.2 The Variables That Affect TG Measurements

A discussion of the variables that can affect TG measurements is now required. But before this, an explanation of the existence of temperature gradients is required. Temperature gradients exist between the furnace wall and the sample container, and between the outer edges and the centre of the sample. These gradients are a result of the finite time taken for heat transfer to occur, and the magnitude of the gradients is attributable as to whether the phenomenon of heat transfer is easy or difficult in the medium being studied.

1. The Buoyancy Effect.

If a thermally inert crucible is heated when empty, there is usually an apparent weight gain as the temperature of the furnace increases. This is caused by hot gas rising along the walls of the furnace and this causes a displacement of gas down the centre of the furnace which in turn causes an apparent weight gain.

2. Container Design

The geometry of the crucible affects results. The crucible must be of a size and shape which allows homogeneous heating of the sample and easy release of volatile products. The container must be made of a material of high heat conductivity so that heat is transferred quickly to the sample in order to minimise the temperature gradient between the sample and furnace temperature. Also, the material of which the container is made should not react with the material under investigation. Allowance should be made in the design for samples which creep, swell or decrepitate.

3. Sample Weight and the State of Sample Subdivision.

The state of subdivision is important. The use of large particles may result in apparent very rapid weight losses during heating, but on closer examination, the cause of this loss may be due to a mechanical loss of part or all of the sample by forcible ejection from the sample pan. This also applies to large samples.

Grinding may change the crystal structure of the sample. Also, the finer the particle size, the easier it is for gaseous decomposition products to escape from the sample. Thus a sharper rate of weight loss will be observed from more finely ground samples.

As small a sample as possible, within the constraints imposed by the sensitivity of the apparatus, should be used in order that the existence of temperature gradients is minimised.

4. Temperature Measurement.

The temperature recorded by the thermobalance may either be the actual sample temperature obtained by placing the thermocouple in the sample, or, more commonly, the temperature at some point in the furnace close to the

sample. With the latter case, it must be realized that these measurements contain certain errors caused by continually increasing the furnace temperature.

A thermal lag will occur between the sample and the furnace, and also between the outside and centre of the sample. This is related to the sample mass, its heat capacity, its thermal conductivity, the particle size of the material, the rate of flow of gas in the furnace, and the heating rate.

5. The Effect of Heating Rate.

For a single-stage exothermic reaction, the temperature at which the reaction is complete i.e. when the weight first reaches its final value, is higher at a fast heating rate than for a slow heating rate. The same is true for the initiation temperature i.e. the temperature at which a weight change is first detected by the thermobalance. Also, at a given temperature, the degree of reaction is greater at the slower heating rate.

Generally, a low rate of heating allows reactions to be well resolved as the reactions operating in the sample after a certain temperature range are give more time to reach completion and thus will not extend into the temperature

region of the next reaction to as great an extent as for a faster heating rate.

A greater heating rate will also increase the temperature gradient within the sample. This is because it takes a finite amount of tine for heat to be transferred through the sample, and at fast heating rates, the time available for this transfer is less.
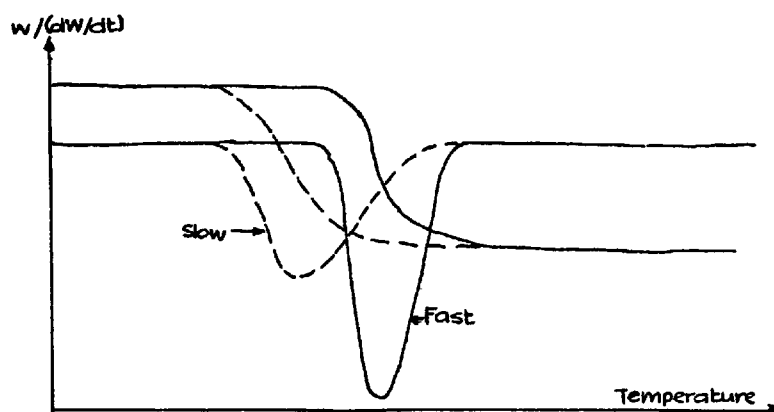
Fig. 3.19: The Effect of Fast and Slow Heating Rates.

6.   The Effect of Atmosphere.

During decomposition, the atmosphere around the sample is continuously changing, thus care must be taken, especially in a "manufactured" atmosphere, that the composition of the atmosphere is known. So, some kind of atmosphere control is required.

A downward flow of gas over the sample is preferred because the atmosphere comes into direct contact with the sample and will carry away the gaseous products. Modifications must be made to the apparatus to prevent damage to the balance or erroneous weight changes if corrosive or combustible gases are to be used.

7. Heat of Reaction.

This affects the way the sample temperature, if measured indirectly, precedes or succedes the measured temperature. The difference depends upon whether the reaction is exo- or endothermic.

8. Miscellaneous Effects.

Care should be taken that volatile matter does not condense on the cooler parts of the weighing mechanism or the sample holder thus resulting in erroneous weight changes.

Other odd effects can occur depending upon the reaction being studied and all possible sources of error should be investigated before experimentation.
Such effects as the creation of magnetic fields by induction from the furnace winding, convection currents, etc.   come

under this classification.

3.5.3 Interpretation of TG Curves.
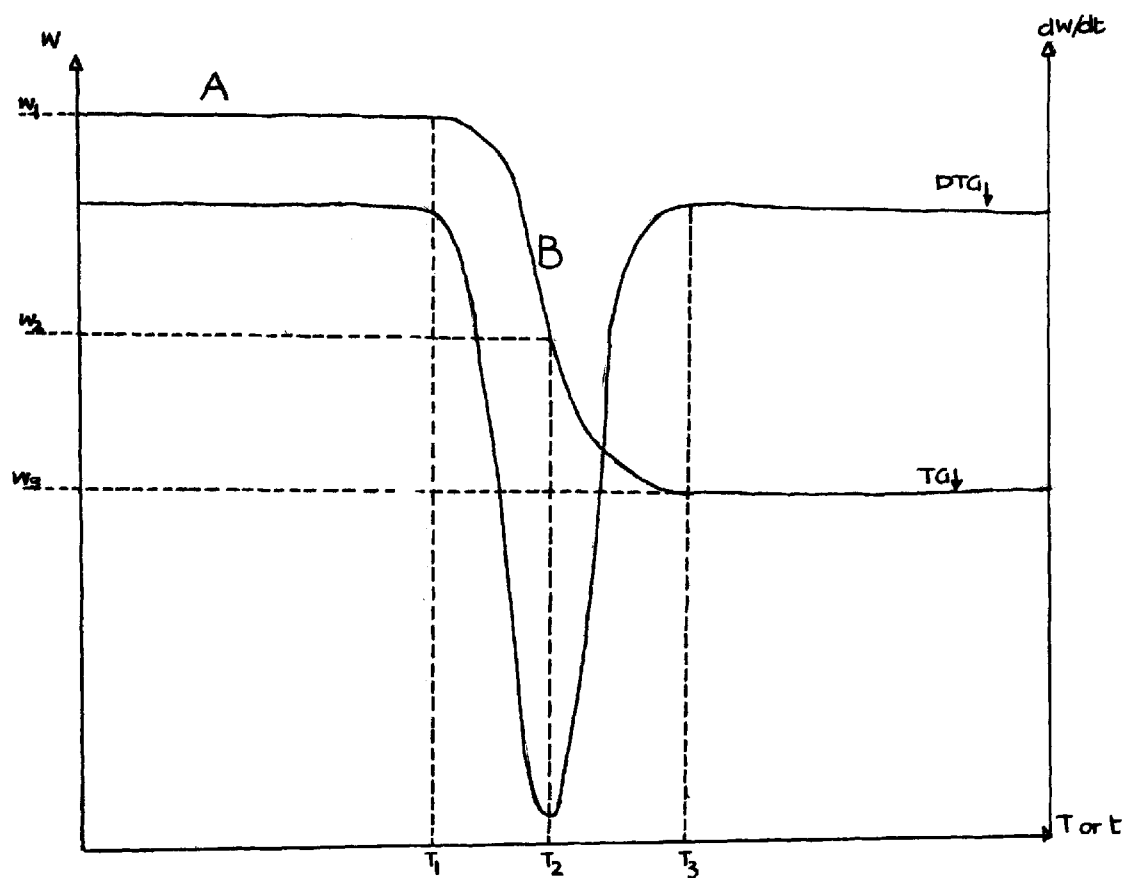
Fig. 3.20: Points Used to Interpret TG Curves.

Figure 3.20 above shows the points commonly used to interpret TG curves. These points correspond to important

parts of the reaction being studied.

W_1 and T_1 are the weight and temperature, respectively, at the point where the weight change is initiated. W_1 is known as the initial sample weight, and T_1 is known as the initiation temperature.

W_2 and T_2 are the weight and temperature at the point where the rate of weight change is a maximum. More specifically T_2 is the temperature of maximum rate of weight change.

W_3 and T_3 are the weight and temperature values at the point where the wieight change ends i.e. the point at which the reaction is complete. W_3 is the final sample weight.

On the TG curve region A is a plateau of constant weight, region B is a region of weight change and the steepness of this region is related to the rate of weight loss.

3.6 KINETICS.

The field of chemical kinetics studies the effects of concentration, temperature and pressure on chemical reactions with a view to elucidation of a reaction mechanism[127]. the rate of reaction is expressed in terms of the rate of decrease in concentration of a reactant or rate of increase in concentration of a product. Thus if the concentration of a product is c at a time t then the rate k is given by

$$k = -\frac{dc}{dt} \qquad (3.1)$$

The rate of reaction is a temperature dependent variable. The Arrhenius Equation[128] links the temperature to the rate of reaction

$$k = A \exp (-E/RT) \qquad (3.2)$$

Where A = pre-exponential factor

  E = activation energy, must be independent of temperature

  R = universal gas constant

  T = absolute temperature

Normally, kinetic studies are carried out in the gas phase or in solution where it is relatively easy to follow the changes in the concentration of reactants or products. In the case of coal pyrolysis, a solid of unknown molecular structure and molecular weight decomposes to give numerous possible gaseous products, the concentration of which is not easy to follow. Given that the composition of coal varies between particle and particle, it would seem that to carry out kinetic analyses would be a fruitless venture, especially as no single reaction proceeds on its own i.e. several reactions occcur simultaneously at any one point in time. Despite this, a kinetic analysis of experimental results can yield important information about the activity of a catalyst upon a particular region of the reaction. It must be understood that any kinetic parmeters obtained for coal are not absolute thermodynamic values. To proceed from these values to the calculation of absolute values needs a knowledge of the mechanism of the reaction, identification of the rate controlling reaction, and changes in the heats of adsorption/desorption of reactants and products. It can be seen from the preceding sections that this information is far from being complete.

Traditionally, kinetic studies ore carried out isothermaly, thus making a series of experiments at various temperatures necessary to construct an Arrhenius plot. From this Arrhenius graph, the pre-exponential factor and activation energy can be obtained.

If the kinetic parameters can be calculated from a series of reproducible thermogravimetric experiments then this gives a practical advantage over the traditional isothermal methods.

Because of the indeterminancy of the molecular weight of coal, kinetic models based upon concentrations[7,14] are unsuitable for the work presented herein. Models which required the measurement of individual product species[35,49,55] are also unsuitable as facilities for these detailed measurements were not available for this research. Complex models[34,52] have been rejected on the basis that the extent of knowledge required about coal structure and the mechanism of decomposition does not justify these methods.

After exclusion of unsuitable models there are two remaining models that could be used[36,42, 43,44]. Both are very similar and are based upon sample weight rather than concentrations. The model used by Serageldin and Pan[43,44]

was chosen as it includes both the initial and final sample weights which correct for slight differences in sample weight.

The themal decomposition of coal in an inert atmosphere may be represented by the rate equation[127,130]

$$-\frac{dm}{dt} = k(1-C)^n \qquad (3.3)$$

where $-dm/dt$ = rate of change of sample mass

k = rate constant

C = the sample conversion

n = the order of reaction

The conversion may be written in terms of mass

$$C = 1 - \frac{m - m_f}{m_i - m_f} \qquad (3.4)$$

where m = mass at time t

m_i = initial mass at time $t=0$

m_f = final mass at the end of the experiment

It is assumed that the rate constant, k, varies with temperature in accordance with the Arrhenius Equation (equation ..2). By combining equations 3.2, 3.3, and 3.4 the following equation is obtained

$$-\frac{dm/dt}{m_i - m_f} = A \exp \frac{-E}{R} \left[\frac{m - m_f}{m_i - m_f} \right]^n \qquad (3.5)$$

n is assumed to be unity in accordance with Van Krevelen[7,13,14,45] and supported by Serageldin and Pan[44]. Taking logs and rearranging equation 3.5 we get

$$\log \frac{-dm/dt}{m_i - m_f} \cdot \left[\frac{m_i - m_f}{m - m_f} \right] = \log A - \frac{E}{2.3RT} \qquad (3.6)$$

An Arrhenius plot can be constructed by plotting the left-hand side of the equation against the reciprocal of the temperature. A series of regions of Arrhenius linearity are obtained, the gradients being equal to E/2.3R and the intercept on the y-axis giving logA.

A sample calculation using this method is given in Appendix F.

3.7 CATALYSIS.

The aim of investigating the effects of possible catalysts in the present work is to examine the way in which activation energies of reactions operating during pyrolysis are affected. Metals from the transition metal series of the periodic table were chosen as many of them are common catalysts in industry. Also, as far as the author is aware, they have not been used in the study of coal pyrolysis by thermogravimetry before. Figure 3.21 shows the metals used and their positions in the Periodic Table.

Group	IVB	VB	VIB	VIIB	VIIIB			IB	IIB
Period 3	Ti	V	Cr	Mn	Fe	Co	Ni*	Cu	Zn*
Period 4	Zr		Mo						
Period 5			W						

Note * indicates the oxide was used.

Fig. 3.21:Metals Used in the Catalytic Studies.

The availability of time and money did not allow the complete series of transition metal elements to be examined for their possible catalytic effect upon coal pyrolysis. Zinc oxide was used because of the low melting point of zinc metal, By using the metals of Period 3, the progression of activation energy change across the Period is shown. The progression down groups IVB and VIB is also investigated.

A catalyst is a substance which in small amounts changes the rate of a reaction without it being appreciably consumed in the process[131]. The basic concept of catalysis is that a catalysed reaction involves the transitory adsorption of one or more of the reactants onto the surface of the catalyst, rearrangement of the bonding, and desorption of the products. This series of events takes place at a reaction site which is a specific location on the surface of the catalyst[132]. It is usually difficult to identify the sites and their structures precisely, in some cases a site may be a group or a cluster of neighbouring atoms on the catalyst, or it may be a species adsorbed onto the catalyst. Also, a site that may be active for one reaction may not be so for another. It should not be inferred that the catalyst remains unchanged, indeed a catalyst may undergo major structural and compositional changes.

The function of a catalyst is to accelerate the rate of approach to the equlibrium state of the reaction, it <u>cannot</u> change the ultimate equilibrium of the reaction as determined by thermodynamics. The relative increase in the rate of reaction caused by a catalyst (measured relative to other catalysts or the uncatalysed reaction) is a measure of its activity; the greater the increase, the more active the catalyst. The most common use of a catalyst is to accelerate the rate of the desired reaction within a group of reactions so that the desired product is produced before other products. This means that the most stable products of the reaction are not necessarily formed.

As it has not been possible to record the changes in the gaseous products of coal pyrolysis during this work, it has not been possible to assess the effect of the metals upon the production of CO, CO_2, H_2, and CH_4. The result of this is that the activation energy of the various regions of Arrhenius linearity, and the temperatures at which they occur will be examined to assess the relative activity of the metals.

CHAPTER 4.

EXPERIMENTAL.

4.1 COAL SAMPLES.

The coal samples were chosen to be representative of the types of coal found in the South Wales Coalfield. The collieries from which they originated are: Cynheidre, Penrikyber, Ogmore, Cwm, Celynen South, and Llanharan. Proximate and Ultimate analyses were performed to ascertain the rank of the coals. The particle size of the samples used in all experiments was that used for Proximate analysis i.e. $<21\mu m$.

4.1.1 Proximate Analysis.

The Proximate analyses were carried out in accordance with BS1016 part3, 1957. The results are given in the table given in figure 41. The ranks of the coal were assessed using the NCB system of coal classification.

AS RECEIVED BASIS

NCB Rank		%H$_2$O	%VM	%FC	%Ash
101	Cynheidre	1.6	5.2	87.0	6.2
201A	Penrikyber	0.8	10.9	82.6	5.7
203	Ogmore	0.6	15.9	77.6	5.9
301A	Cwm	0.5	20.8	70.9	7.8
301B	Celynen South	0.8	28.8	62.3	8.4
501	Llanharan	1.7	30.5	62.2	5.6
701	Llanharan	1.8	30.4	60.1	7.7

DAF BASIS

%VM	%C	VM/FC
5.6	94.4	0.059
11.7	88.3	0.132
17.0	83.0	0.205
22.7	77.3	0.293
31.7	68.3	0.462
32.9	67.1	0.490
33.6	66.4	0.506

ULTIMATE ANALYSIS (daf basis)

%C	%H	%O*	%N	%S	C/H	(C+H)/O
85.4	2.76	1.86	0.90	0.88	30.94	47.39
84.2	3.70	2.86	1.10	1.44	22.76	30.74
84.0	4.09	3.29	1.30	0.92	20.54	26.77
81.7	4.33	3.14	1.30	0.93	18.87	27.39
77.6	4.40	6.41	1.10	0.69	17.64	12.79
77.9	4.63	7.74	1.30	0.93	16.82	10.66
75.9	4.44	7.78	1.30	1.08	17.09	10.33

%O calculated by difference.

Proximate Analysis results supplied by the NCB.
Ultimate Analysis results supplied by Minton, Trehearne and Davies (Cardiff)

Fig. 4.1 Proximate and Ultimate Analysis Results.

4.1.2 Ultimate Analysis.

Ultimate analysis of the coal samples was carried out to BS1016 by Minton, Treharne and Davies Ltd of Cardiff. These results are tabulated in Fig. 4.1.

The main results of the Proximate and Ultimate analyses are shown in figures 4.2 and 4.3.

4.2 THE METALS USED IN THE CATALYTIC STUDIES.

The metals used for the catalytic studies are shown in fig. 4.4, together with details of the supplier, the particle size used, and the purity of the metal. From the results of the initial thermogravimetric investigations, two coal samples were chosen to be studied with the possible catalysts. Each catalyst was added to the sample in both 5% and 10% proportions by weight. the samples with the catalysts were well stirred to ensure a well mixed sample.
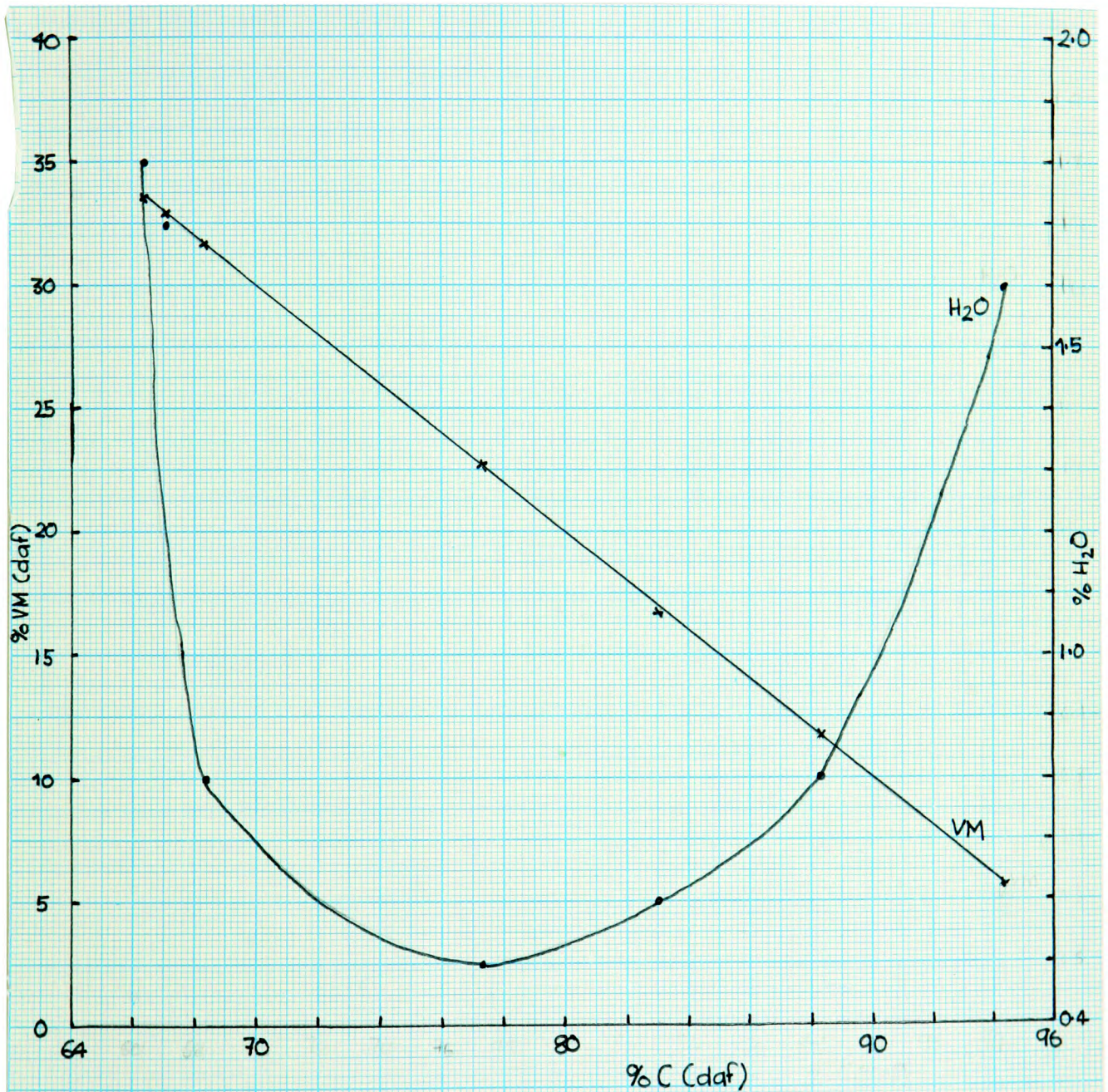
Fig 4.2 : The variation of moisture content and volatile matter content with the carbon content for the coal samples.
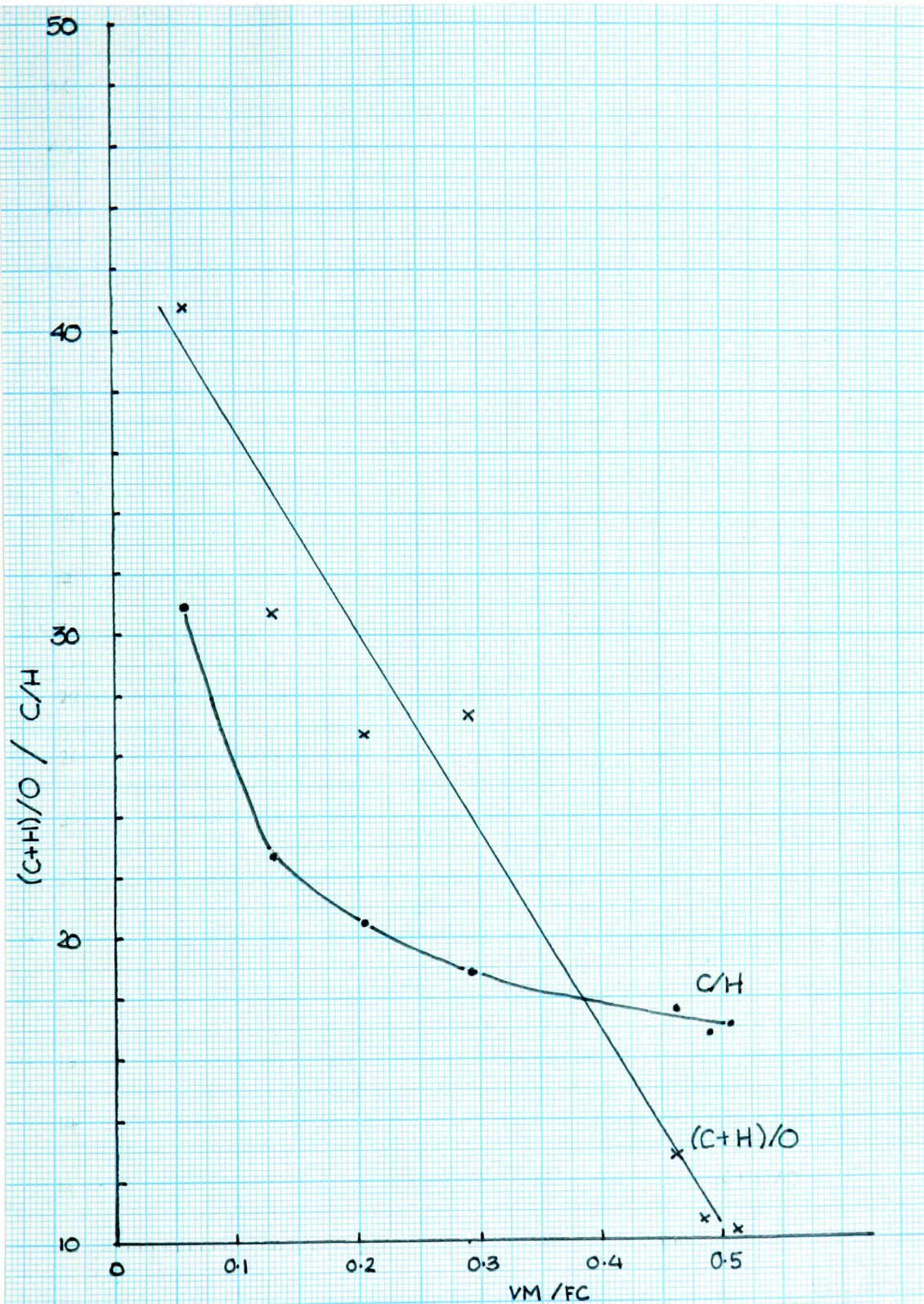
Fig. 4.3 : The variation of the ratios C/H and (C+H)/O with VM/FC for the samples.

Page 129 b.

Metal	Supplier	Particle size	Purity
V	Fluka	>38<75μm	>99.5%
Zr	New Metals and Chemicals	<40μm	97%
Fe	BDH	<38μm	95%
W	New Metals and Chemicals	2.5μm	99.9%
Mo	New Metals and Chemicals	>1<5μm	99.5%
NiO	BDH	<38μm	–
Ti	Goodfellow Metals	<38μm	99.5%
Cr	Goodfellow Metals	<38μm	99.0%
Mn	Goodfellow Metals	<5μm	98.3%
ZnO	BDH	<38μm	99.9%
Cu	Fluka	<38μm	99.99%
Co	Fluka	<38μm	99.8%

Fig. 4.4

4.3 THERMOGRAVIMETRY.

4.3.1 Apparatus

A Perkin-Elmer TGS-2 Thermobalance using a Perkin-Elmer Differential Scanning Calorimeter as a temperature programmer was used for the thermogravimetric studies. The interfacing of a BBC Model B microcomputer to the TGS-2, and the resultant development of computer programs, allowed computerized data acquisition, storage and analysis with a much greater sensitivity and accuracy than the chart recorder usually employed for this function. The computer reads the weight with an error of 0.3%, the chart recorder with an error of 1%[136].

Fig. 4.5 shows a cut-away diagram of the essential components of the TGS-2 thermobalance.

The balance consists of two pans connected by Nichrome hangdown wires to a light beam balance. The sample pan holder is located within a microfurnace when the balance is operational. The sample hangdown wire and the balance mechanism are protected from heat by a baffle. The baffle also acts as a channel to direct the flowing purge gas,
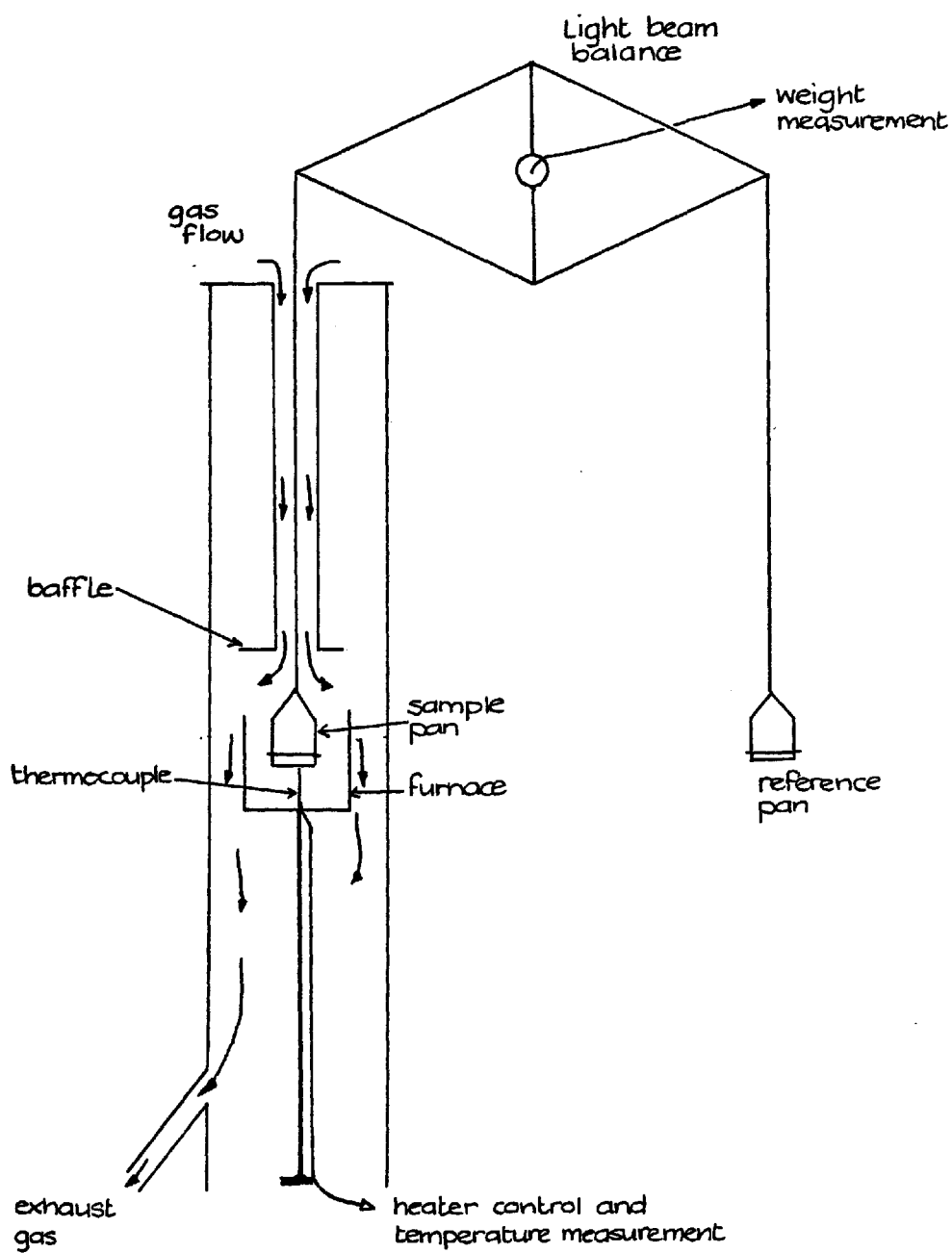
Fig. 4.5: Cut-away Diagram of Thermobalance.

which controls the atmosphere around the sample in the furnace. The apparatus is designed to work only at atmospheric pressure. The baffle also prevents any reactive gaseous products form entering the balance housing and damaging the mechanism. The flow rate of the purge gas is measured by a bubble flow meter connected to the exhaust gs tube. This allows the atmospheric conditions to be regulated with accuracy and repeatability.

The sample pan has a diameter of 6mm and is manufactured from Iconel. This is placed within the sample pan holder which is fashioned from platinum. The weight of the sample pan is tared off the sample weight so that only the sample weight is recorded. The whole assembly is suspended within the microfurnace and a thermocouple is positioned just below the sample. The thermocouple is used to relay temperature information to the DSC-2 so that the temperature of the furnace can be maintained isothermally or carefully controlled in a linear heating programme. 10 heating rates in the range 0.32 to $160^\circ Cmin^{-1}$ can be used. The thermocouple is calibrated by the use of magnetic transition standards.

In the more conventional thermobalances, a two-pen chart recorder is used to record the weight of the sample (either

as a percentage, or in weight units) and whether the temperature or the rate of weight change (derivative signal). But in the experimental set up used for this research, a computer was used to collect the weight and temperature data for each experiment. The rate of weight change can then be calculated using another computer program. Fig. 4.6 shows a block diagram of the experiment.

```
┌─────────┐    ┌──────────────┐    ┌────────────────┐
│ Balance ├────┤ Balance Unit ├────┤ Weight Output  ├──────────────┐
└─────────┘    └──────────────┘    └────────────────┘              │
                                                                    │
┌─────────┐    ┌──────────────┐    ┌────────────────┐  ┌─────────┐  │
│ Furnace ├────┤ Thermocouple ├────┤ Temperature    ├──┤ Heater  │  │
└─────────┘    └──────────────┘    │ Output         │  │ Control │  │
                                   └────────┬───────┘  └─────────┘  │
                                            │                       │
                                   ┌────────┴───────────┐           │
                                   │ Computer Disc File ├───────────┘
                      ┌────────────┴─────┐ └───┬────────┘
                      │ Analysis         │     │
                      │ of Results       ├─────┤
                      └──────────────────┘     │
                                       ┌───────┴──────┐
                                       │ TG/DTG Graph │
                                       └──────────────┘
```
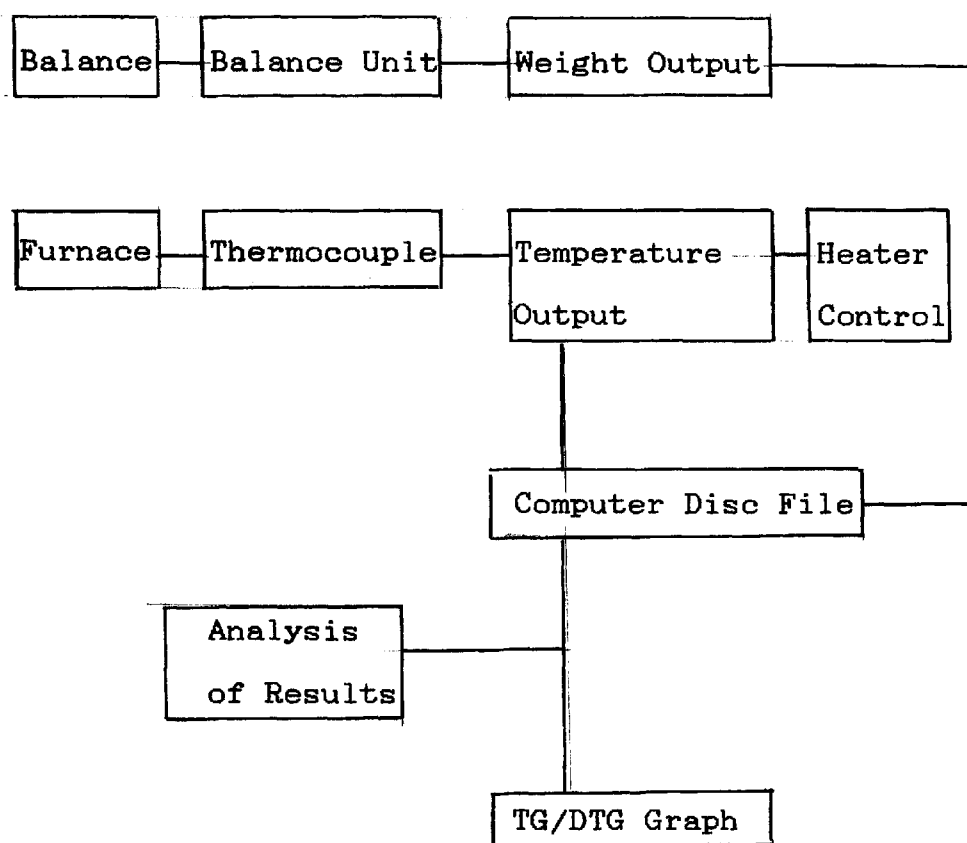
Fig. 4.6: Block Diagram of Thermogravimetric Instrumentation

4.3.2 Experimental Conditions.

Given below are the experimental conditions used in the thermogravimetric studies. Heating rate is the only major variable to be varied as it has been shown in an exhaustive study[36] that heating rate is the only variable to significantly affect thermogravimetric results. Other variables have been nominally chosen. The rate of flow of the nitrogen purge gas used is the maximum possible without causing any instabilities in the balance or furnace. The flow needs to be high enough to take away the gaseous products before any secondary reactions can take place and to prevent condensation of the products on the sample pan/hangdown wire, the result of which would be inaccuracies in the measurement of the sample weight. The pressure within the TGS-2 was ambient atmospheric. The temperature range was chosen so that the samples could be pre-heated to 130°C to remove the moisture in the sample so that the weight loss recorded is that of the volatile component of the sample. A slightly higher temperature of 150°C was used for the computer to begin recording the weight loss. This was a result of the requirements for the computer program to work successfully. The sample weight was chosen to be the minimum possible where the background noise would not

present a problem, and where heat would be transferred quickly throughout the sample so that the thermocouple gives a true sample temperature. The particle size was as for the proximate analysis, i.e. <211µm.

Heating rate = 20, 40 and 80°Cmin^{-1}

Atmosphere = dry nitrogen gas (B.O.C)

Atmosphere purge rate = 40cm^{3}min^{-1}

Atmosphere pressure = ambient atmospheric

Sample weight = 7-14mg

Temperature range = 150-900°C

Coal particle size = <211µm

For the catalytic studies the following conditions were used.

Heating rate = 20°Cmin^{-1}

Atmosphere = dry nitrogen gas (B.O.C)

Atmosphere purge rate = 40cm^{3}min^{-1}

Atmosphere pressure = ambient atmospheric

Sample weight = 7-14mg

Coal particle size = <211µm

Metal particle size = as specified in section 4.2

%metal by weight = 5%, 10%

For each sample under each set of conditions, a series of five thermogravimetric experiments were completed in order to give a set of reproducible results. So many were needed because of the increased sensitivity of the computerized data collection and the inherent heterogeneity of coal; i.e. small variations in the coal composition which result in slight variations in the mode of decomposition of the sample and these are recorded as slight variations in the weight and rate of weight changes by the computerized data collection system.

4.4 THE COMPUTER INTERFACE AND PROGRAMS.

A 32K BBC Model B Microcomputer, complete with dual disc drives, colour monitor, and printer, was used to collect and record the temperature and weight data. The temperature and weight signals that are produced by the TGS-2 are analogue in form and in the voltage range 0-10V. For the BBC computer to record and use these signals, they must be in the voltage range 0-1.8V and of a digital form. A resistor pack placed in the computer-TGS-2 interface scales the voltage, and the analogue to digital converter (ADC) incorporated into the computer digitizes the signal.

The computer programming necessary to produce a TG/DTG plot and to perform a kinetic analysis of the data and produce an Arrhenius plot was accomplished in a series of short programs. It was necessary that the programs were split because of the limitations of the computer's memory, and for ease of improvement and change of the programs.

One problem encountered with the increased sensitivity of the computerized data collection system is that some "noise" is encountered on the derivative TG graph. The source of this noise is mainly electronic in nature and emanates from the electronic circuitry within the TGS-2 control system. Some of the noise has its source in fluctuation of the sample weight caused by unavoidable phenomena such as the buouyancy effect (see section 3.5.3).

This noise must be taken into account during any results analysis. TG/DTG curves for an inert sample provide the means for this. The noise level varies with the heating rate. The following maximum rates of weight change were found for various heating rates.

Heating Rate	Noise Level
($^{\circ}Cmin^{-1}$)	($mgmin^{-1}$)
80	±0.060
40	±0.017
20	±0.009
10	±0.009

The noise level is minimised at heating rates of $20^{\circ}Cmin^{-1}$ or less. This suggests that the noise may be related to the time interval between the recording of the datum temperatures and weights - the slower the heating rate, the longer the time period between datum points. Thus, for detailed studies the slower heating rates are suggested. A typical graph showing the noise for an inert sample is shown in figure 4.7.

Fig. 4.7 : A Thermogravimetric Curve for an Inert Sample
Showing the Background Noise from the TGS-2.
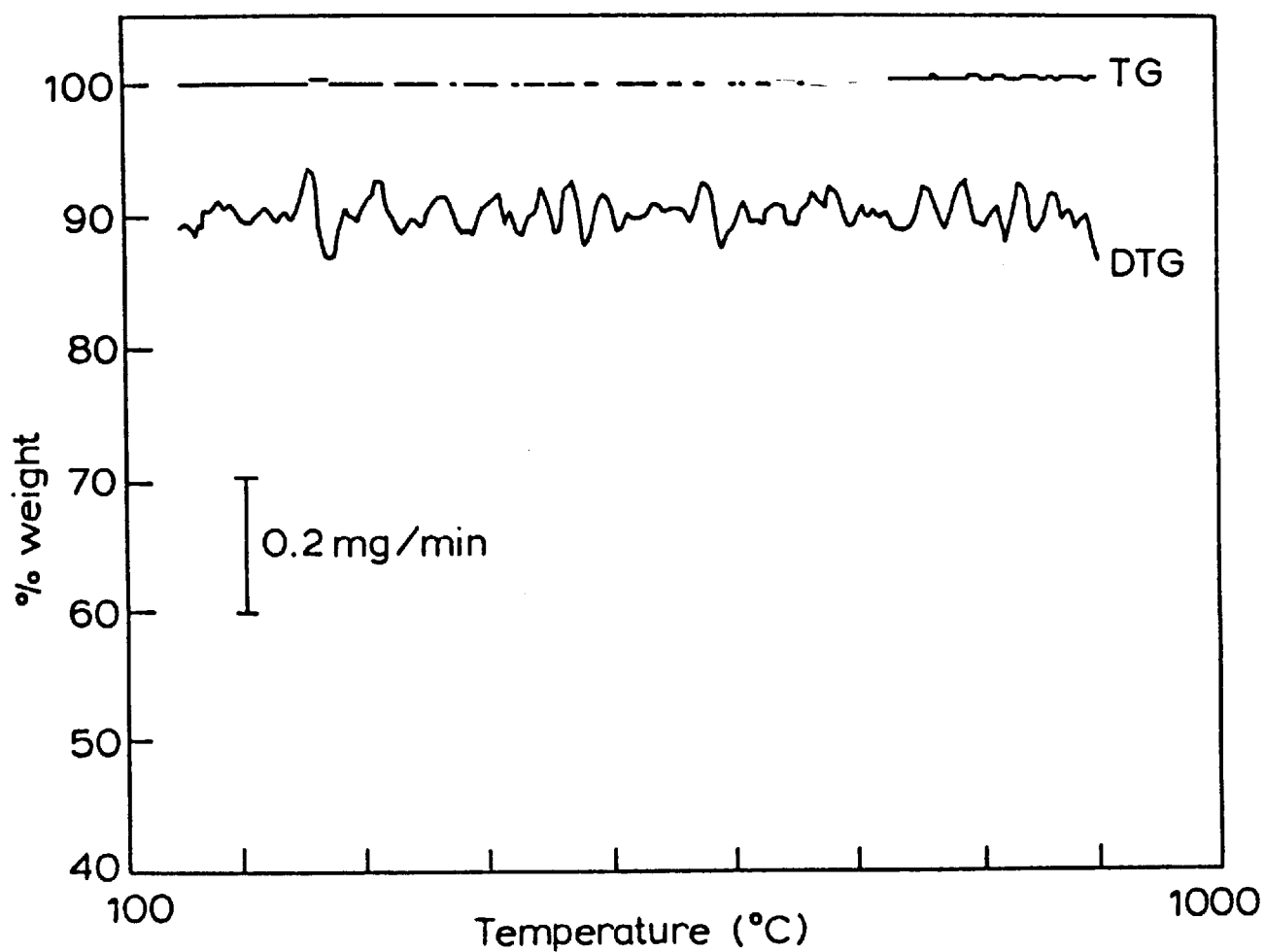
Heating rate = 80°C min⁻¹

Sample weight = 5 mg

Nitrogen flow rate = 40 cm³ min⁻¹

4.4.1 The Data Collection Program.

Before this program was written, two calibration curves needed to be constructed to enable the digitised signals to be converted to their corresponding temperature and weight values. Digital values for various weights and temperatures were recorded and plotted against their respective weight or temperature values to give the calibration curves. Straight lines were obtained which passed through the origin and thus the gradients of the lines were the required conversions. These curves need to be calibrated each time the TGS-2 is calibrated.

The program records the weight of the sample at a certain temperature interval. This interval is set within the program as 5°C as this was found to give the optimum compromise between the electronic noise and the sensitivity. Also, as the temperature was found to fluctuate slightly over a period of time, as did the weight, an average of 10 readings was taken to enable the temperature to be pinpointed with accuracy. The time taken for these 10 readings to be recorded and averaged is about 0.04s. The results are then stored to a file called, say F1, on disc and a graph can be plotted of the sample weight on the monitor screen.

4.4.2 The Derivative TG Program.

This program uses the data from the temperature/weight file created by the data collection program to calculate the rate of weight change, or derivative TG, and the percentage at the data points. The program uses the 5-point parabolic least squares method of numerical differentiation. The resultant rate of weight change data together with the corresponding initial and final sample weights, the percentage weights, and the temperature at which the results were taken are stored in an new disc file, F2.

4.4.3 The Graph Plotting Program.

The temperature, weight and rate of weight change data contained within the second disc file are plotted, first on the monitor screen and then with the printer, as a conventional TG/DTG plot with the Y-axis labelled as the %sample weight, a scale bar for the DTG curve, and the X-axis as the temperature scale.

4.4.4 Program to Give Information About the DTG Peaks.

This program uses the second file to pinpoint the peaks on the DTG curves and to print out the temperature, percentage weight and rate of weight change for all peaks with a rate of weight change value greater than a quarter of the maximum rate of weight change value. This eliminates all peaks which may be due to or greatly altered by the background noise.

4.4.5 The Kinetics Program.

This program uses the data contained within the derivative files (F2) to calculate the kinetic parameters using the Serageldin and Pan[43,44] method. For each sample a series of five runs was undertaken and <u>all</u> five files are used in this program to provide average results. The log of the reaction rate constant and the reciprocal of the corresponding temperature are calculated and stored in a new file F3. The standard deviation of the averages is calculated for each point and if the standard deviation is greater that 0.2 the point is not used in any subsequent calculations and graphs. This is a result of the heterogeneity of coal and of the noise and such points

cannot be regarded as being representative of the sample. These points are then used to draw Arrhenius graphs of the kinetic results from which the apparent activation energy for the various regions of Arrhenius linearity can be calculated.
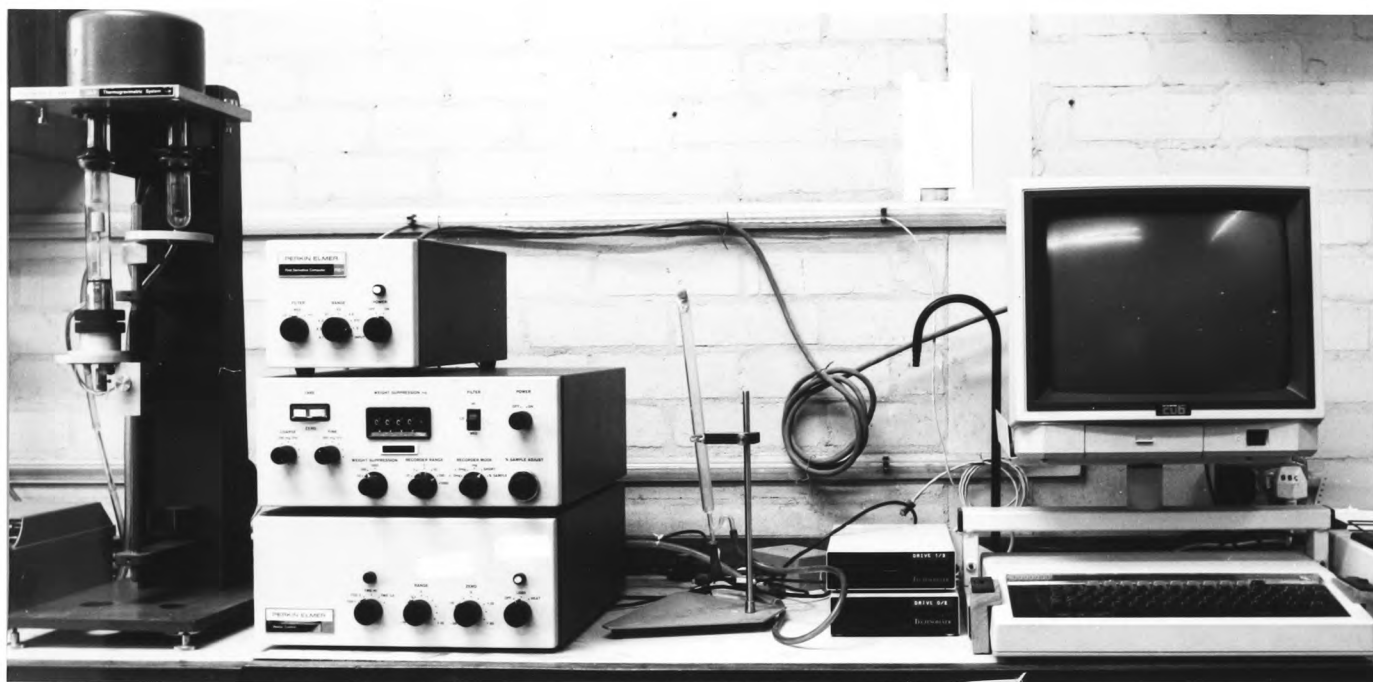
Fig. 4.8 : Photograph of the Apparatus Used.

4.5 VERIFICATION OF THE COMPUTERIZED DATA COLLECTION.

Before the computer programs were designed and used some thermogravimetric experiments were conducted with the coal samples using the chart recorder to record the TG/DTG curves. The result of one of these experiments, shown in figure 4. 9, is for a sample of 301B Celynen South coal heated at $20^\circ Cmin^{-1}$ in an atmosphere of nitrogen. the DTG peak maximum occured at around $500^\circ C$. The sample weight was 2.7704mg and the maximum rate of weight loss was $-0.142mgmin^{-1}$. Figure 4.10 shows the same sample under the same conditions except that the sample weight used was 8.3634mg, the maximum rate of weight loss was $0.4053mgmin^{-1}$ and the temperature at which this occured was $520^\circ C$. The difference in peak temperature is attributable to the computerized system directly reading the thermocouple temperature, whereas for the chart recorder the temperature is inferred from the X-axis time scale. The computerized system is also more "sensitive" to weight changes as data smoothing and filters to cut out the noise and give perfect curves are not used in the computer system. It is also believed that the method of differentiation used to obtain the derivative curve differs in the computer programs. Despite this there is good agreement between the values for

the maximum rate of weight loss from both the chart recorder and the computer. There is a linear relationship between the initial sample weight and the maximum rate of weight loss. By making both initial sample weights the same, the maximum rate of weight loss for the chart recorded experiment would be -0.4287, and for the computer method it is -0.4053. The difference between these values is 5.4% and is within experimental error, especially for such a heterogeneous substance as coal. Similar results were found for other samples studied using the chart recorder for data recording.

Fig. 4. 9 : Chart Recorder TG/DTG Curve.

301B
20°C min⁻¹
40cm³ N₂ min⁻¹

-0.02 mg min⁻¹

% Sample weight.

DTG

TG

Temperature (°C)
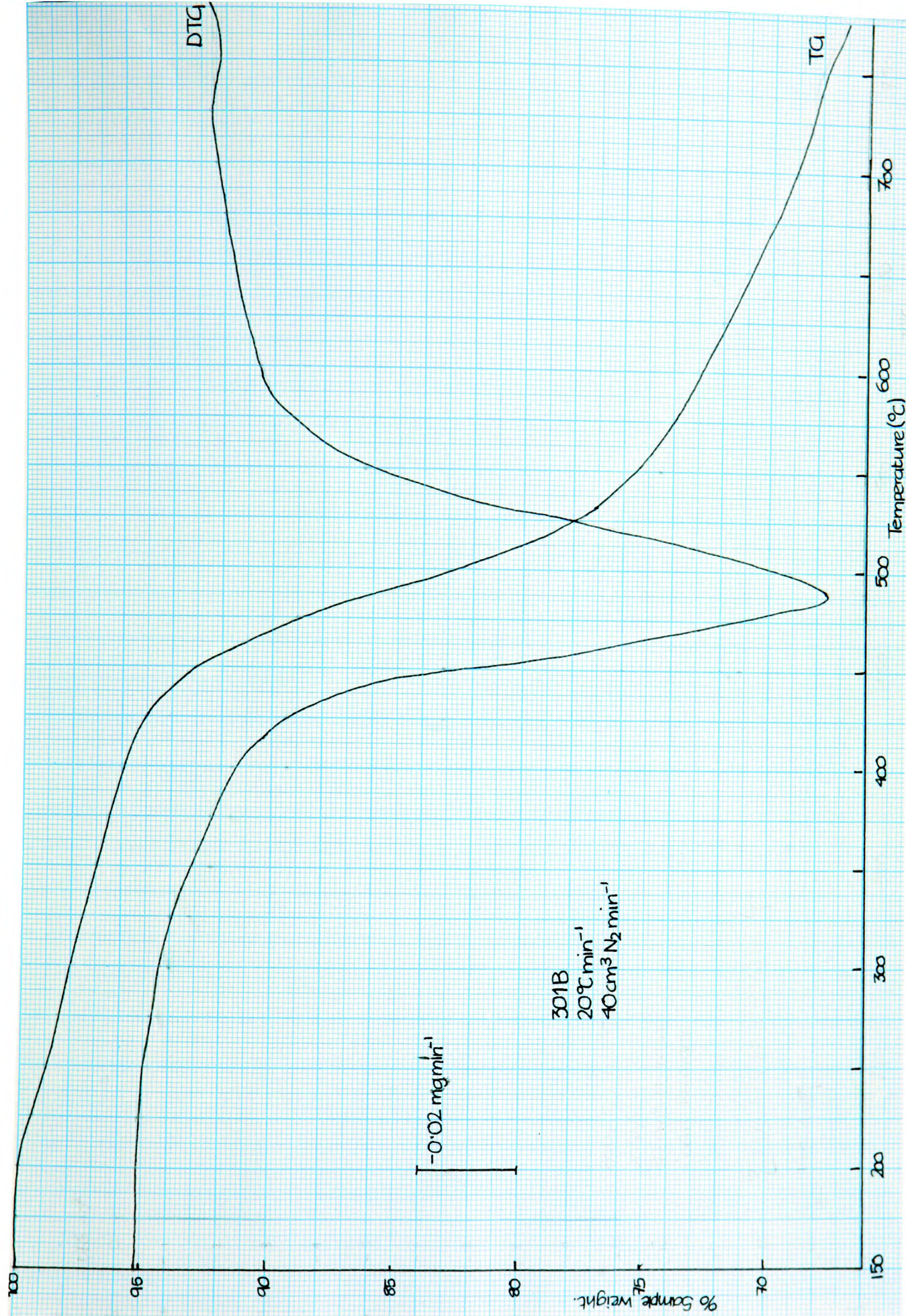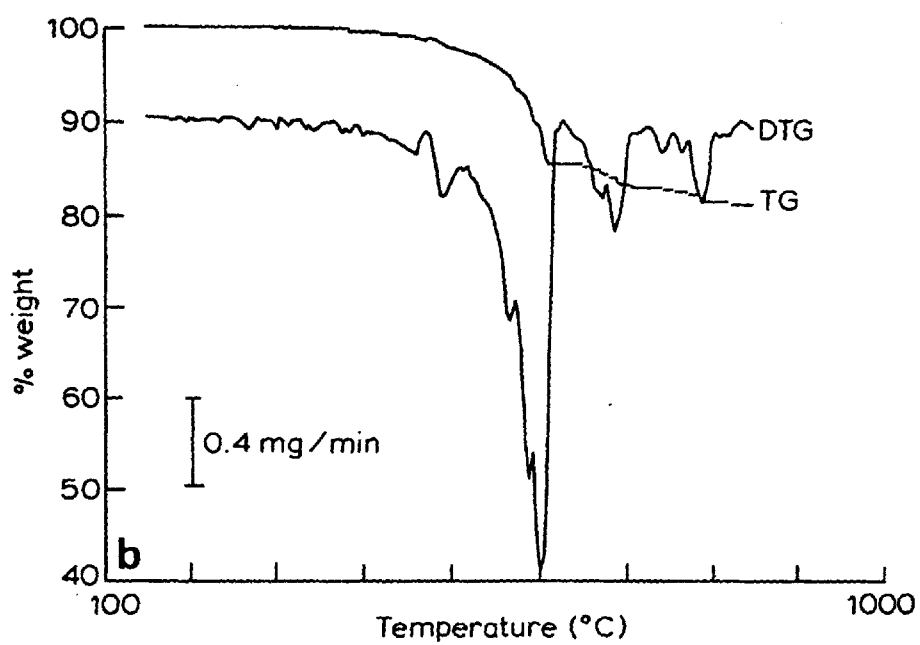
Fig. 4.10 : Computer TG/DTG Curve.

4.6 HOT-STAGE MICROSCOPY.

4.6.1 Apparatus.

Hot-stage microscopy allows the visual observation of the physical changes which samples undergo during heating. The apparatus used for this work is a Stanton-Redcroft HSM-5 hot stage and temperature programmer. The microscope usd is an Olympus X-Tr stereoscopic model fitted with a trinocular head for photomicrography. The camera used for the photomicrography is an Olympus PM6 35mm camera. 2x objectives (f=50) are used with the microscope and the optical specifications are as shown in fig. 4.11. Photographs can be taken at any time without affecting the visual observation of phenomena.

The body of the hot-stage is water cooled for safe high-temperature handling. The furnace is a microfurnace of a low thermal mass which allows the use of high heating and cooling rates. A chrome-alumel thermocouple is placed in contact with the furnace and is used to control the temperature programmer. The furnace sample chamber contains a plate type thermocouple (Pt/Pt-13%Rh) on which the sample pan, formed of Iconel, containing the sample sits.

Drum position	Eyepieces	Total magnification	Field diameter(mm)	Working distance(mm)
6.3		–	–	
10		–	–	
16	10x	31.5x	7.7	
25		50 x	4.9	
40		80 x	3.1	
				45
12.5		–	–	
20		40 x	6.1	
31.5	20x	63 x	3.9	
50		100 x	2.4	
80		160 x	1.5	

Fig. 4.11 : Optical specifications for the Olympus Microscope with 2x Objectives.

A removable lid fitted with a quartz window, to allow viewing of the sample, covers the sample chamber. The lid can be rotated through 360° whilst still maintaining a gas-tight seal, and this ensures an unobstructed view of the sample at all times for most samples. The furnace atmosphere can be controlled and in this research, nitrogen gas was used.

The furnace temperature programmer allows a temperature range from ambient to 1000°C to be used. Heating and cooling rates of 1,2,3,5,10,20,30,50, and 100°Cmin⁻¹ are available. The furnace may also be used isothermally. The temperature of the furnace may be checked by I.C.T.A standards. A fibre optic light is used to illuminate the sample.

For each experiment the following conditions were used:

Heating rate = 50°Cmin⁻¹

Atmosphere = nitrogen

Atmosphere purge rate = 100cm³min⁻¹

Cooling water flow rate = 25lhr⁻¹
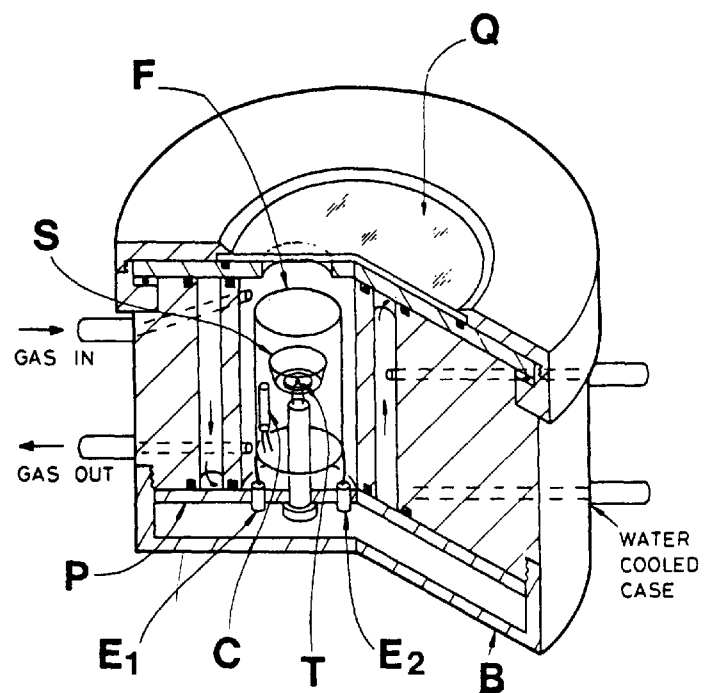
Key Q = quartz window
    F = furnace
    S = sample container
    P = baseplate
    E_1 & E_2 = furnace connections
    C = control thermocouple
    T = Pt v Pt-13% Rh thermocouple
    B '= removable base plate

Fig. 4.12 : Cut-Away Section of the Hot-Stage.
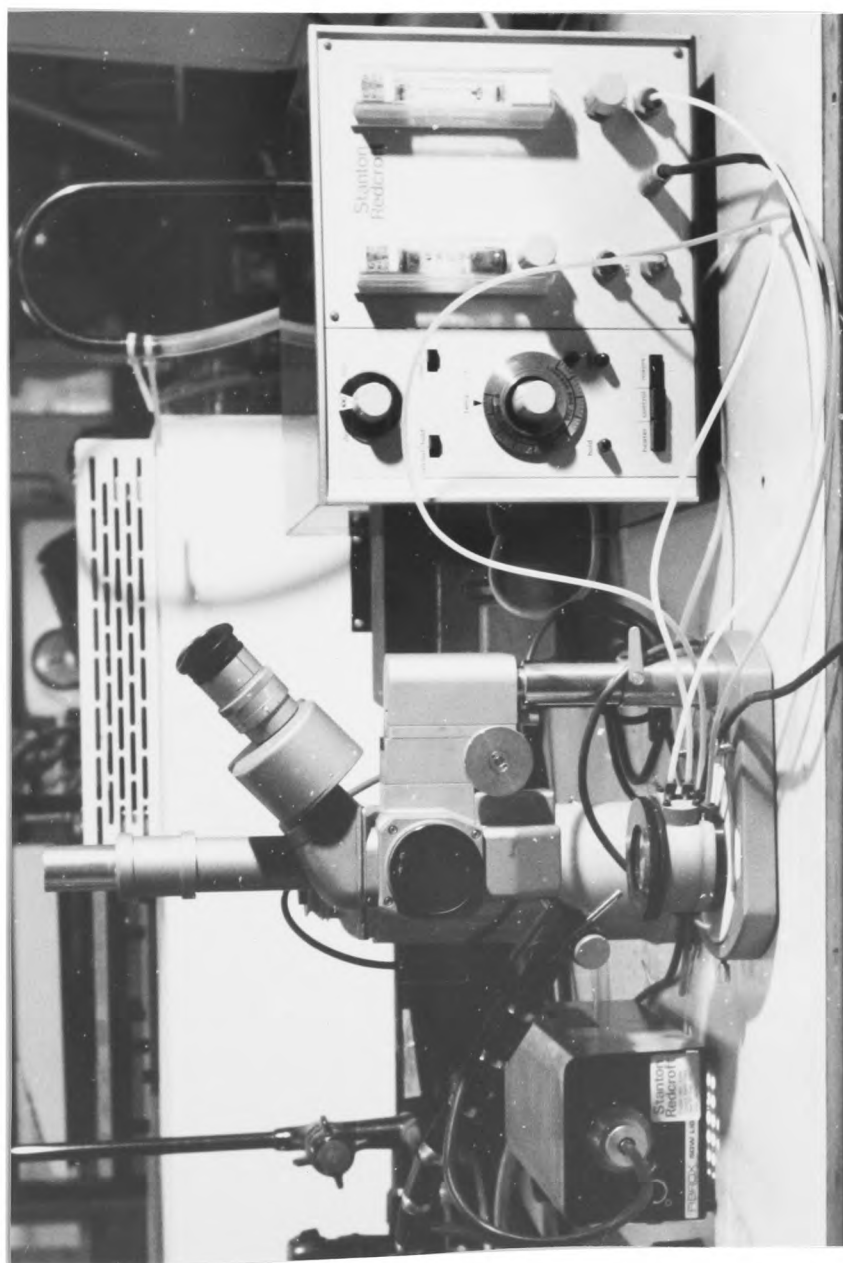
Fig. 4.13: Photograph of Hot-stage Microscopy Apparatus

CHAPTER 5

HOT STAGE MICROSCOPY.

5.1 INTRODUCTION.

The hot-stage microscope gives a purely qualitative view of the physical changes that a sample undergoes during heating in a controlled atmosphere, in this case nitrogen. The observations made using the hot-stage microscope are helpful in interpreting other results.

Both photographs and written observations were taken of the changes which the coals underwent as they were heated. Unfortunately, two problems were encountered in obtaining photographs. The first was that the depth of field of the photographic system was very narrow and caused problems in getting the camera correctly focused. The second problem was the condensation of the tarry volatiles upon the quartz window. This persisted despite the use of a high purge rate to carry the volatiles away before they had a chance to condense. Photographing the coal through the haze of the

volatiles proved to be a pointless exercise as clear photographs could not be obtained due to light being reflected back from the haze of tar. Fortunately, observations could be made through this haze and photographs were taken of the samples before and after pyrolysis to act as references for hand-drawn illustrations of what happens to the sample. These photographs are presented in figure 5.1 and the illustrations in figure 5.2. Descriptions of what was observed are given below for each sample with the exception of 101 Cynheidre which undergoes no observable physical changes.

5.2 PYROLYSIS OF 201A PENRIKYBER.

Initially, the sample is a fine powder consisting of homogeneously sized, angular particles. Many of these particles are highly reflective and thus appear to be white or grey due to the light they reflect. Upon pyrolysis, no visible changes occured until a temperature of 380°C is reached. At this point, tar, produced by the pyrolytic breakdown of the coal substance, oozes out of the coal particles and, upon inflation by the encapsulation of

volatile gases, forms bubbles. As the temperature increases, more gases are produced and are trapped within the tar bubbles, which eventually burst when the internal pressure becomes excessive and the gases escape. As the temperature approaches 500°C, some of the gaseous volatiles begin to condense upon the quartz hot-stage cover and form a yellow, tarry deposit. This indicates that the light tar fraction is vapourizing from the sample, and these molecules may possibly result from the larger tar molecules decomposing. Concurrent with the formation of this tarry condensate is the observation that the particles within the sample can be observed to melt and fuse into a darker, more lustrous solid which has smoother, less angular contours. At this stage, the main part of the pyrolysis is complete. As the sample temperature increases still further to 800°C, the solid shrinks slightly, and its edges creep away from the sides of the sample pan. A slight swelling of the sample may also be observed and this is caused by the earlier formation of tar bubbles within the sample.

5.3 PYROLYSIS OF 203 OGMORE.

Before heating, this sample is composed of a fine powder with evenly sized, angular particles. Widely distrubuted are particles with a high reflectivity which are observed as pinpoints of light. Upon pyrolysis, tarry volatiles first begin to condense on the quartz cover at around 420°C. As the sample temperature increases to 470-500°C, the coal particles begin to swell, crack and exude tar which is blown into bubbles as volatile gases are produced and trapped within the tar. These globules appear as tiny beads spread over the surface of the sample. As the sample temperature increases to 560°C, the tar formation accelerates, the condensation of tarry volatiles upon the quartz cover increases markedly and the melting of particles of coal can be seen. By 630°C, the coal particles have begun to fuse together to produce a more solid sample which has rounded contours and particles and an increased lustre. With a further increase in sample temperature to 730°C, cracks in the sample together with with a small amount of shrinkage in sample size occurs, resulting in a final shrunken, cracked, lustrous solid.

5.4 PYROLYSIS OF 301A CWM.

The initial sample consists of fine grains interspersed by large, angular particles. Most of the sample particles are reflective and appear silvery-grey or almost white. As the sample is heated, no signs of pyrolysis are observed until a temperature of 350°C is reached. At this temperature, volatiles produced by the decomposition of the sample begin to condense on the quartz cover and form a misty haze. At around 400°C volatiles can be seen to condense in the furnace atmosphere as a fine yellowish mist. Also at this temperature, yellow tar begins to condense upon the hot-stage quartz cover. As the temperature approaches 430°C, the first signs of a thick, heavy tar oozing out of the coal particles is observed and by 450°C some of the coal particles begin to swell, crack and exude tar. The tar is blown into bubbles as the gaseous volatile products which are formed are trapped within the tar. At 510°C the evolution of tar is extensive and the coal sample has begun to swell and melt. By 520°C, the sample has begun to "boil and bubble" rather like black treacle or toffee boiling. Tar bubbles are constantly being formed and then bursting. As

these bubbles burst, a network of large, open pores is formed. These reactions continue until a temperature of around 600°C is reached when they rapidly cease, and by 640°C the reaction is complete. The resultant solid is a porous, swollen, lustrous coke which has rounded contours.

5.5 PYROLYSIS OF 301B CELYNEN SOUTH.

The unpyrolysed sample comprises mainly of fine grains interspersed with a few angular "lumps". Most of the grains in the sample are highly reflective. As the sample is pyrolsed, and the sample temperature approaches 350°C light, misty volatiles begin to condense upon the quartz cover of the hot-stage. By 440°C these volatiles change in nature to a yellow, oily condensate, and at 440°C the coal particles begin to exude tar. At 490°C tar formation is extensive throughout the whole of the sample, and by 500°C the whole of the sample appears to have melted and boils and bubbles rather like boiling treacle. This liquid state is viscous and shiny, the bubbling being caused by the evolution of gaseous products from the coal which also cause the sample to swell and to develop a system of large, open pores. As the temperature rises, this reaction diminishes in ferocity and by 570°C the reaction is almost complete. The final

solid is a highly swollen, greatly porous, lustrous coke with rounded and smooth contours. The large pores are formed by the collection of gaseous products within the viscous, fluid during the plastic stage of pyrolysis. When the pressure within the trapped bubbles of gaseous products has reached a high enough level, the fluid layer bursts and the gases escape. This process is also the cause of the swelling of the sample. The formation of this fluid mass and the "boiling" in both this sample and the sample of 301A Cwm, corresponds to the softening, degassing and condensation processes of coke formation as formulated by Van Krevelen et. al.[13,14,15]

5.6 PYROLYSIS OF 501 LLANHARAN.

At the start of the experiment, the sample comprised of a fine powder with some reflective particles dispersed throughout it. As the sample temperature is raised, no visible signs of pyrolysis are noted until a temperature of 250°C is reached when some volatiles begin to condense on the quartz window of the hot-stage. This condensation gradually increases as the temperature increases and at 400°C the sample begins to swell slightly and the formation of tar bubbles can be observed. These tar bubbles begin to

fuse the individual particles of the sample together. By 450°C there is extensive volatile condensation on the quartz window. Also, cracks begin to appear in the sample due to the start of sample shrinkage. The tar bubbles begin to burst at around 470°C as the rate of volatile release increases; concurrent with this is an increase in the rate of formation and number of tar bubbles. By 530°C the reaction has begun to ease off, and has almost ceased by 550°C. Shrinkage of the solid continues and the cracks in the sample widen. This reaction has stopped by 800°C. The final sample is a cracked, shrunken, lustrous solid whose surface is "bubbly" and porous in appearance.

5.7 PYROLYSIS OF 701 LLANHARAN.

The initial sample consists of a fine powder with numerous shiny motes dispersed throughout the sample. Volatiles begin to condense on the quartz window at around 290°C, and by 350°C this condensation is extensive. Also at this temperature, tiny tar bubbles begin to appear upon the sample surface. The condensation of the tarry volatiles continues to such and extent that by 550°C it becomes difficult to see through the condensate to the sample. All that could be made out was that there were myriad tiny tar

bubbles over the sample surface. Once the upper temperature had been reached and the sample cooled and viewed without the quartz window, the final solid could be seen to be very shrunken, lustrous and smooth.

From the illustrations, photographs, and recorded observations, it is obvious that each coal sample decomposes in a characteristic way. It is the temperature at which various reactions are observed to begin and end that are important rather than the actual reactions, although the sudden releaase of volatile matter through bursting tar bubbles with a resultant loss in weight may be of importance in the interpretation of the thermogravimetric results.
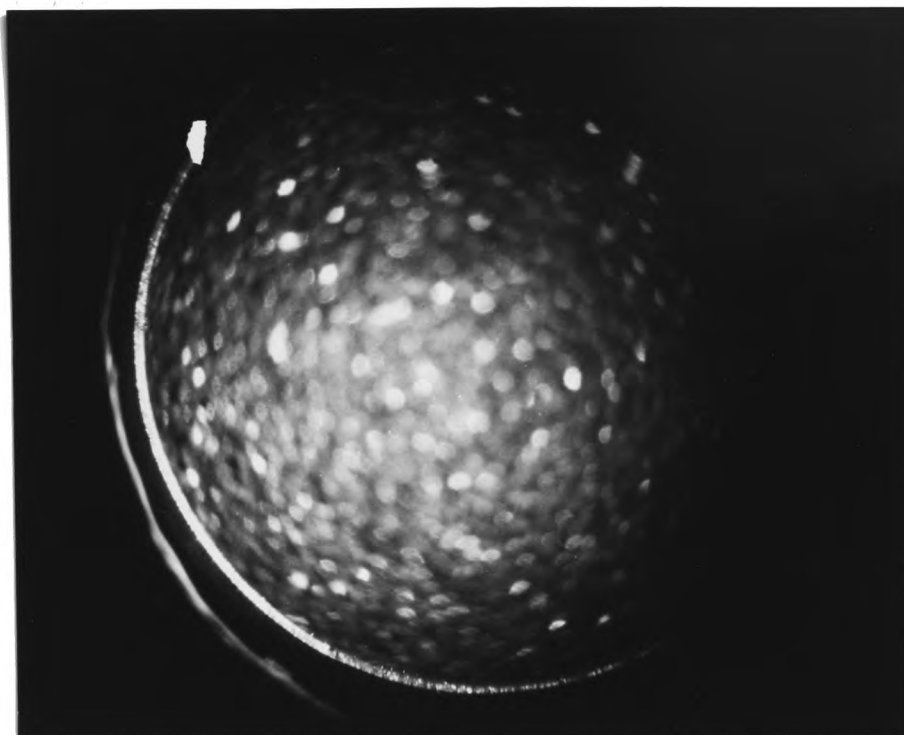
Before
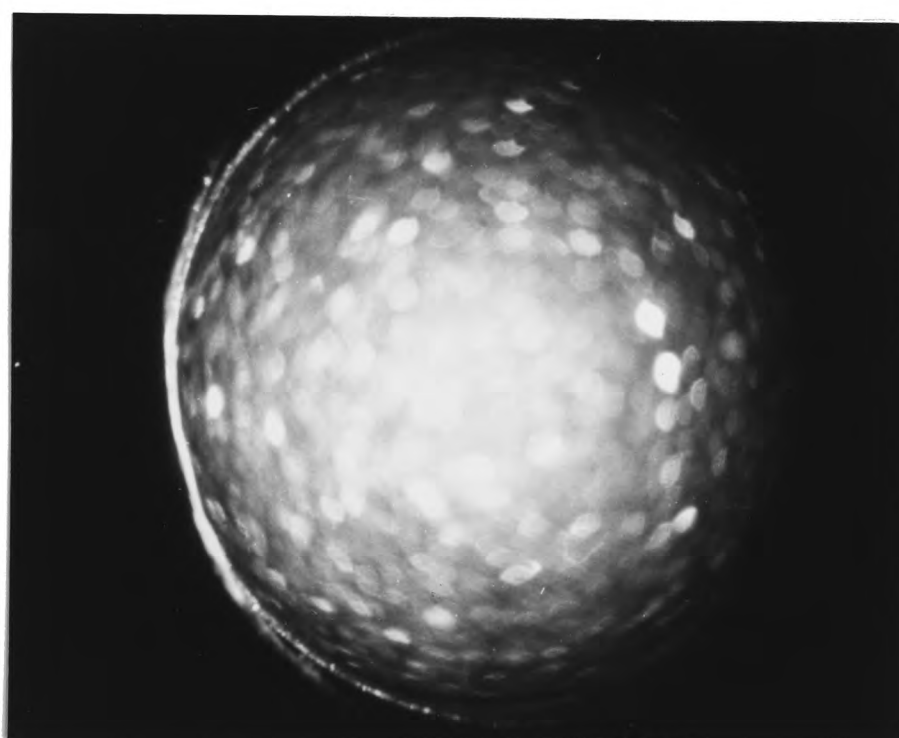
After.

Fig 5.1 a. 201A Penrikyber

Fig 5.1 : Photographs of the Samples Before and After Pyrolysis.

Page 163
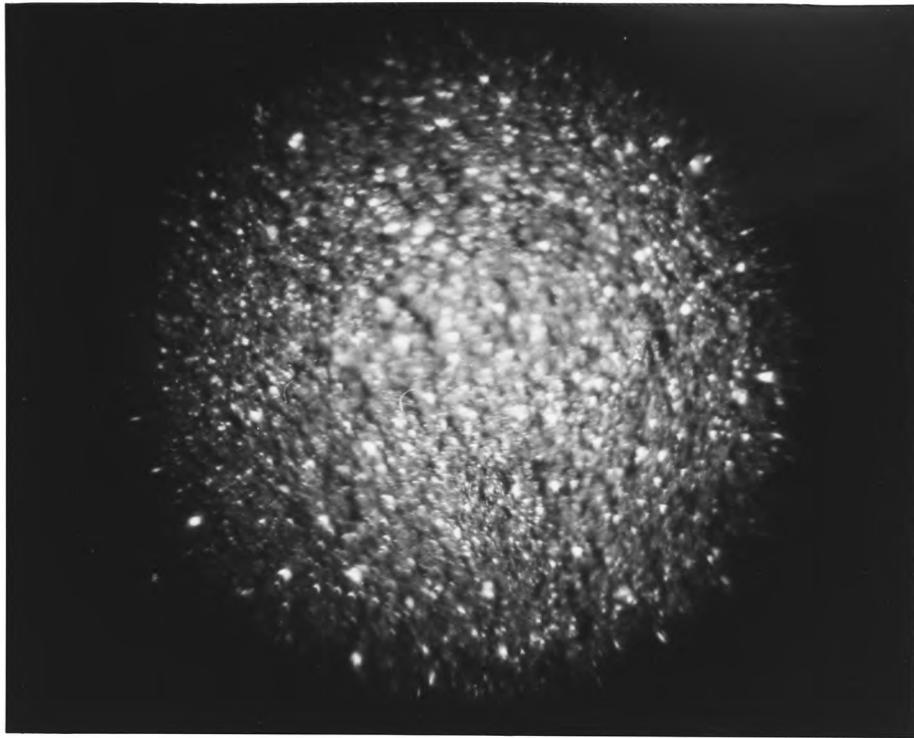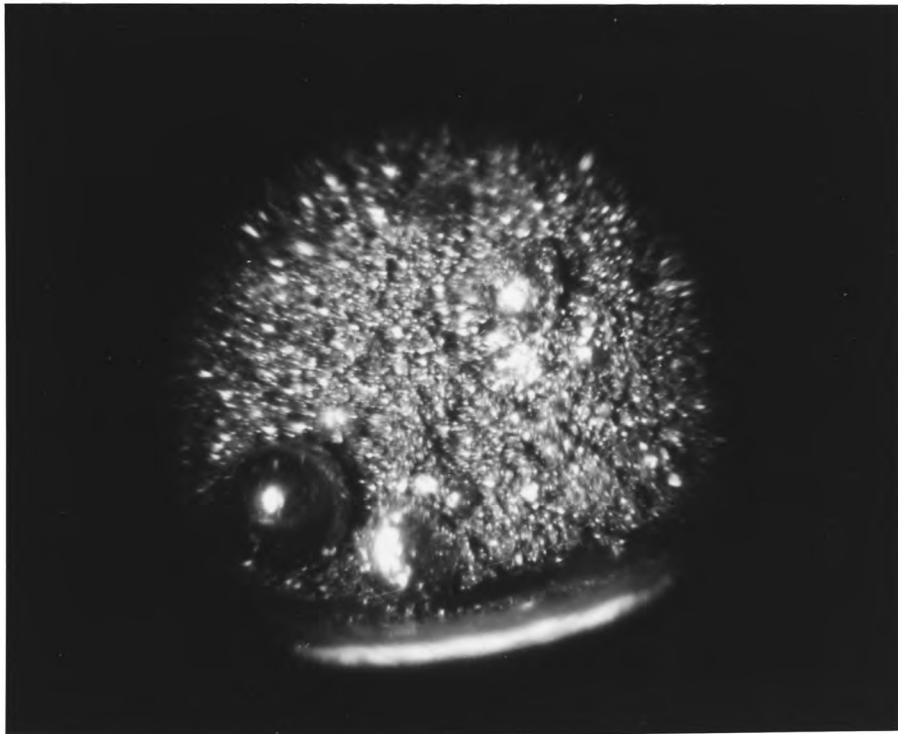
Before

After

Fig 5.1 (b): 203 Ogmore
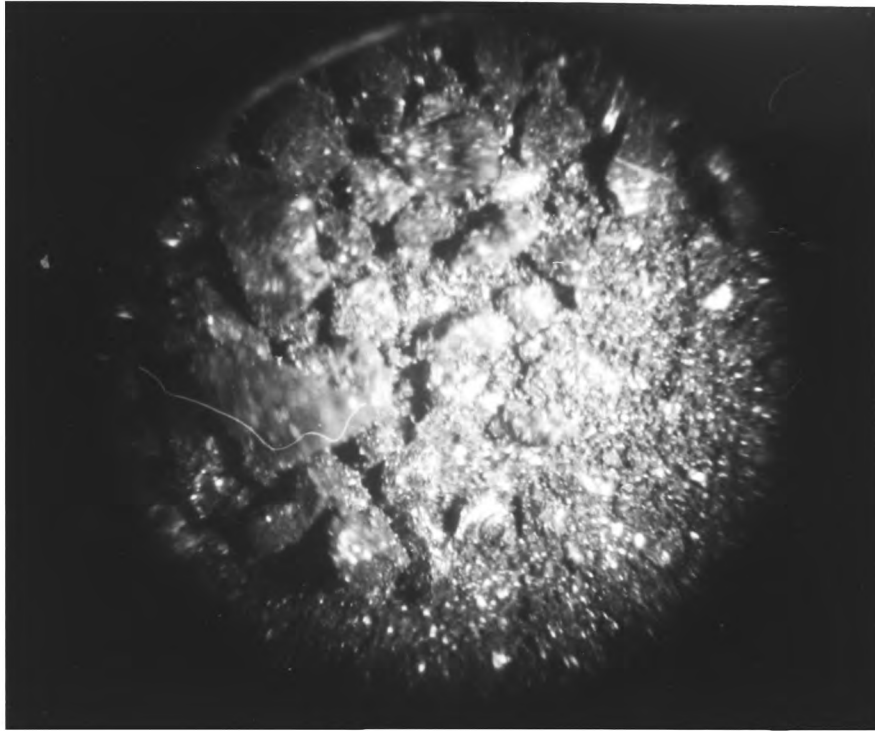
Before

After.

Fig 5.1 (c)   301A Cwm

Page 165
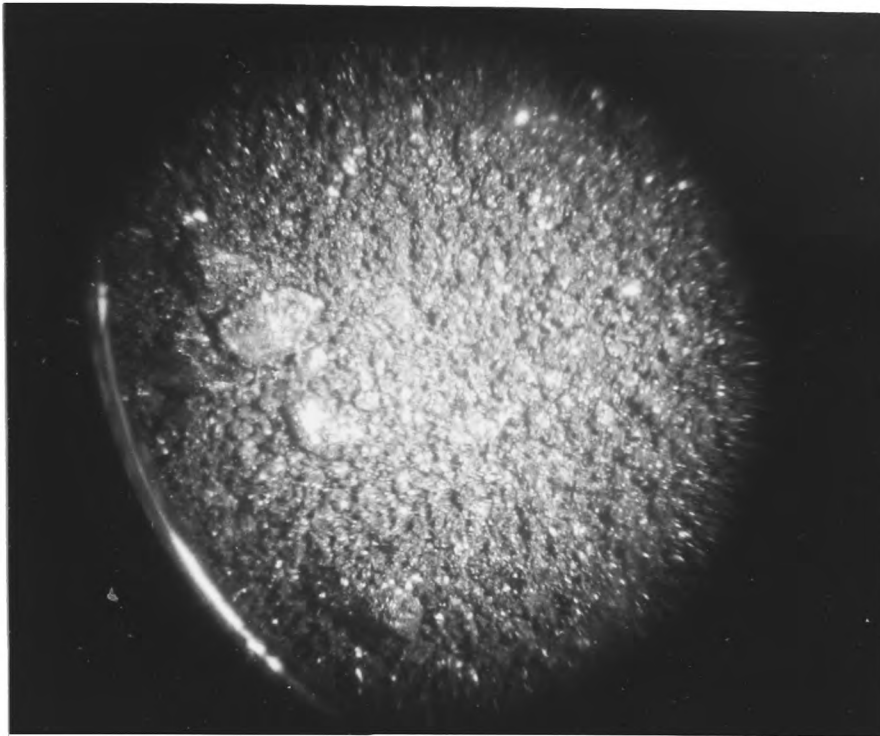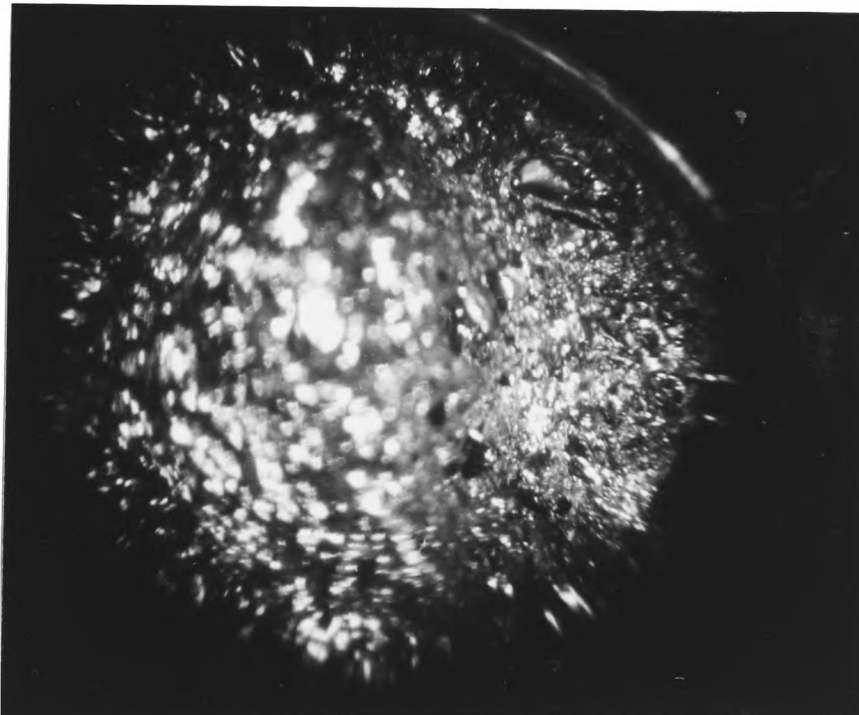
Before.

After.

Fig 5.1 (d) 3018 Celynen South
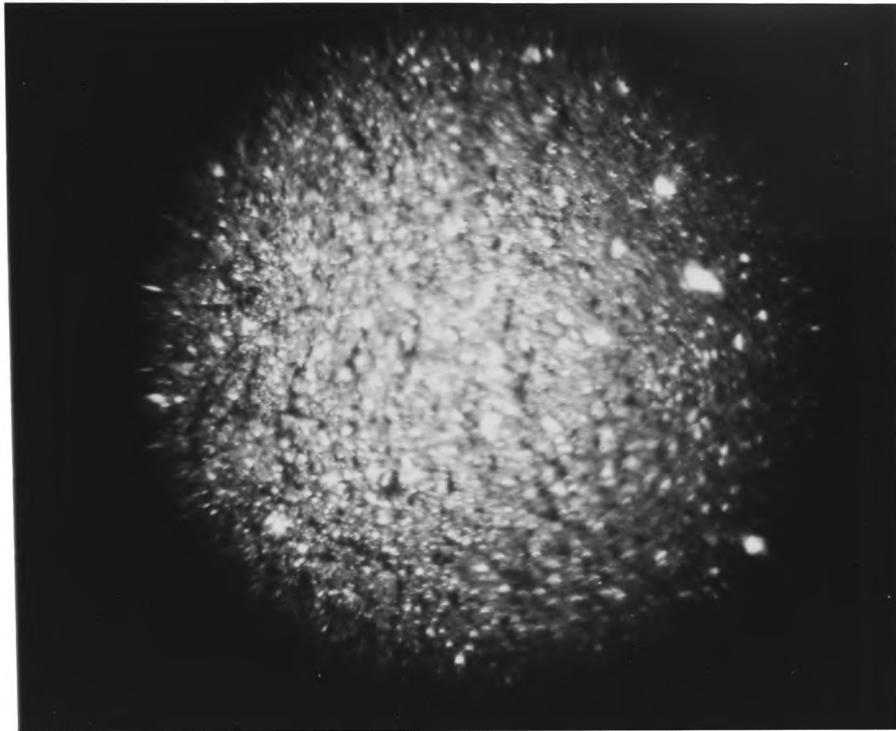
Before
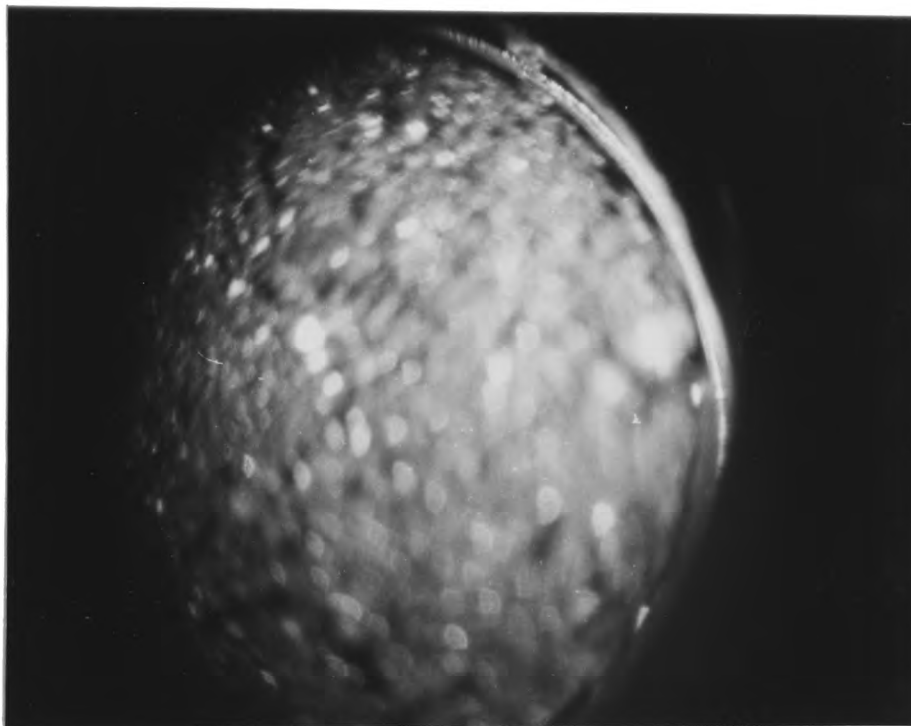
After.

Fig. 5.1 (e)   501 Llanharan
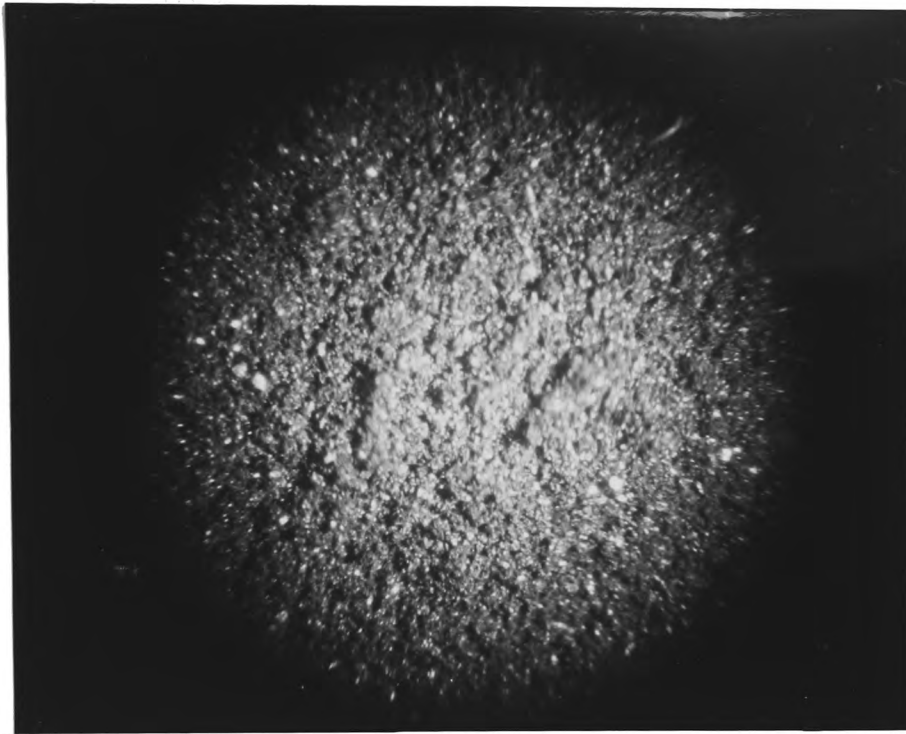
Before
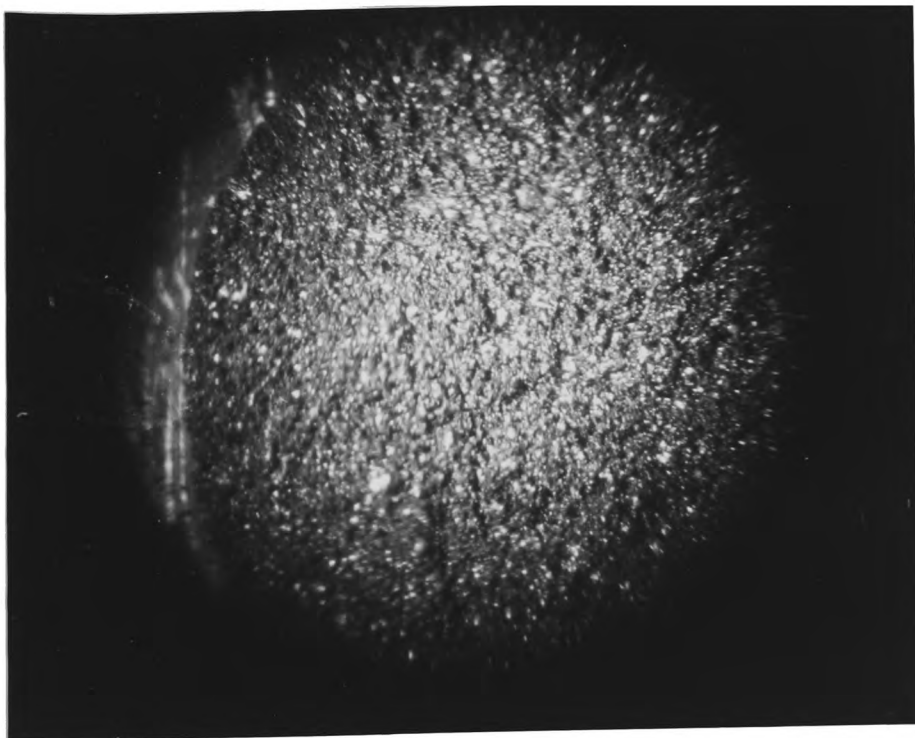
After

Fig. 5.1 (F)   701 Llanharan

(a) 201A initial sample   201A 380°C   201A final solid

(b) 203 initial sample   203 560°C   203 Final solid
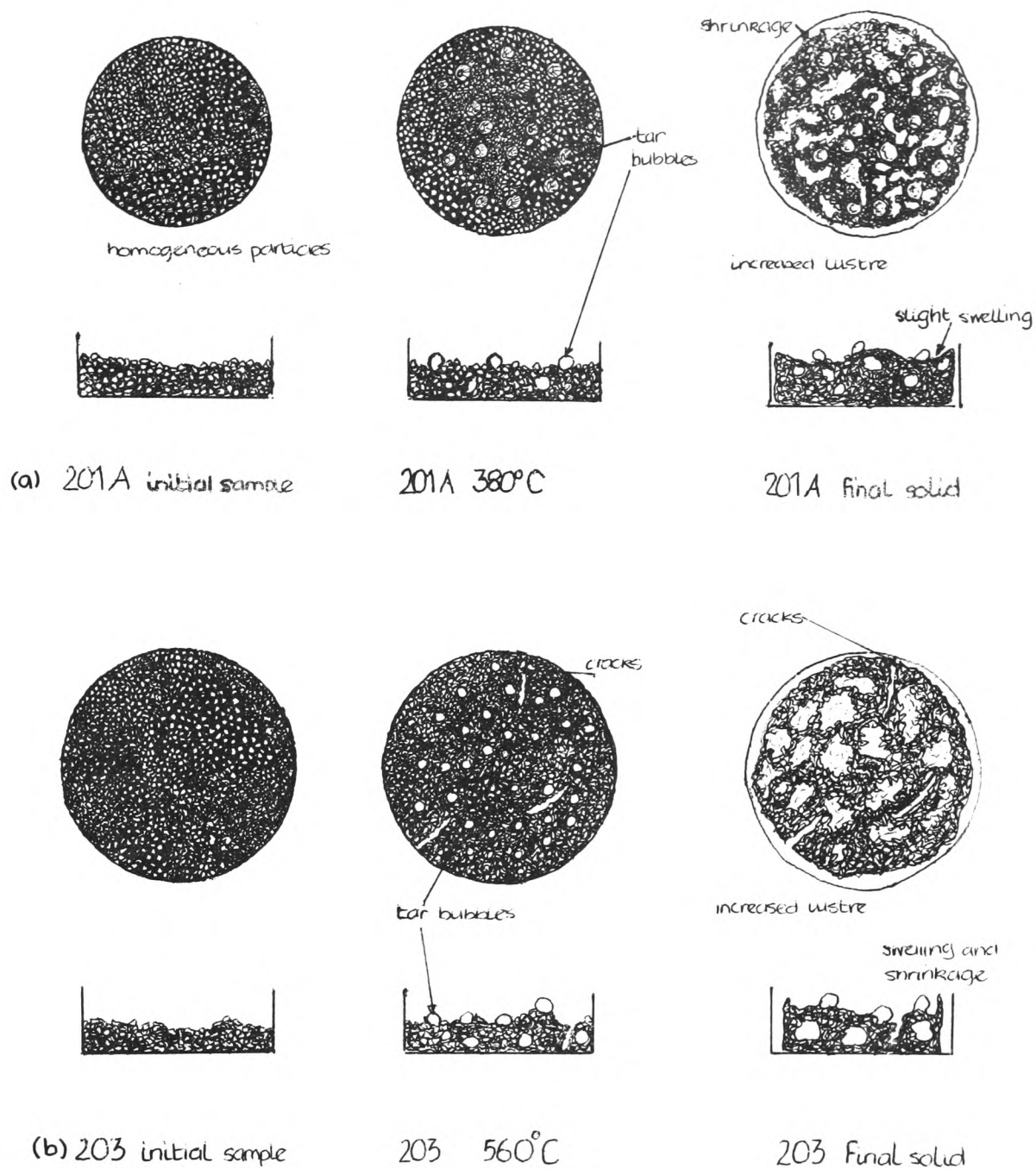
Figure 5.2   Hot Stage Illustrations.

tar bubble — fluid mass — shiny, smooth solid coke

some large particles present — bursting tar bubble — large pores developed

301A Initial Sample — 301A 570°C — 301A Final Coke.

fluid mass

tar bubble — pore development

301B Initial Sample — 301B 530°C — 301B Final Coke.

Fig 5.2 cont.

shrinkage

cracks

tar bubbles
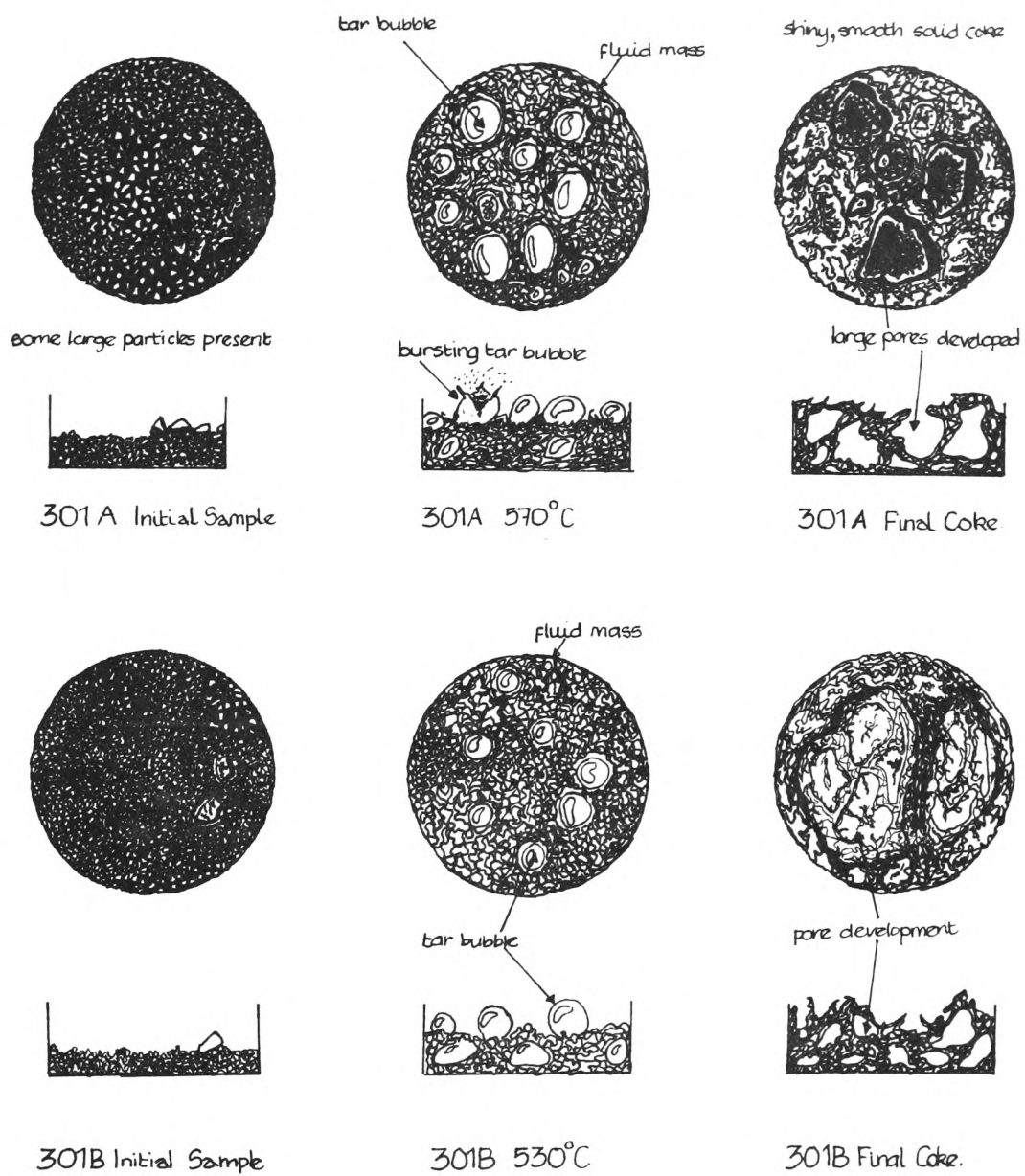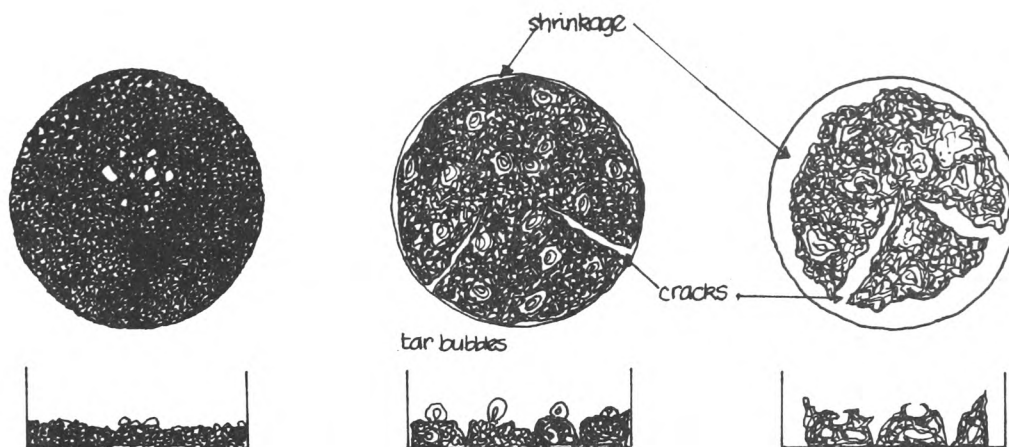
501 Initial Sample   501 510°C   501 Final Solid

small tar bubbles

shrinkage
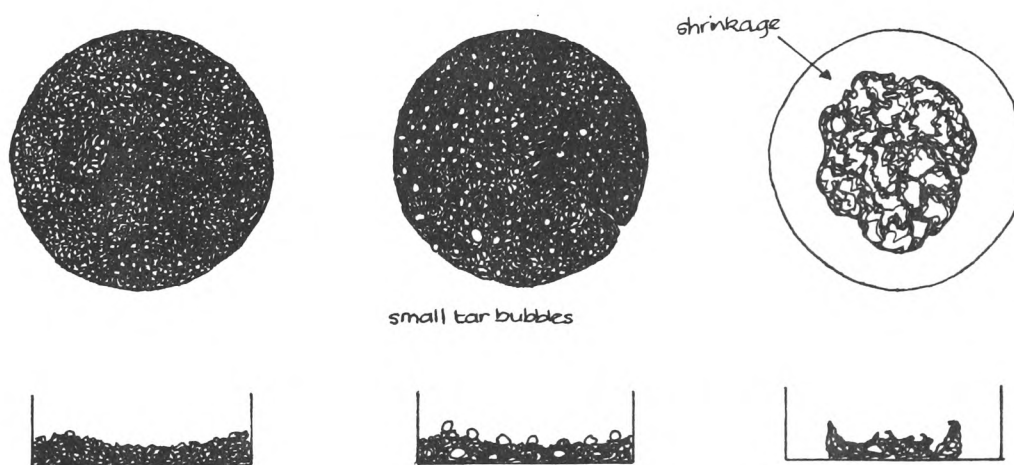
701 Initial Sample   701 480°C   701 Final Solid

Fig. 5.2   cont.

Page 171

CHAPTER 6.

THERMOGRAVIMETRIC CHARACTERIZATION OF THE PYROLYTIC
BEHAVIOUR OF THE COAL SAMPLES.

6.1 INTRODUCTION.

At the start, a discussion is necessary of the numeric rate
of weight loss results used in the account. The results
have all been standardized for an initial sample weight of
10 mg. This does not affect the %weight loss (TG) curve,
nor the shape of the rate of weight loss (DTG) curve, but it
does change the values of the rate of weight loss on the DTG
curve. This manipulation of data is performed to allow the
easy comparison of results from samples of slightly
different starting weights. This can be done quite easily
as there is a simple linear relationship between the initial
weight and the rate of weight loss at any point. For
instance, if the initial weight is halved, then dW/dt at any
point will also bee halved. Thus a simple forumula may be
used for conversion.

$$DTG_{stand} = DTG_{original} \times (10 \text{ / original sample weight})$$

This initial part of the investigation aims to

1. characterize the pyrolytic behaviour of the coal samples in order to establish trends in behaviour over the series of coals studied

2. select two samples to be studied with the addition of transition metal elements in order to assess any catalytic effects

3. select the optimum experimental conditions for these catalytic studies.

Much of the work completed at a heating rate of $80^{\circ}Cmin^{-1}$ has been previously published by the author[136].

6.2 THE EFFECT OF COMPUTERISED DATA COLLECTION.

In an earlier chapter (Chapter 4), the computerised method of data collection was verified. Figure 4.9 gave a comparison of a chart recorder TG/DTG curve of the same coal. From this figure it can be seen that the computer produced graph contains a much greater number of DTG peaks and thus contains much more information. It is this increased amount of information which gives the computerised system its value.

Unfortunately, the increased sensitivity of the system is not without a problem. This is that of electronic noise in the TGS-2/computer system. If all of this were to be filtered out then the computerised system would be effectively reduced to the level of an ordinary chart recorder and would yield no extra information. But, with the noise being recorded and a greater number of identical experimental runs carried out under each set of experimental conditions with each sample, then any spurious peaks which are directly attributable to the noise can be eliminated during subsequent investigations or calculations. Indeed, the curves over the major region of weight loss for any one experiment are practically identical, small variations are more likely to be due to the heterogenous nature of coal itself.

The greater number of DTG peaks is directly attributable to the increased sensitivity of the data recording system, which is more capable of differentiating between smaller variations in the sample weight than is the chart recorder system. It is postulated here that each of these peaks is either produced by a different type of reaction occurring within the sample or is directly related to the production of tar bubbles within the sample, as seen in the hot-stage investigations, which trap volatile products, and their

subsequent bursting, which will result in a sudden weight loss. It is likely that both of these propositions are correct, and it ; is a combination of these which results in the fine structure seen in the DTG curve. It is proposed that this fine structure could be used in a system of fingerprinting the pyrolysis behaviour of coals.

6.3 TRENDS IN BEHAVIOUR OBSERVED WITH VARIATIONS IN COAL RANK AND HEATING RATE.

Previous researchers[36] have established that the heating rate is the only experimental variable to significantly affect thermogravimetric (TG) results and thus is the only operating parameter to be varied in this investigation. The following discussion will begin with a study of the effects of rank and heating rate and will then proceed with the presentation of a method for fingerprinting the pyrolytic behaviour of coals, and the conclusion will consist of a coordinating of results.

Typical TG/DTG curves for the samples studied at each of the three heating rates are shown in figures 6.1, 6.2 and 6.3. Upon inspection of these curves, it will be seen that for a decrease in rank at any one heating rate

1. the total weight loss increases

2. the maximum rate of weight loss (DTG_{max}) increases

3. the temperature at wihich DTG_{max} occurs (T_D) decreases

4. the temperature range over which the rate of weight loss (dW/dt) is greatest i.e. where most of the pyrolysable sample is decomposed and gaseous products are liberated, generally narrows

5. the resolution of the DTG curves improves markedly

and, for any one sample with increasing heating rate that

1. DTG_{max} increases

2. T_D increases

3. the temperature range over which most of the weight is lost generally widens.

These observations are in agreement with those from previous researchers[1,13,37].

Another feature of the TG/DTG curves which may be observed, particularly in the coking samples, is the occurrence of a secondary region of weight loss at higher temperatures than the major region of weight loss. This region is not as pronounced in the coals studied here as for those noted by other researchers (see Chapter 3.). These two distinct regions are well documented in the literature.

Graphical summaries of these observations are given in figures 6.4, 6.5, 6.6.

Figure 6.4 shows the variation of T_D both with rank (represented by the volatile matter to fixed carbon ratio (VM/FC)) and with heating rate. The shape of the rank curves does not vary with heating rate thus suggesting that the trend of T_D with rank is an inherent property of the South Wales coal series. The heating rate affects the values of T_D, but not the overall trend.

Figure 6.5 presents the variation of DTG_{max} with the VM/FC ratio for each heating rate. Once again, each curve has a similar shape. Again, the heating rate affects the value of DTG_{max}, but not the overall trend.

Figure 6.6 is a composite of figures 6.4 and 6.5 with DTG_{max} being plotted against T_D for each heating rate. Here also, there is a distinctive shape of curve illustrating the trends in pyrolytic behaviour. Once more, the heating rate only affects the values and not the patterns.

It is now necessary to explain the appearance of these trends, so we start with the variations due to changes in rank.

Initial weight = 5·7808 mg
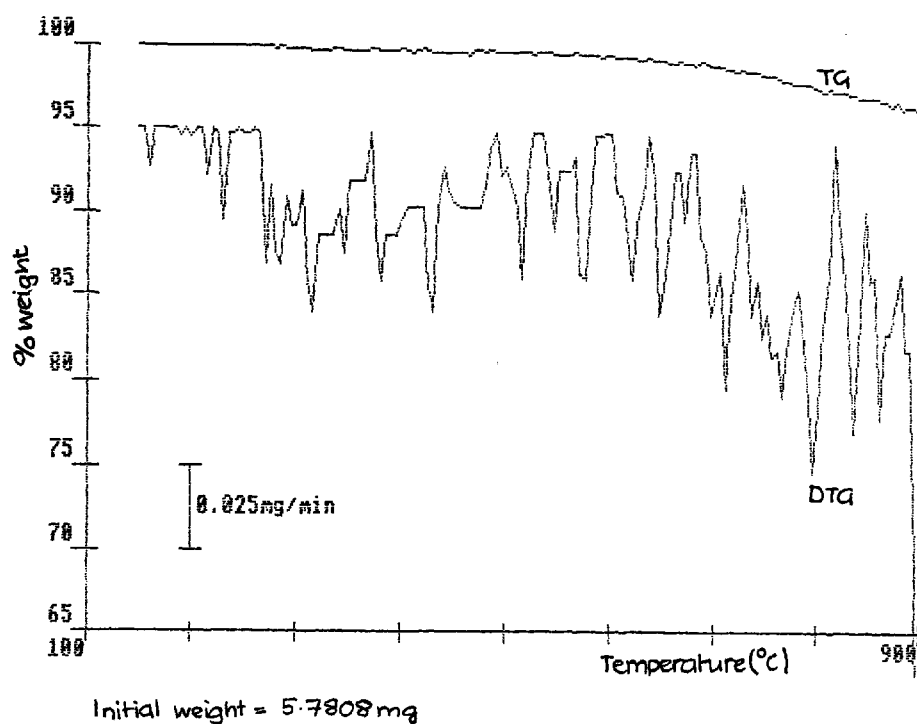
Figure 6.1a : 101 Cynheidre at 80degC/min

Initial weight= 6·4821 mg
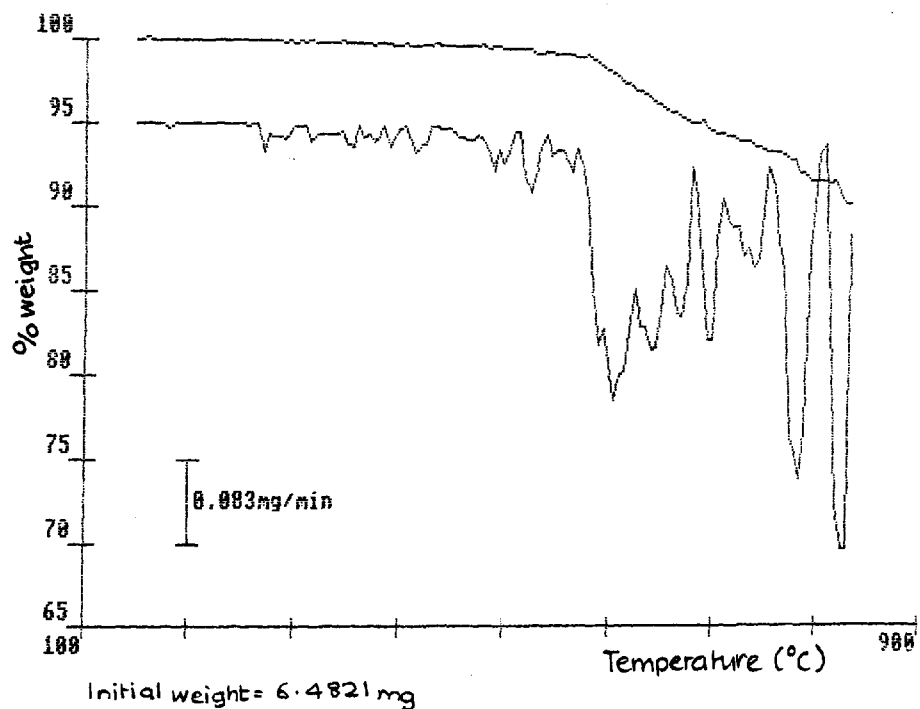
Figure 6.1b : 201A Penrikyber at 80degC/min
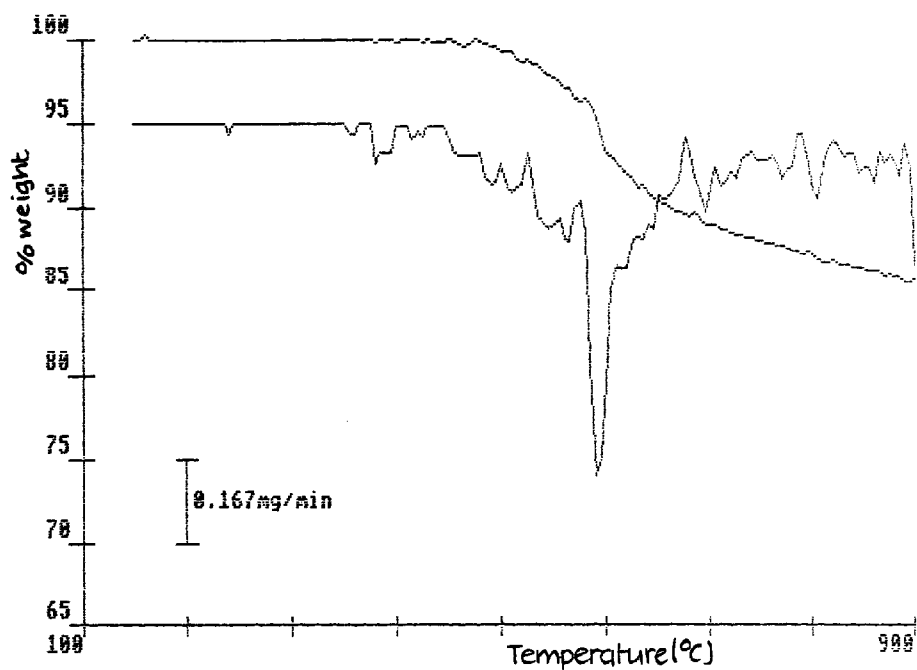
Initial weight = 5.2867 mg

Figure 6.1c : 203 Ogmore at 80degC/min
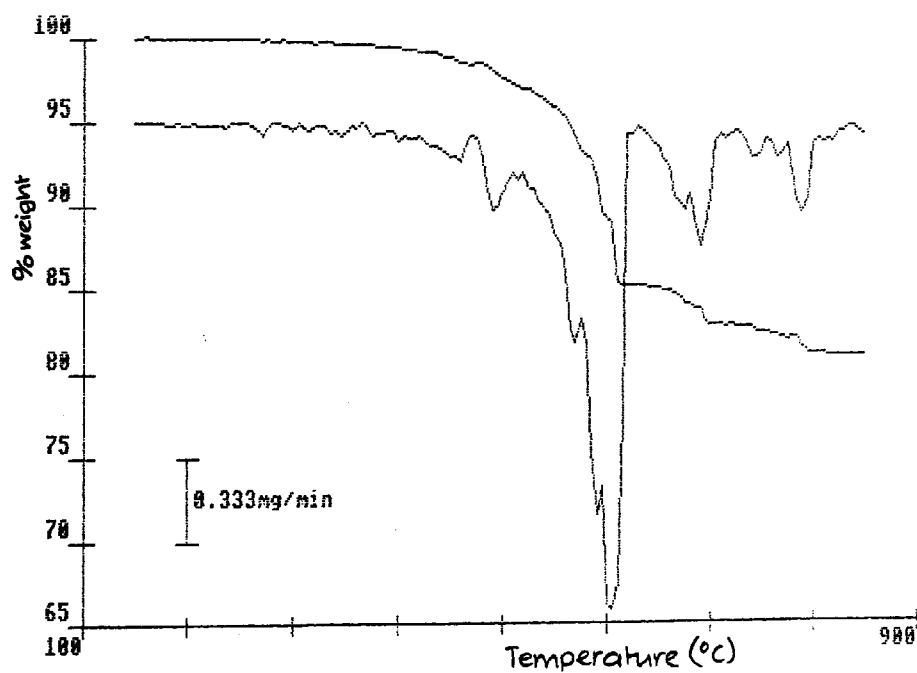
Initial weight = 9.4007 mg

Figure 6.1d : 301A Cwm at 80degC/min

Page 179
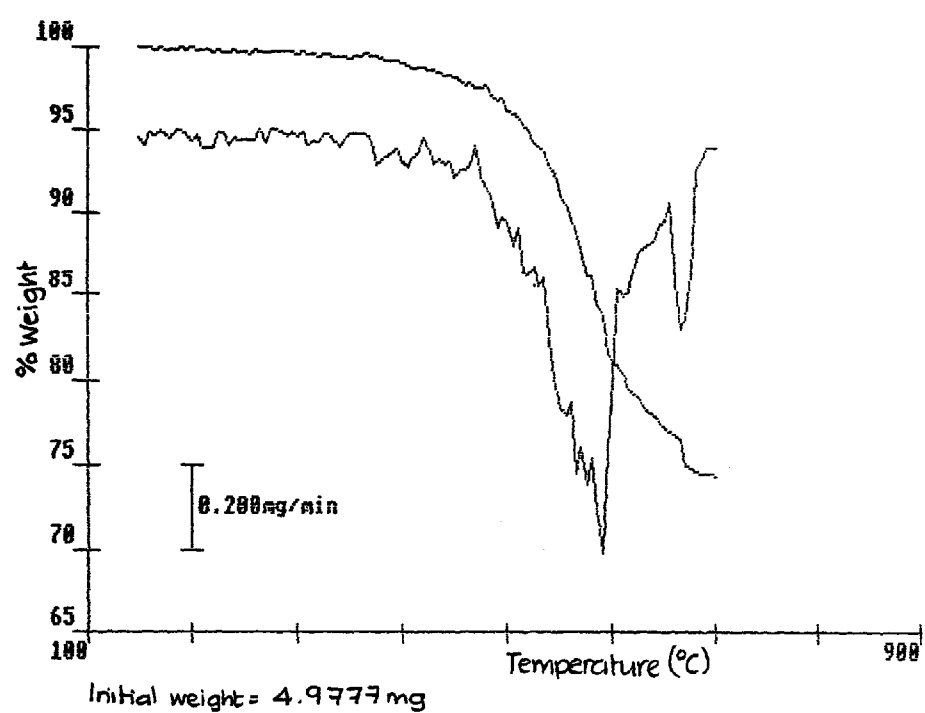
Figure 6.1e : 301B Celynen South at 80degC/min

Initial weight = 4.9777 mg
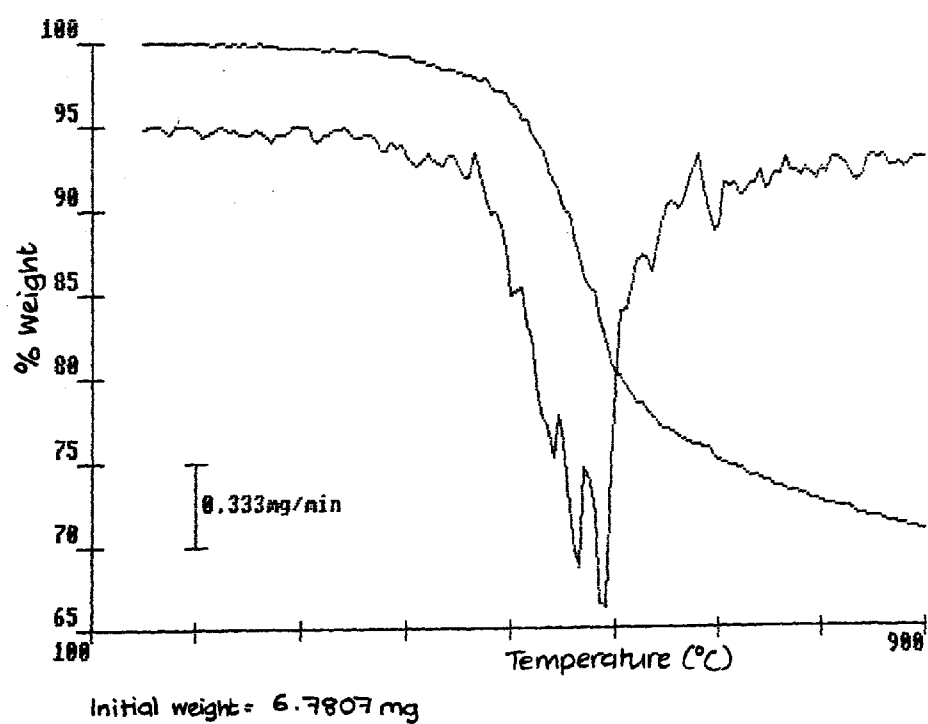
Figure 6.1f : 501 Llanharan at 80degC/min

Initial weight = 6.7807 mg

Initial weight= 6.6001 mg
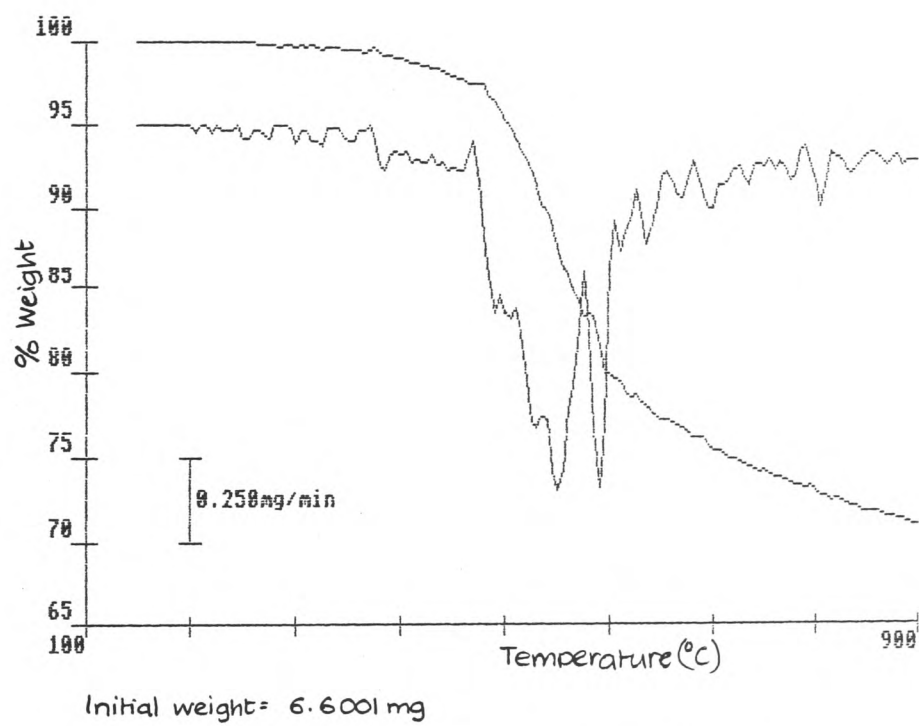
Figure 6.1g : 701 Llanharan at 80°C/min

Figure 6.1: Pyrolysis of the Coal Samples at a Heating Rate of 80°C/min . N₂ atmosphere.

Initial weight= 6.8262 mg
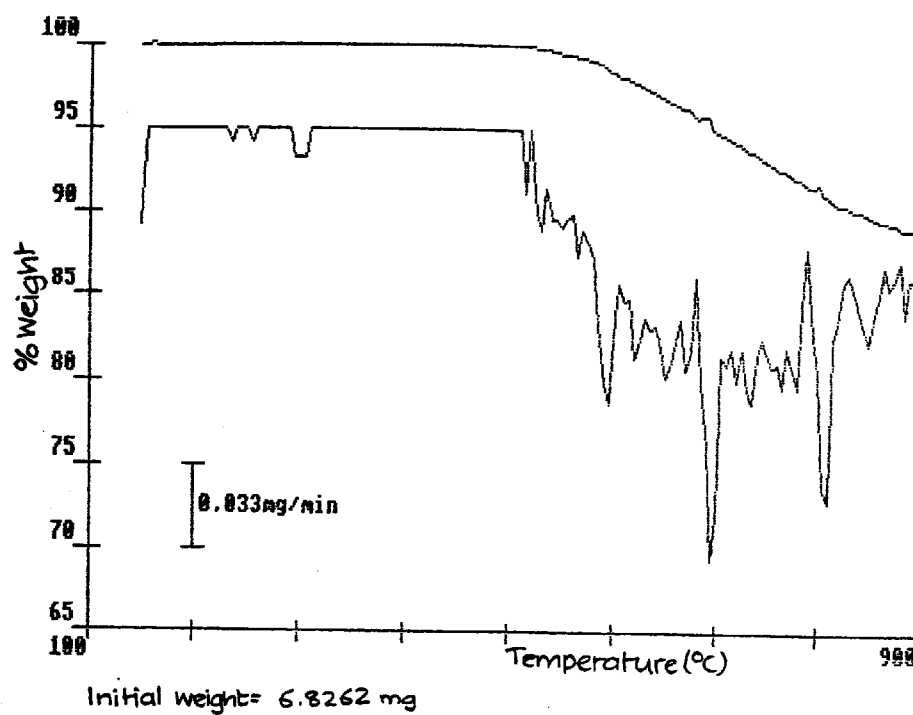
Figure 6.2a : 201A Penrikyber at 40degC/min

Initial weight= 7.1361 mg
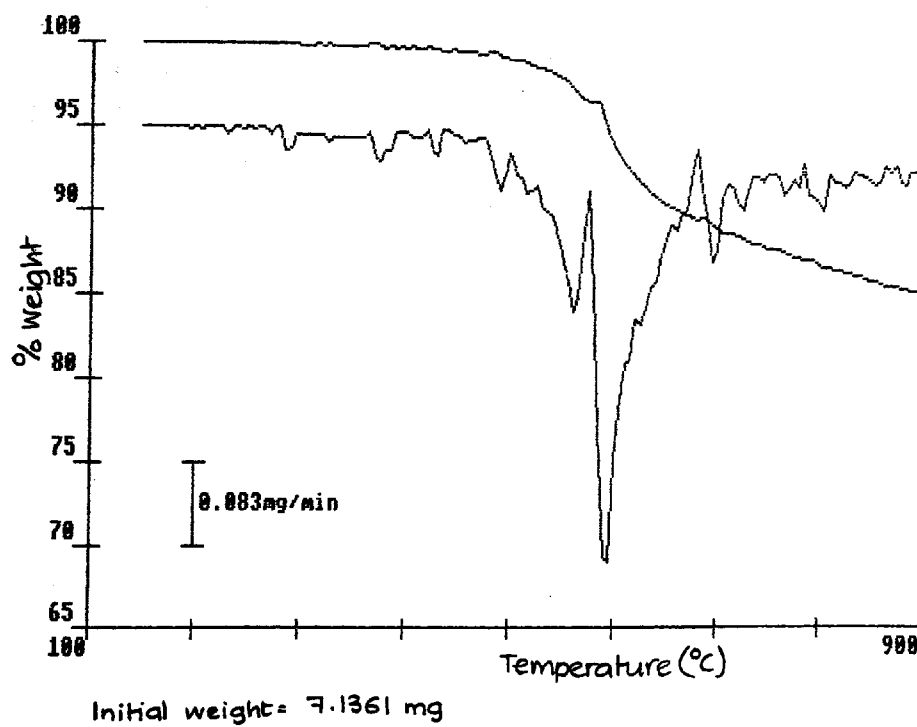
Figure 6.2b : 203 Ogmore at 40degC/min
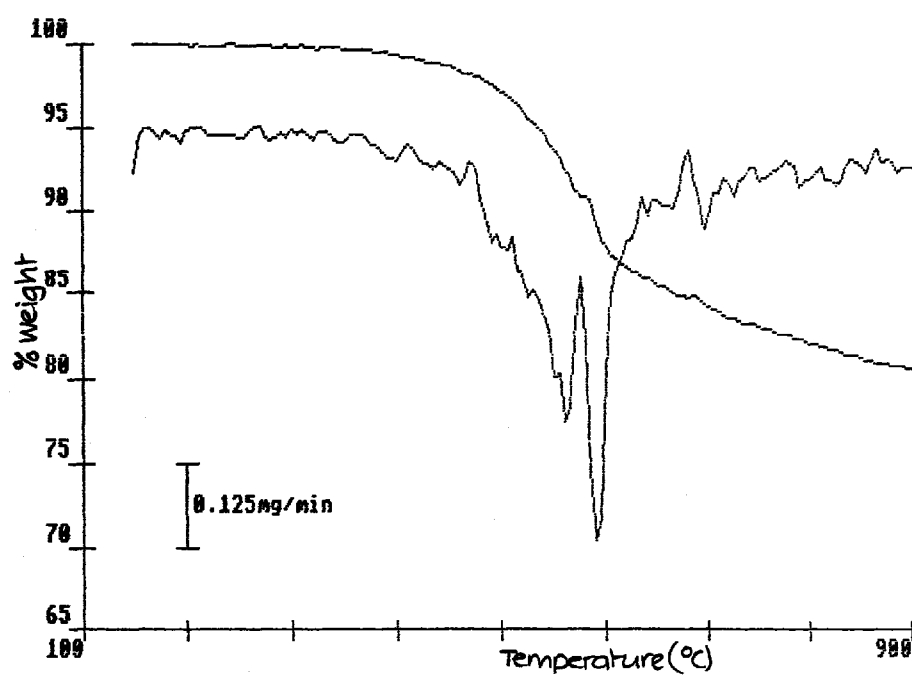
Initial weight = 9.0047 mg.

Figure 6.2c : 301A Cwm at 40degC/min
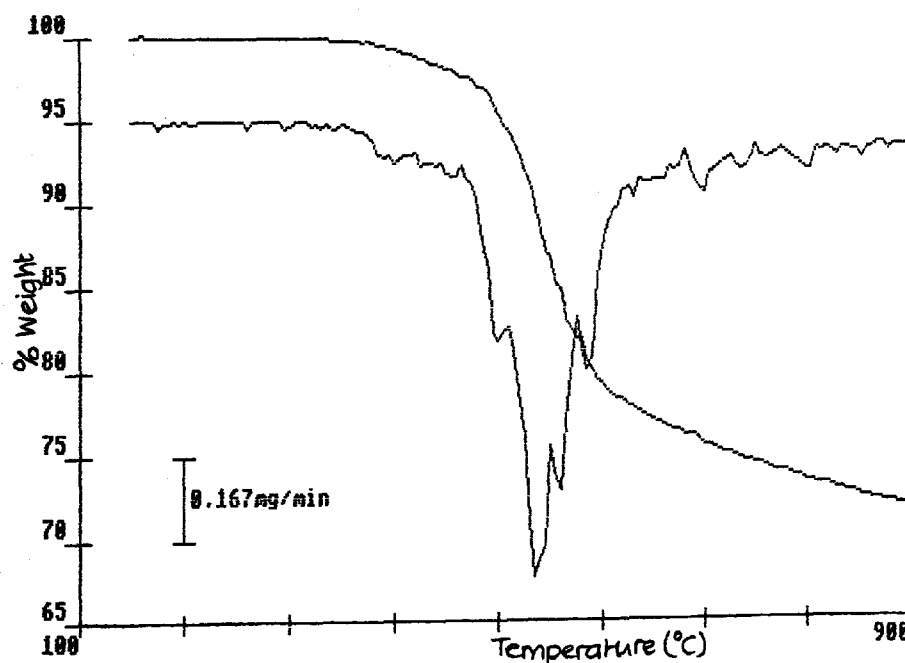
Initial weight = 8.9490 mg

Figure 6.2d : 301B Celynen South at 40degC/min.

Initial weight = 8.8269 mg
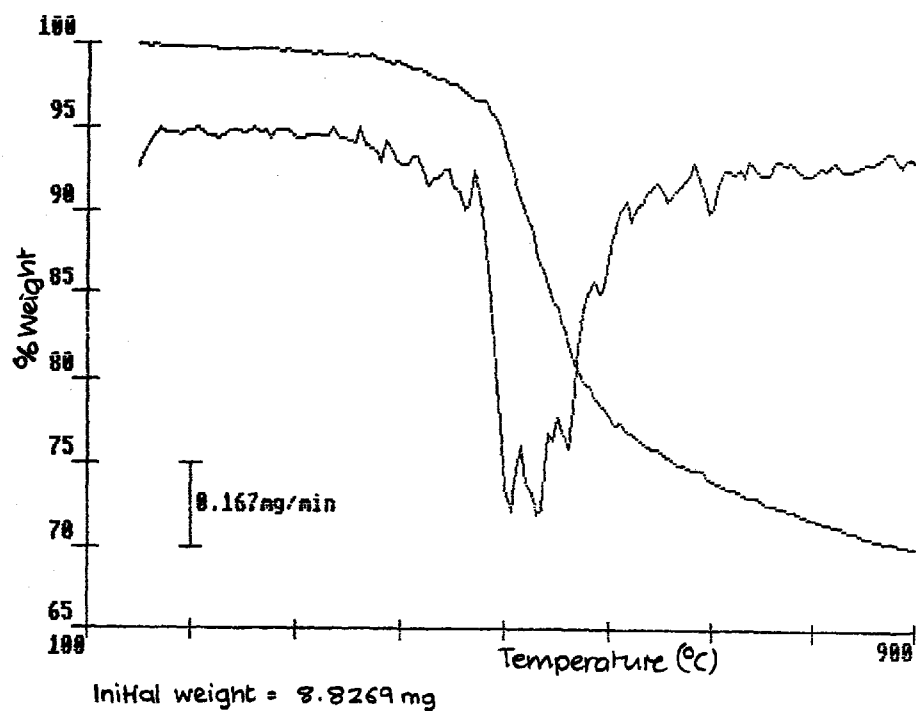
Figure 6.2e : 501 Llanharan at 40degC/min.

Initial weight = 7.8780 mg
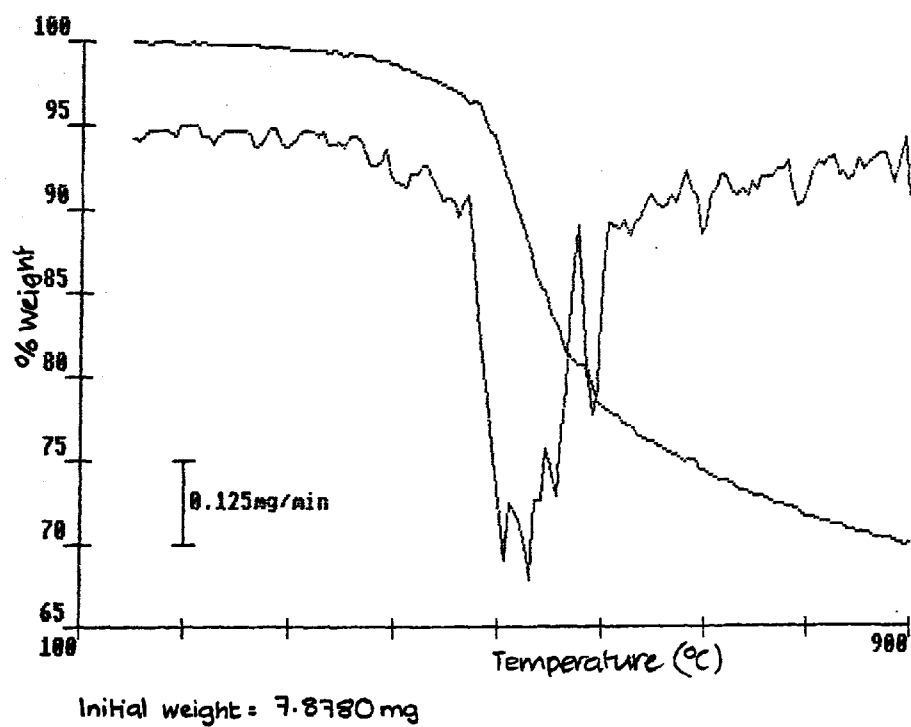
Figure 6.2f : 701 Llanharan at 40degC/min.

Figure 6.2 : Pyrolysis of the Coal Samples at a Heating Rate of 40°C min⁻¹

Initial weight= 7.4492 mg
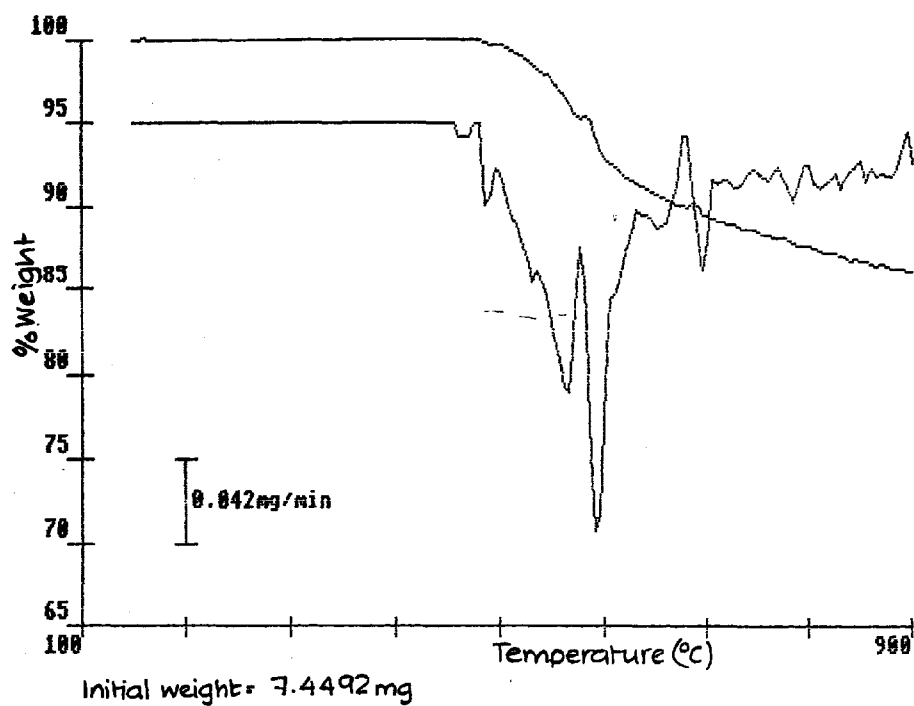
Figure 6.3a : 203 Ogmore at 20degC/min.

Initial weight = 9.8131 mg
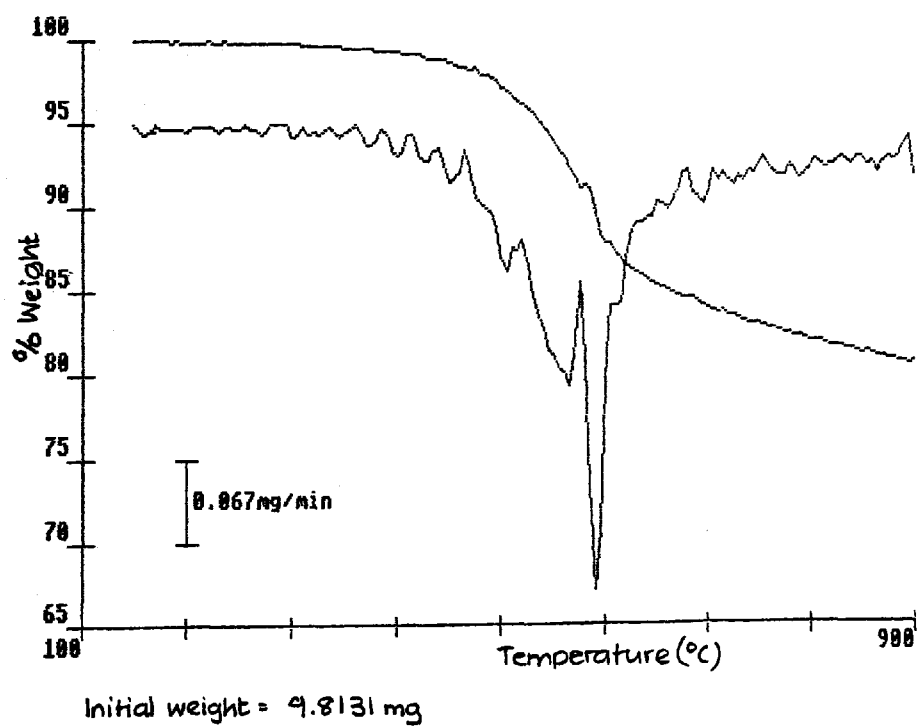
Figure 6.3b : 301A Cwm at 20degC/min.

Page 185
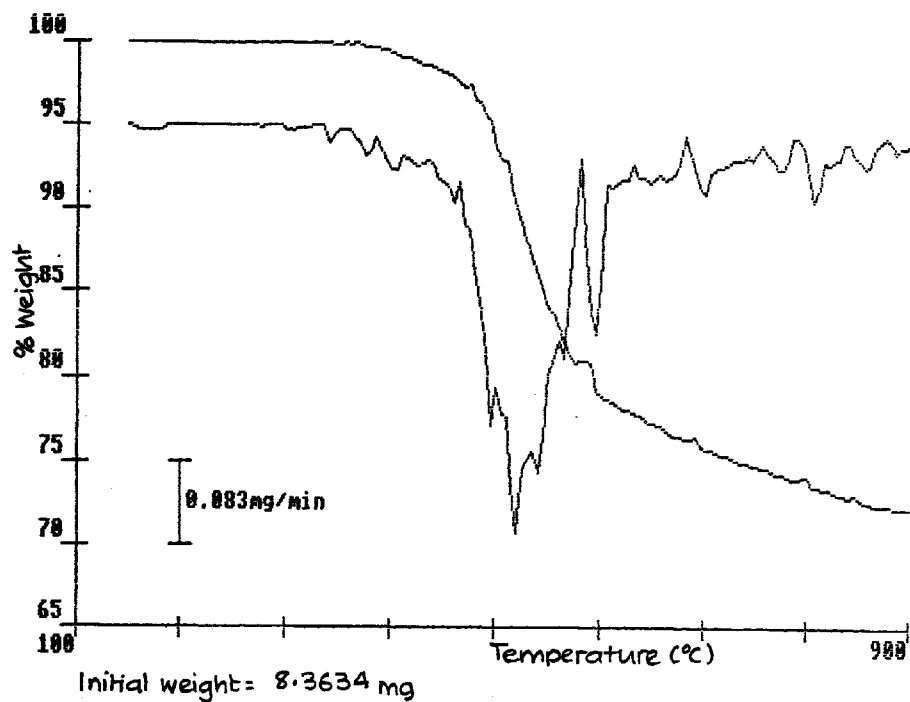
Figure 6.3c : 301B Celynen South at 20degC/min.

Initial weight= 8.3634 mg
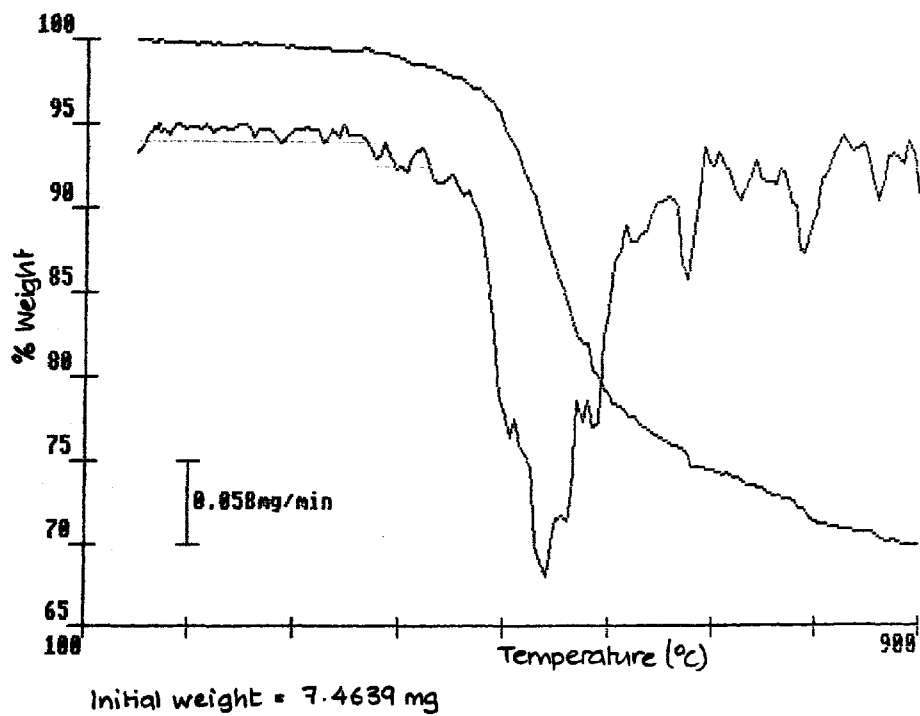
Figure 6.3d : 501 Llanharan at 20degC/min.

Initial weight = 7.4639 mg

Page 186
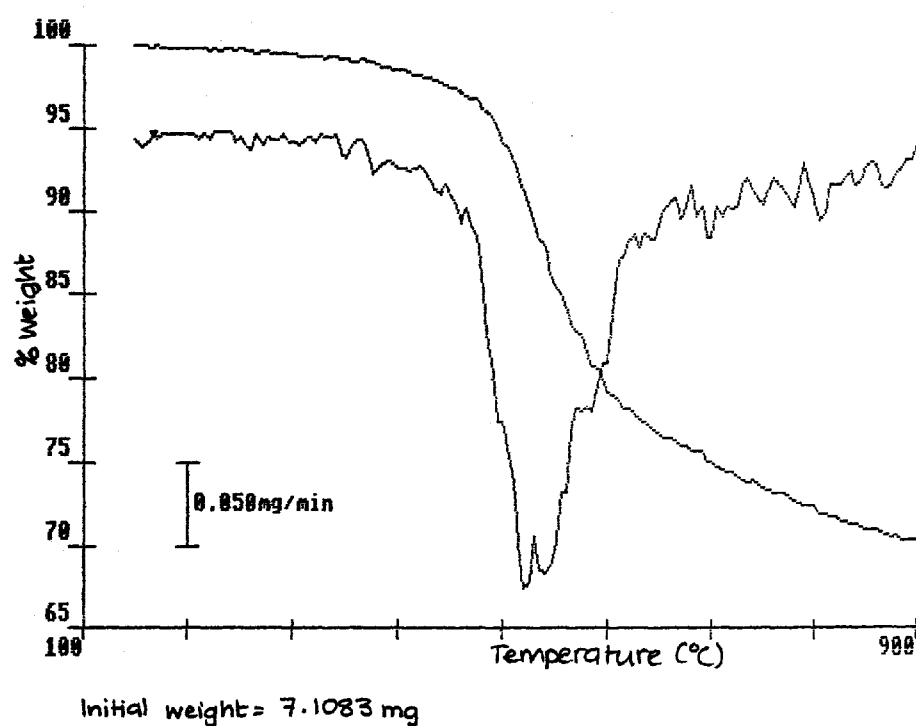
Figure 6.3e : 701 Llanharan at 20degC/min.

Initial weight = 7.1083 mg

Figure 6.3: Pyrolysis of the Coal Samples at a Heating Rate of 20°C min⁻¹.
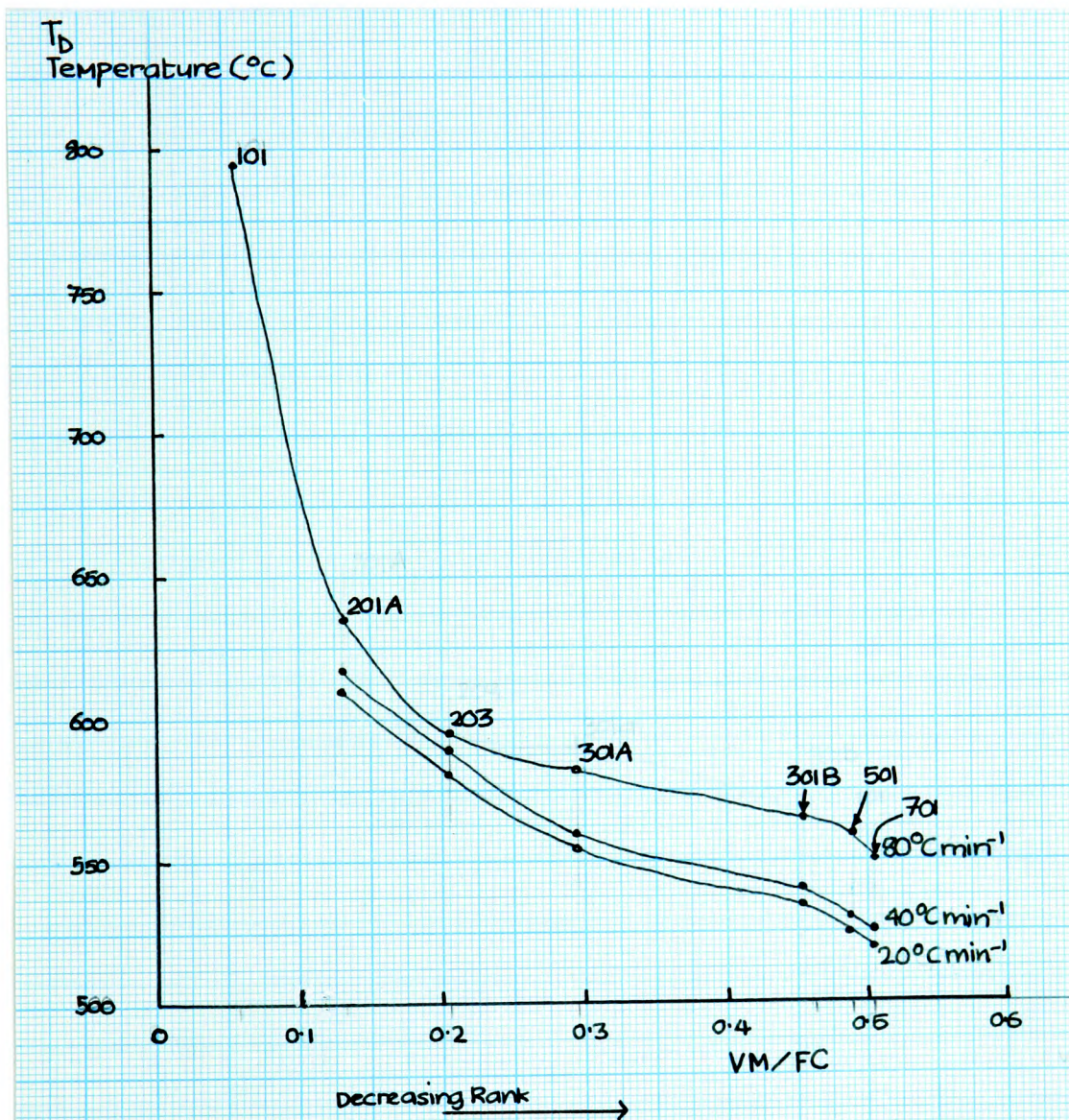
Figure 6.4 : Graph Showing the Variation of T_D with Rank for the Coal Samples at the 3 Heating Rates Used.
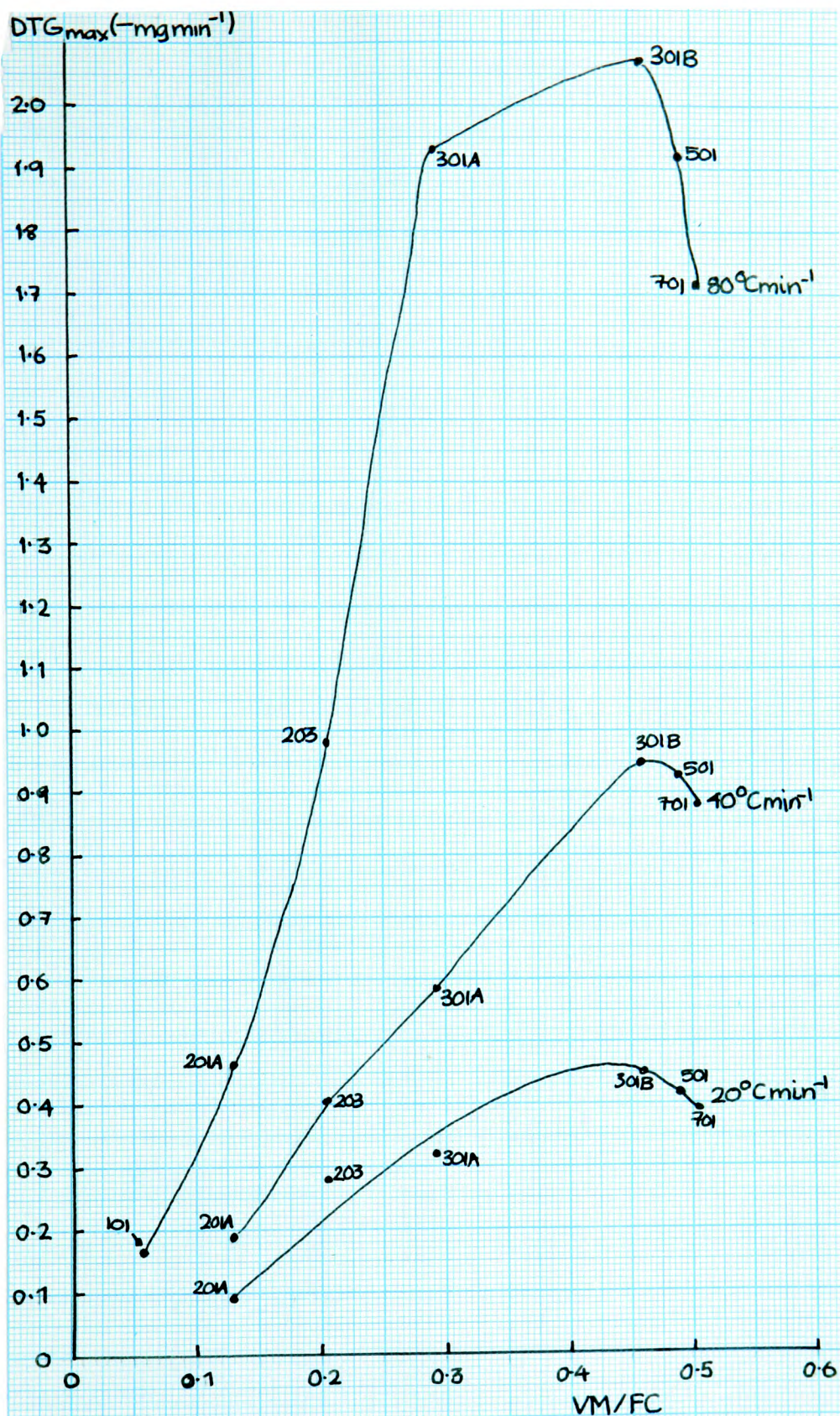
Figure 6.5 : Graph Showing the Variation of DTG max With Rank for the Coal Samples at the 3 Heating Rates Used.
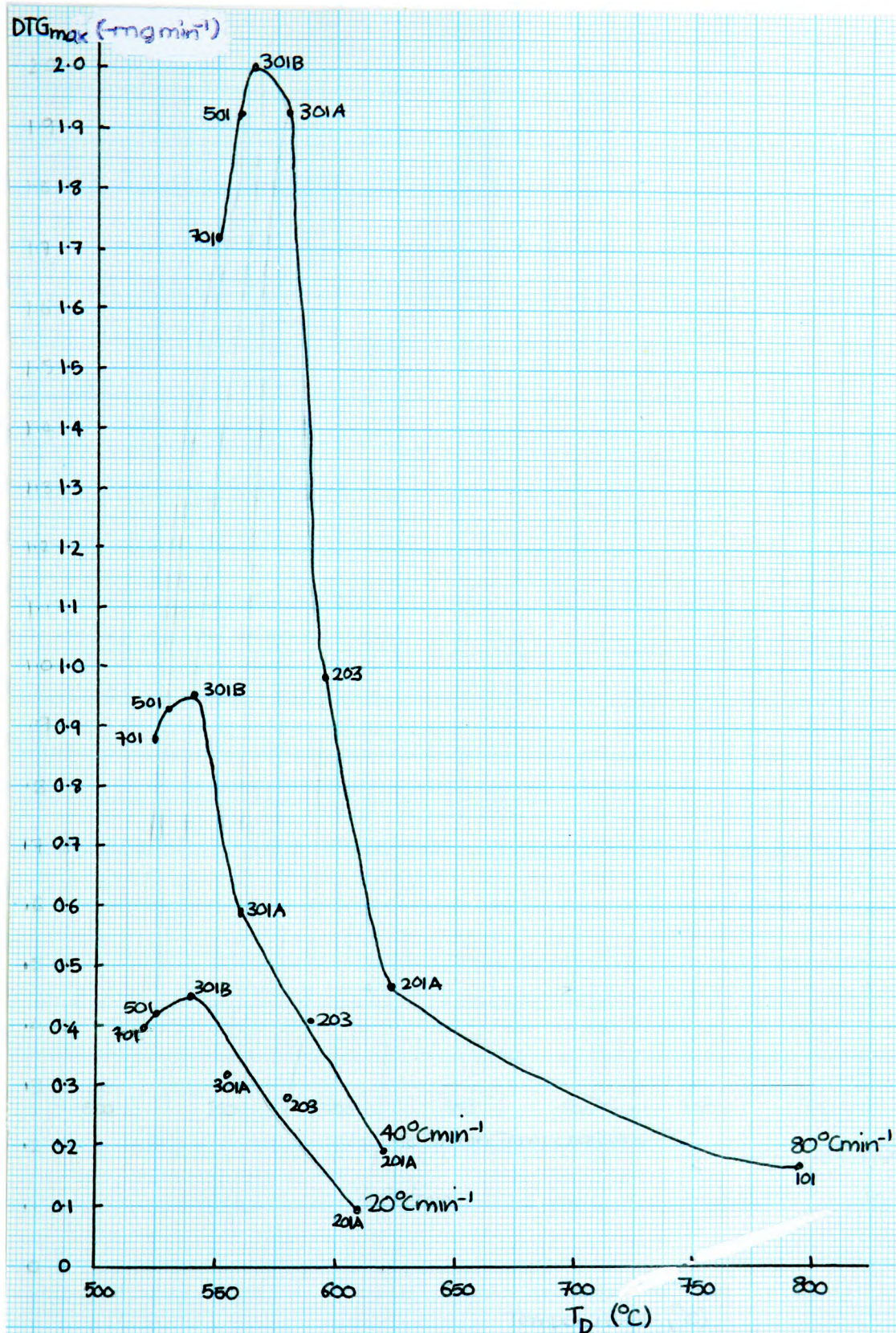
Figure 6.6 : Variation of DTGmax with T_D for Coal Samples at 3 Heating Rates

6.4 THE EXPLANATION FOR THE EFFECT OF RANK.

As rank increases, the weight loss decreases, T_D increases, and, $DTG(max)$ decreases. This is a direct result of the maturation processes that coal experiences with time. As a particular seam of coal matures, the carbon content increases, the aromaticity also increases and the closer the coal becomes to the conceptual end-point of the coal series viz. graphite. The result of increasing maturity is that the volatile matter content of the coal decreases. The consequence of this is that the total weight loss of the coal decreases with increasing rank. This is also the reason for the decrease in the rate of weight loss values — there is less weight to lose. The explanation for the decomposition occurring at a higher temperature as rank increass is found when the conditions which drive the maturation process are examined. Heat and pressure are the forces that drive the maturation process. They cause a homogenization of the coal structure, with weak bonds being broken, and the resultant volatile products being driven off from the coal, and a resultant condensation and aromatisation process occurs. The effect of this heat and pressure treatment is to cause the coal to be composed of stronger bonds. In other words, as the rank increases, the

coal becomes more resistant to decomposition by heat, i.e.,in the context of this research, to pyrolysis. Thus the temperature at which decomposition occurs increases with increasing rank.

The expected result of the homogenization of the coal structure might be a sharpening of the dW/dt peaks. But this is not observed. The reason for this is that the increased sensitivity of the computerized data collection system registers electronic background noise from the TGS-2 system and this is then superimposed upon the DTG trace. In a sample where the weight loss is large, then this noise does not prove to be a nuisance, but in the higher ranked samples, this noise causes confused DTG traces. This means that useful quantitative results are limited, and that it is hard to ascertain the true shape of the curve. This is also the reason why the higher ranked 101 Cynheidre and 201A Penrikyber samples will not be investigated at lower heating rates to any great extent since the DTG_{max} and dW/dt values decrease with decreasing heating rate. Although the noise level also decreases, few meaningful results can be obtained. It may be argued that this noise should be filtered out, but to do this would deprive the computerized system of its sensitivity and render it no more than a

"high-tech" chart recorder. Much more valuable information
can be gained by accepting this noise and allowing for its
presence, as explained in section 6.1.

6.5 THE EXPLANATION FOR THE EFFECT OF HEATING RATE.

As noted above, as the heating rate increases for any one
sample, DTG_{max} and T_D increase while the temperature range
over which most of the pyrolysable weight is lost broadens.
The reason for these changes is as follows.

At any given heating rate, the pyrolysis reaction may be
envisaged as a series of reactions which occur in a series
of small, finite temperature regions. Each reaction needs a
finite amount of time to reach equilibrium/completion. At a
slow heating rate, there may be enough time during each
temperature region for the reactions to approach
equilibrium/completion. If there isn't enough time, then a
small portion of the reaction is carried over into the next
reaction temperature region where equilibrium/completion may
occur. The result of this is that there is a greater amount
of possible reactant in the second region. The same thing
may happen in the second region, and so on. This results in

a series of slightly overlapping reactions. Also, there is at a slow heating rate a good chance that each reaction will be complete within or close to its own temperature region.

At faster heating rates, each temperature region operates for a much shorter period of time, thus much more of the reaction is carried over into the mext region where it still may not reach equilibrium/completion. This results in a shifting of the DTG peaks to higher temperatures. The shorter time over which each temperature region operates is the reason for the increase in the rate of weight loss - if the time available for a certain mass to be lost doubles at a slower heating rate, then the rate of weight loss is halved. This relationship is complicated by the non-completion/equilibrium and overlapping of reactions.

The broadening of the temperature range over which most of the pyrolysable weight is lost is due to the overlapping of reactions.

6.6 FINGERPRINTING OF PYROLYTIC BEHAVIOUR.

The strong behavioural trends illustrated in figures 6.4-6.6 are based upon the basic characteristics of the pyrolytic behaviour exhibited by each sample investigated. These basic values, combined with some extra information form the more detailed DTG curve obtained by using the computerised data collection, can be used in a system of fingerprinting the pyrolytic behaviour of the samples. The object of this exercise is to allow a quick and easy comparison of the behaviour of two different samples under the same conditions, or of the same sample under different conditions, or of the effect of an additive upon different sample, or of different additives upon the same sample, or to predict the effect of changing conditions and additives upon samples not investigated in any way other than by a simple TG analysis.

Although only a few samples have been investigated, it is believed that to add new samples to the standard curves will only take a small amount of time and will extend the range of standard coals. The trends found in the coals investigated in this research may not be apparent once other coals are added, particularly if they originate from other

coalfields, as was experienced by Ghetti[54]. Nevertheless, as standards for this research these curves are important.

The method of fingerprinting is based upon figure 6.6. Upon this curve are superimposed the range of temperatures over which the 4 largest DTG peaks may be found. Within this region, much of the pyrolysable weight of the sample is lost and this range, together with the DTG_{max} and T_D, reflects the individual pyrolytic behaviour of the coal. This system of fingerprinting is illustrated in figure 6.7.

6.7 COORDINATION OF RESULTS.

Upon close inspection of the curves shown in figure 6.7, it can be seen that for the coking coals (301A and 301B) the temperature range over which the four largest DTG peaks occur narrows to a minimum. It is suggested that this narrowing is a result of the coincidence of the reactions which cause the coals to coke i.e. the softening, degassing and condensation reactions as described by Van Krevelen et. al.[13] As described in Chapter 3, the softening process is a depolymerization reaction with the bonds between the structural units of the coal being ruptured and consequently free radicals are produced. The result of these reactions
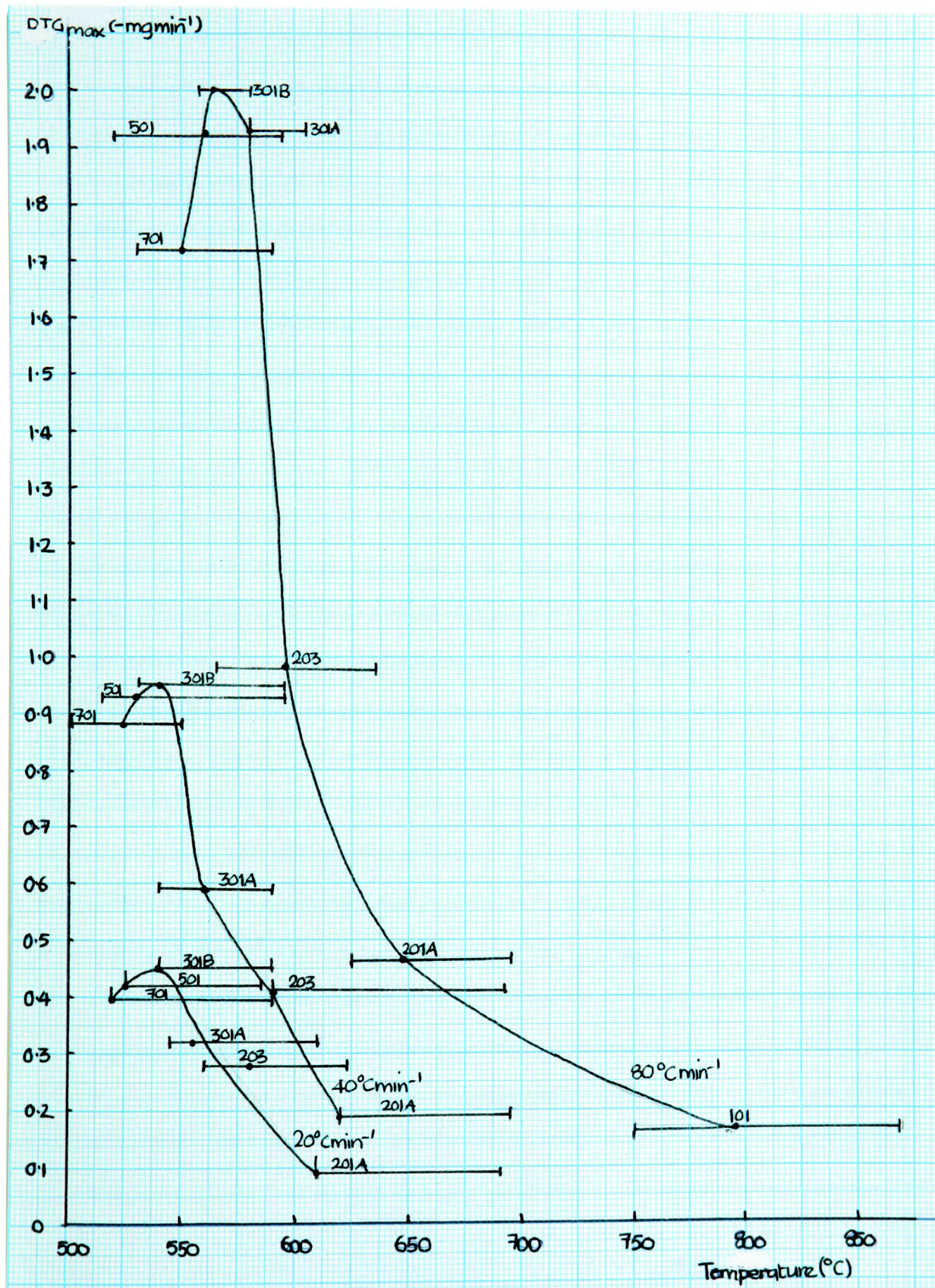
Figure 6.7 : Fingerprinting of the Pyrolysis Behaviour of the Coal Samples.

is the formation of an unstable intermediate which acts as a plasticizer for the coal mass. It is this intermediate which is responsible for the "boiling treacle" stage of the pyrolysis reaction as viewed using the hot stage microscope. As the reaction proceeds, the intermediate undergoes further conversions. The radicals produced condense and increase the aromatic content of the sample; the non-aromatic condensation products ar liberated into the furnace atmosphere and carried away by the purge gas. The solid which results from these reactions is called the semi-coke. and as this undergoes further degassing and condensation reactions, the final coke is formed. The main volatiles to be evolved during the degassing are hydrogen, methane, and other gases.

Generally, the chemical decomposition of coal may be divided into 3 stages[42]

1. the first stage begins well below 200°C with the release of water, oxides of carbon and H_2S. Above 200°C alkylbenzenes are evolved in small quantities.

2. the second stage is called the active decomposition stage and begins around 350-400°C and ceases around 555°C. It contains the region of maximum rate of weight loss. Most of the volatile release occurs here, the volatiles including tar and all lighter condensable hydrocarbons.

3. the third stage is termed secondary degasification, the gradual loss of heteroatoms, principally H and O, occurs. The principal volatile products are H_2O, CO_x, H_2, CH_4 and traces of C_2 hydrocarbons. The resultant char becomes increasingly more aromatic.

The release of tar in the second stage is the result of the distillation and diffusion of other smaller organic molecules with a molecular weight <200 which are trapped in the narrow pore structure of the coal. The rates of diffusion increase exponentially with temperature and in this stage the rates are high enough to allow diffusion of the these molecules out from the coal solid. Thermal degradation of the coal does not begin until about 400°C and proceeds parallel to the gaseous diffusion. Tar, H_2O, CH_4, C_2- and C_3-hydrocarbons are produced simultaneously at temperatures above 400°C. H_2 does not begin to appear until a temperature of 420°C is reached and this signals the start of the condensation processes. At still higher temperatures, CO will also be produced[51].

This is the generally accepted mechanism of pyrolysis of a coking coal. Minor modifications are necessary for other coals, the main ones being the change in temperature at which reactions occur and the way in which they are spread

over greater temperature ranges. In higher ranked coals, the bonds which join various clusters of molecules within the coal matrix are stronger and there are fewer of them, and the result is that the thermal degradation takes place at higher temperatures. The converse is true for the lower ranked coals.

It is proposed that these reactions contribute to the different DTG peaks, although which reaction is responsible for which peak is not known, especially since it is not known whether the reaction or the sudden release of volatile matter from the tar bubbles contribute more to the value of the DTG peak. This may become clearer when the kinetic results are examined more closely. These are the subject of the next chapter.

CHAPTER 7.

THE KINETICS OF COAL PYROLYSIS.

The activation energies for each sample at each heating rate were calculated using the Serageldin and Pan method of kinetic analysis[45,44]. The Arrhenius equation is the basis of this method. It is assumed that the process of coal pyrolysis proceeds via a series of parallel first order reactions. The resultant Arrhenius plot of log k vs. 1/T exhibits a series of regions of Arrhenius linearity, each with its own activation energy. A typical Arrhenius plot is shown in figure 7.1.
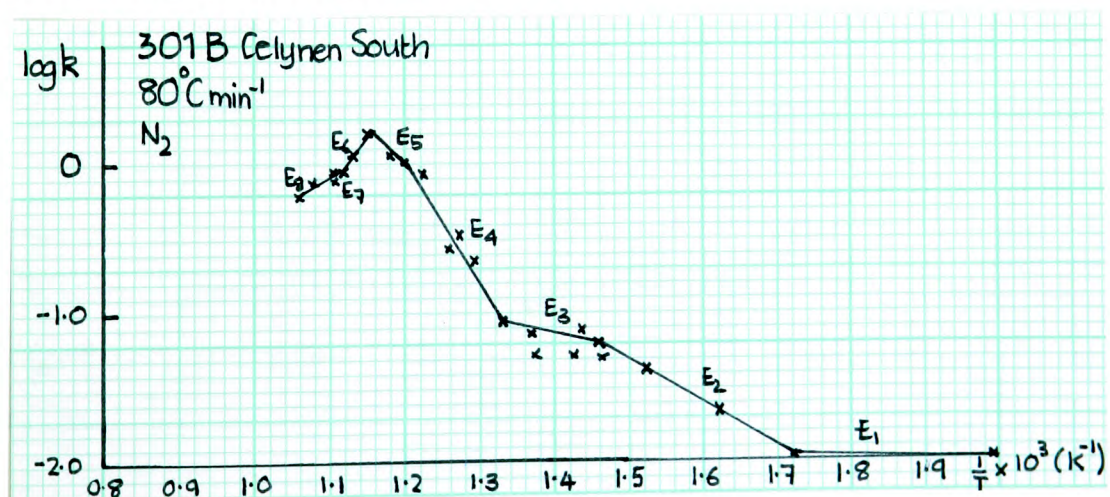
Figure 7.1 : A Typical Arrhenius Plot.

It must be noted here that any calculated kinetic parameters for coal pyrolysis from TG results are not absolute thermodynamic constants. This is because the full mechanism of coal pyrolysis is not known, nor is the chemical structure of each sample before, after and during pyrolysis. Also, as many reactions occur simultaneously during coal pyrolysis, the activation energies thus calculated are the result of several reactions taking place concurrently, and some form of average results. Despite these problems, the activation energies can be used as a measure of reactivity of the coals and for comparison purposes.

The full table of kinetic results for the seven coal samples may be found in Appendix A. The following discussion is based on a few selected results.

Figures 7.2-7.7 show the variation of activation energy (E) with the temperature at which E first comes into operation for each sample at each heating rate. (Note : for clarity, negative activation energies have been omitted.) It can be seen that, generally, as the heating rate decreases, the activation energies increase, and the graphs become more complex.

Figure 7.2 : Activation Energy Values for 201A Penrikyber.
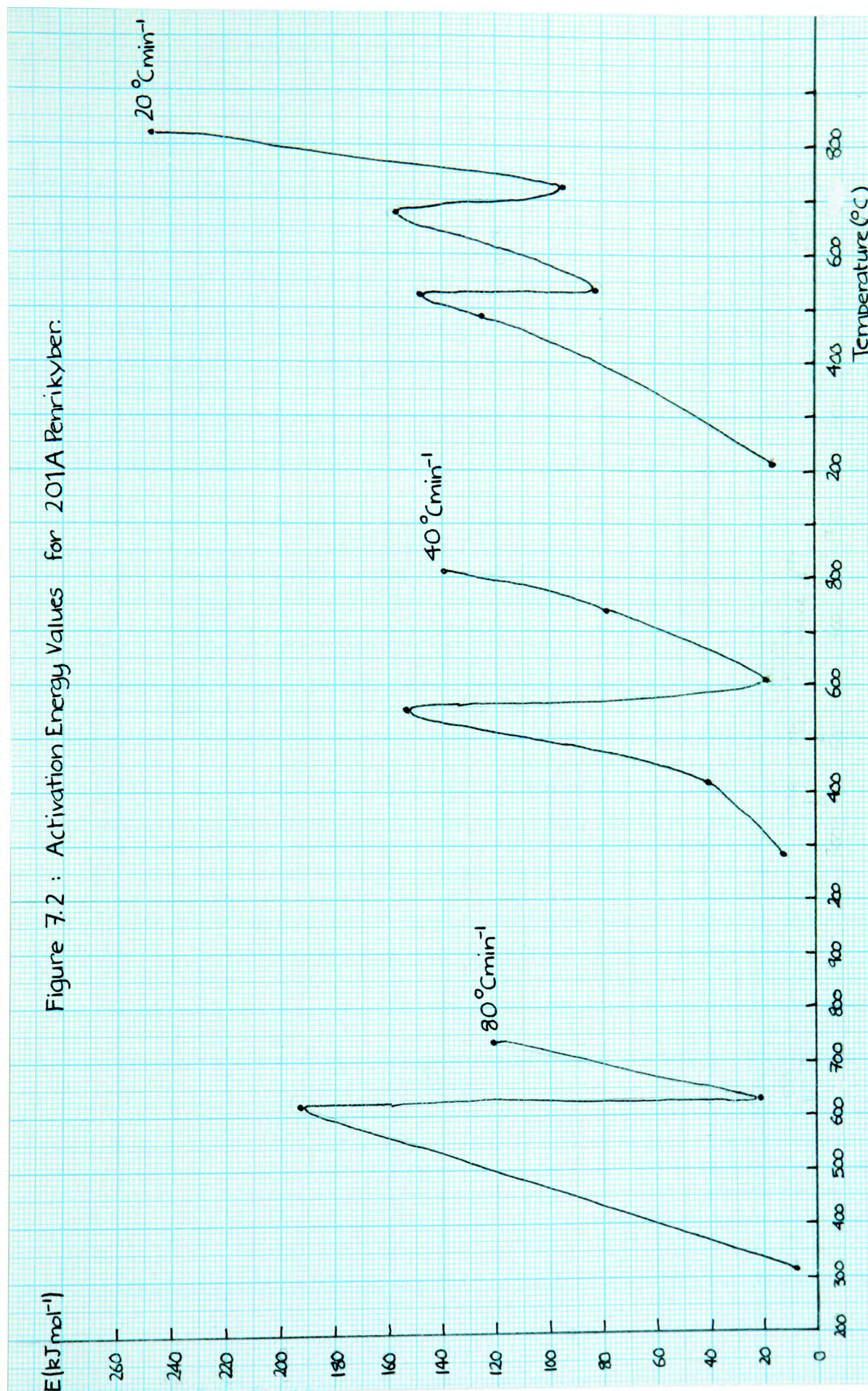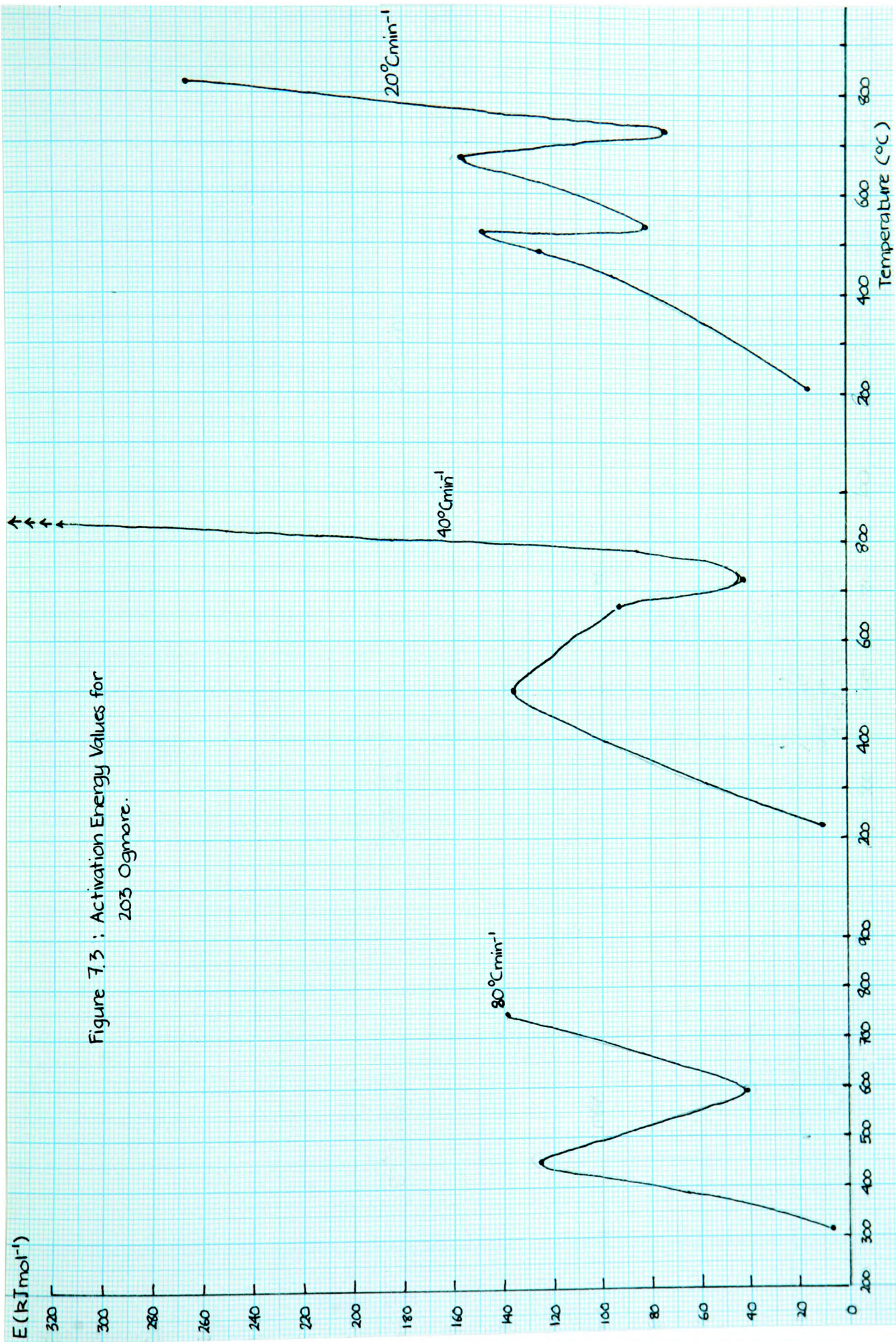
Figure 7.3 : Activation Energy Values for
203 Ogmore.

Figure 7.4 : Activation Energy Values for 301A Cwm.

Figure 7.5 : Activation Energy Values for 301B Celynen South.

Figure 7.6 : Activation Energies for 501Llanharan.

Figure 7.7 : Activation Energies for 701 Llanharan.
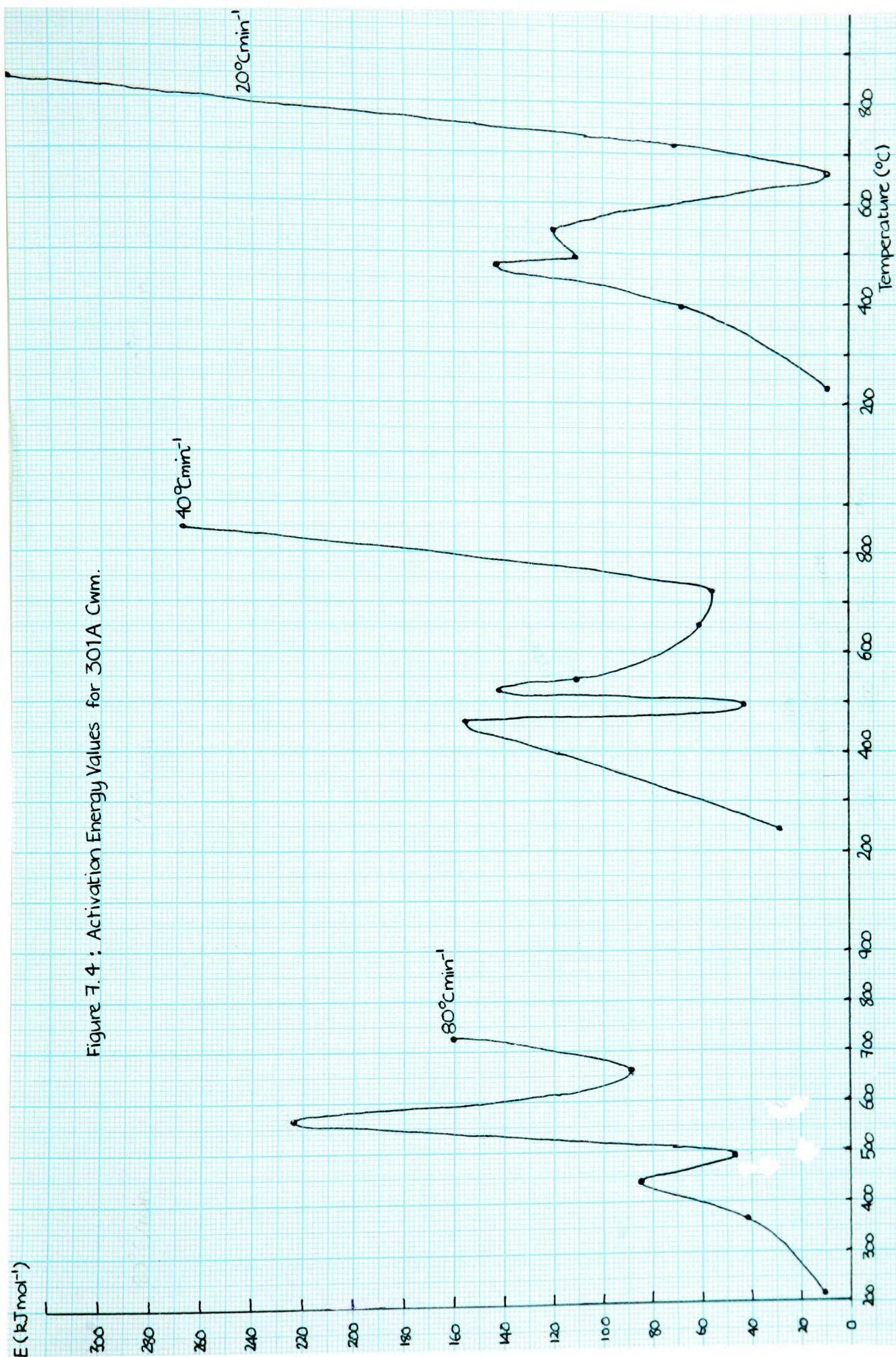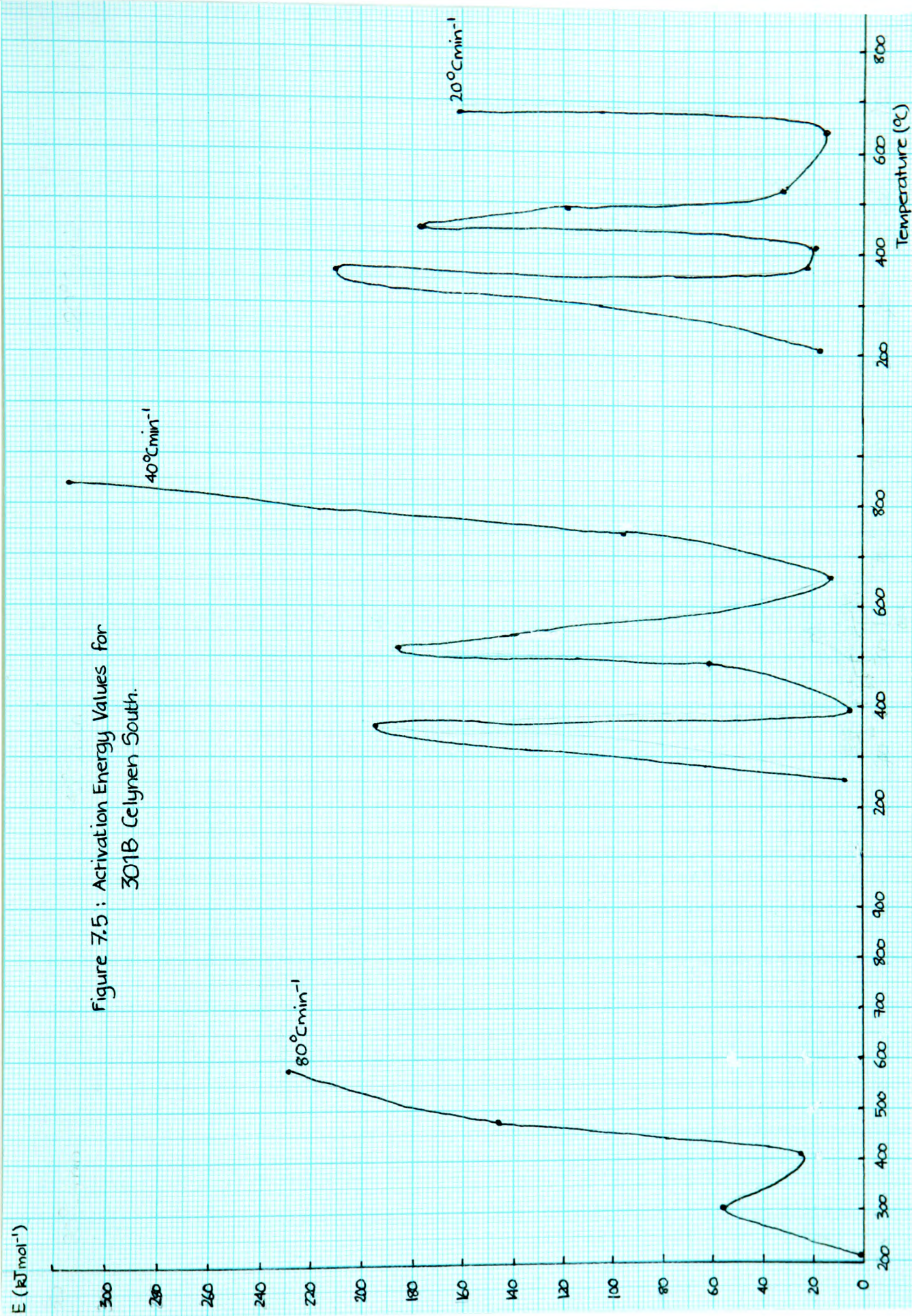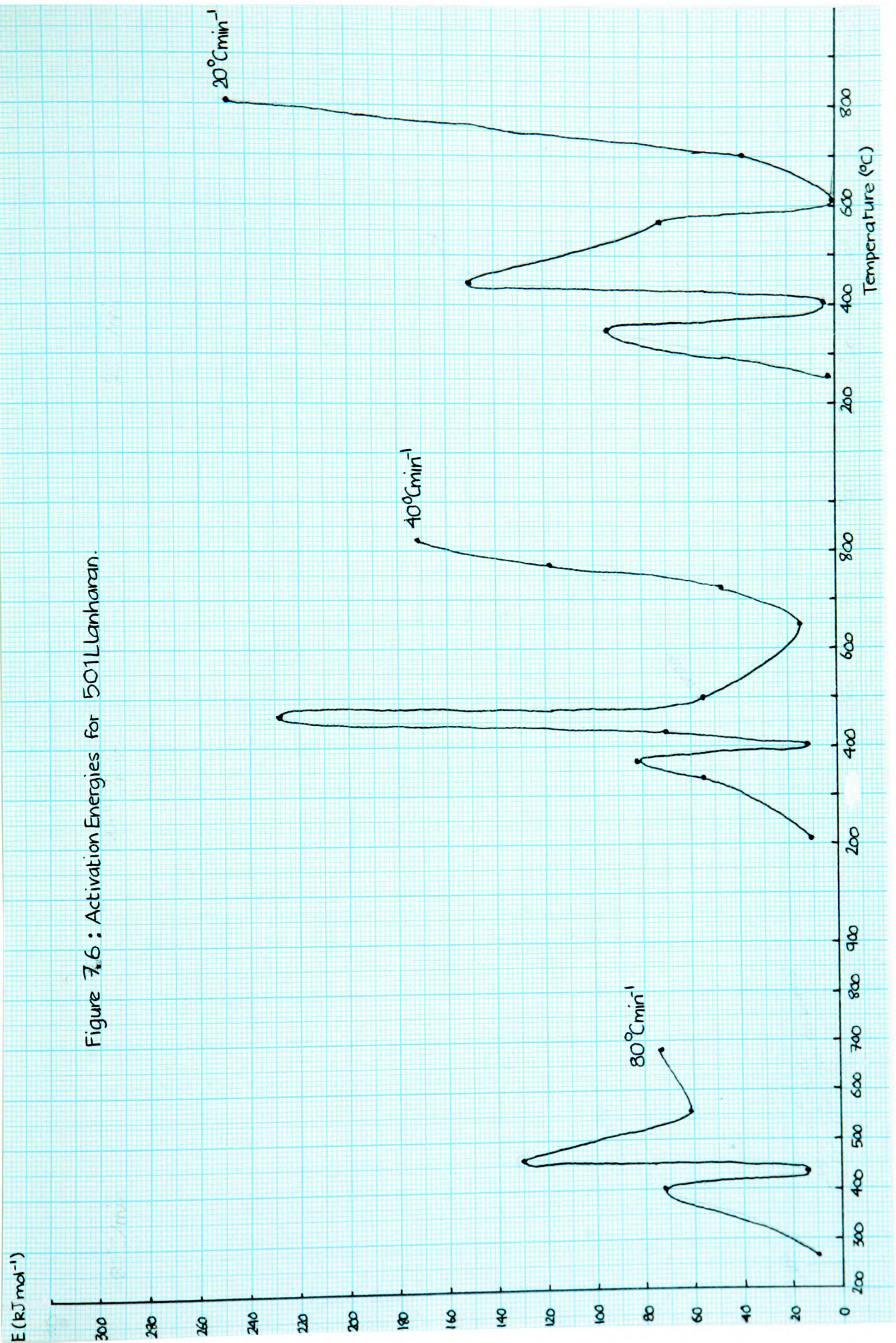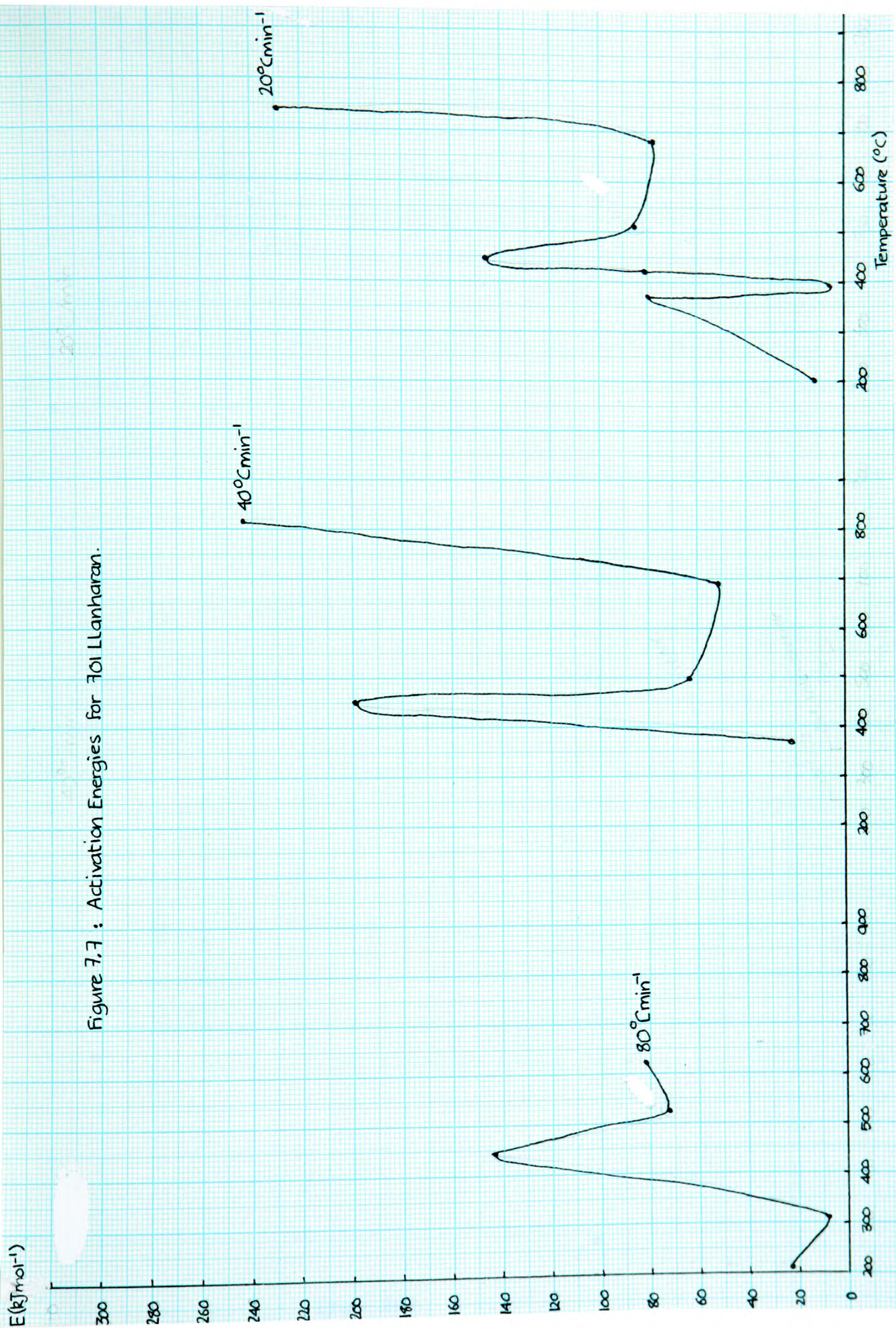
By using the results from the hot-stage microscopy experiments, the TG experiments, and by referring to the pyrolysis model formulated by Juntgen[51], an attempt will be made to relate the various activation energies to the reactions which coal undergoes during pyrolysis.

The first region of activation energy for each sample is the region where gaseous diffusion of trapped water, methane, and lighter aliphatics out of the coal matrix occurs. The activation energies are in the range $0.5-23.2 kJmol^{-1}$ at a heating rate of $80^\circ Cmin^{-1}$, $7.6-28.8 kJmol^{-1}$ at $40^\circ Cmin^{-1}$. and $3.5-17.4 kJmol^{-1}$ at $20^\circ min^{-1}$. These values are typical of the process of gaseous diffusion. The variation in activation energies is most probably due to the variations in pore size distribution and porosity in the samples. The samples with the highest activation energies for this first region viz. 203 and 301A, are coal of a rank where the surface area is at a minimum value[62,45,15,134]. On either side of this range of rank, the surface area increases. This variation in activation energies for the region of gaseous diffusion is illustrated in figure 7.8.

Figure 7.8: Variation of E_I with Rank and Heating Rate

x 80°C min⁻¹
• 40°C min⁻¹
▲ 20°C min⁻¹

Figure 7.9: Variation of E at T_D with Rank and Heating Rate

• 80°C min⁻¹
▲ 40°C min⁻¹
x 20°C min⁻¹
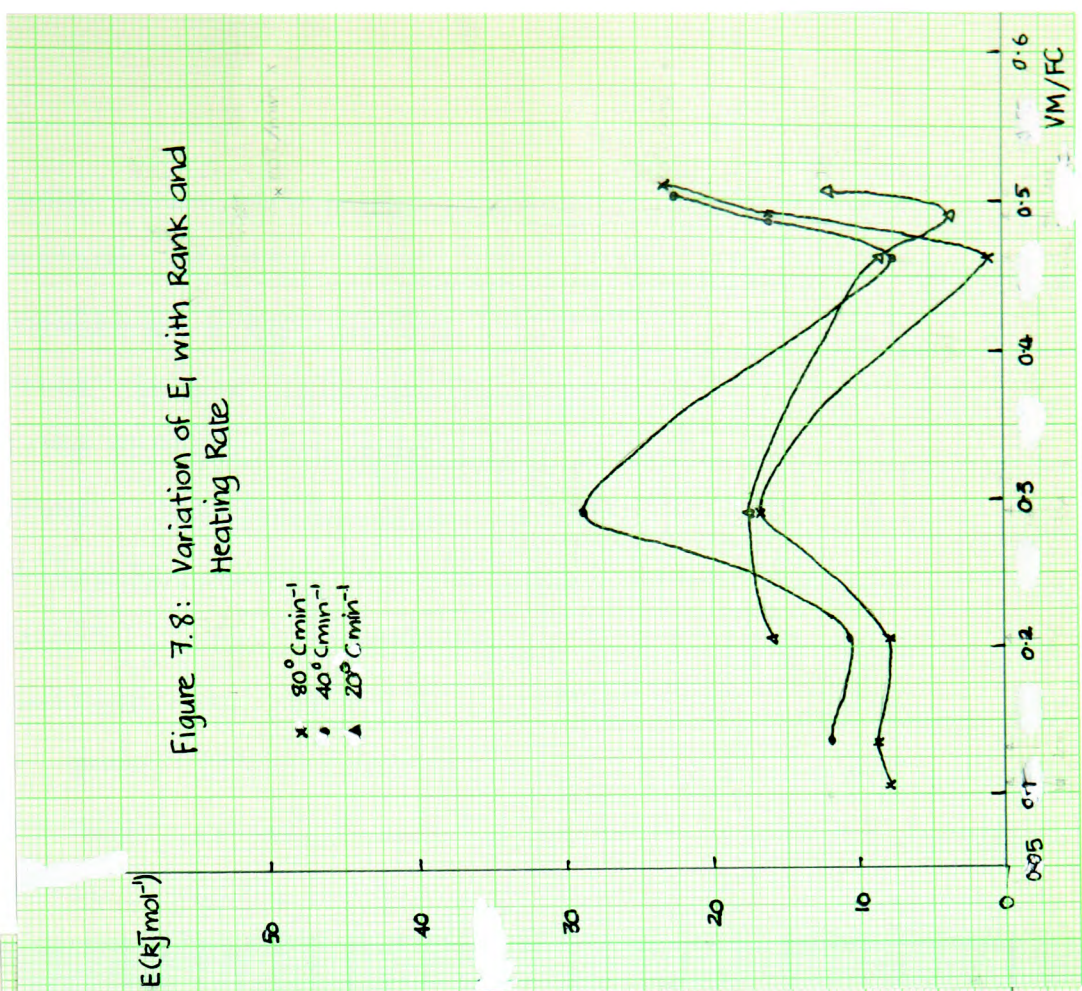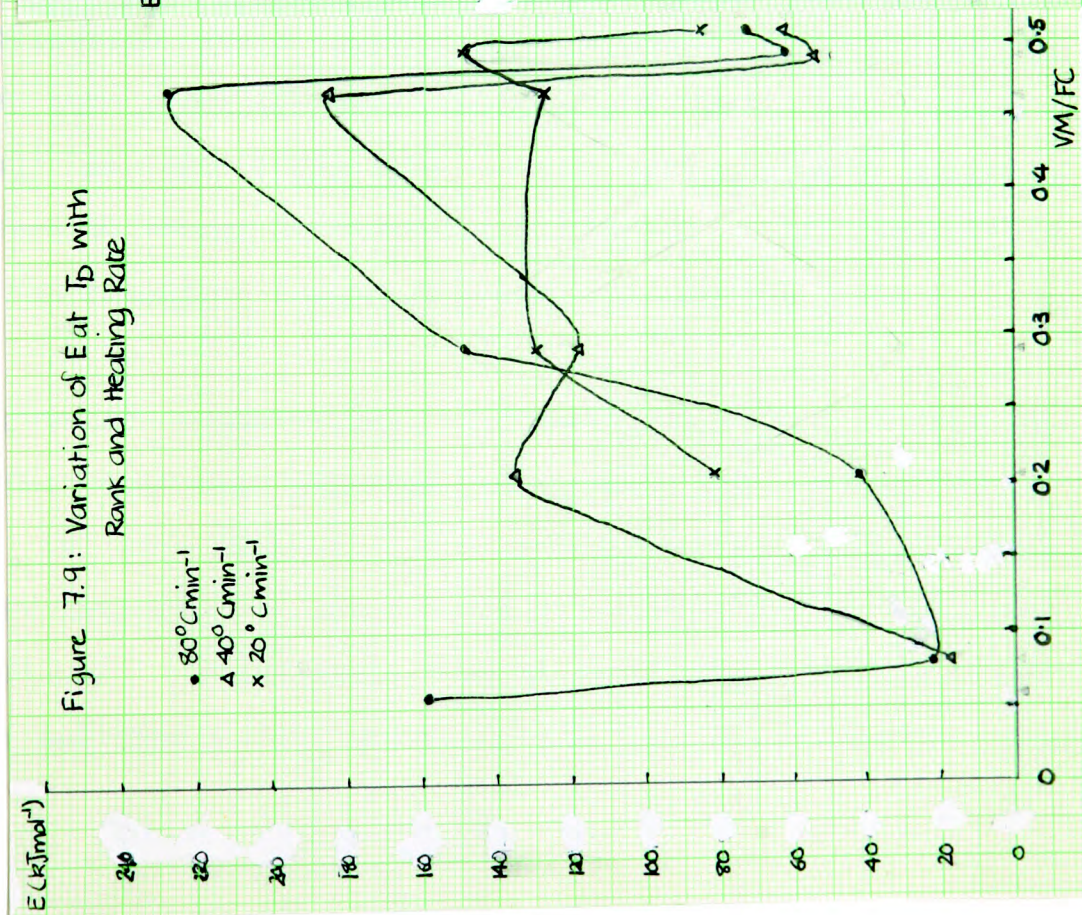
The next stage in the pyrolysis of all the samples is the liberation of oily, yellow volatiles. Under the hot-stage microscope at a heating rate of $50^\circ Cmin^{-1}$ these were first observed in the temperature range $250-420^\circ C$, the higher the rank the greater the temperature at which this phenomenon is observed. Generally, this coincides with the second region of activation energy for the results at a heating rate of $40^\circ Cmin^{-1}$. In the previous chapter, it was noted that as the heating rate increases, the temperatures at which the major peaks occur also increase. Thus it is reasonable to assume that the temperature at which the evolution of tarry volatiles begins will be shifted to a higher/lower temperature when the heating rate is increased/decreased. A complication which arises here is that at a faster heating rate, more reactions will overlap, and this will cause a change in the activation energy for the region since the activation energy in a particular region is an average of all the reactions taking place in that region.

At greater temperatures ($350-480^\circ C$) tar begins to evolve, and this continues into the region where the rate of weight loss is at a maximum. This temperature region corresponds to the beginning of the thermal degradation of the coal substance. This begins with the cracking of bridge carbon bonds and then by the dissociation of the aromatic ring

units; radicals are formed as a result of these reactions. These radicals rapidly recombine to form small aliphatic gas molecules and water which diffuse unhindered into the gas phase. Larger ring fragments become saturated and distil as a tar of medium molecular weight from the solid matter into the gas phase. These processes continue, to varying extents, into the higher temperature regions. The activation energy for the region in which DTG_{max} occurs vary between 21.8 and 193kJmol^{-1} at a heating rate of 80°Cmin^{-1}, 18.5 and 186.6kJmol^{-1} at 40°Cmin^{-1}, and 82.3 and 150.6kJmol^{-1} at 20°Cmin^{-1}. These results are presented graphically in figure 7.9. It can be seen that the pattern of activation energies for this region are similar at each heating rate.

Above these temperatures, the main reactions are those which produce CO, H_2, and CH_4 to yield the final solid. These reactions occur at temperatures greater than T_D and run parallel to the cessation of the formation of tar. The gases are produced as a result of the condensation of the substances of higher molecular weight.

To state precisely which type of reactions occur during any particular region of activation energy is not possible due to a lack of information about the way in which coal decomposes.

The activation energies for the initial gaseous diffusion region and the region where DTG_{max} occurs will be used to assess the effect of the transition metal additives upon the pyrolysis of coal.

CHAPTER 8.

THE EFFECT OF THE ADDITION OF SOME TRANSITION
METAL ELEMENTS.

8.1 INTRODUCTION.

From the results of the TG study of the seven samples, the decision to use a heating rate of $20^\circ Cmin^{-1}$ for the study of the effect of the addition of some transition metal elements was made. The reasons for this choice were

1. the electronic background noise is reduced to a minimum at this heating rate

2. the resolution of the DTG peaks is better than at any other heating rate used.

Choosing the two samples to be used was not so easy. The higher ranked coals were eliminated on the basis that at low heating rates little quantitative information can be obtained from them. Of the remaining samples, the choice was, unfortunately, largely determined by the availability of the samples. During the course of the research, some of the collieries from which coal was obtained, had closed

down, and further samples could not be obtained. 301A Cwm and 501 Llanharan were therefore chosen because of their availability and difference in ranks and properties.

The amount of each transition metal catalyst added to a sample of each coal was arbitrarily decided to be 5% and 10% by weight of each metal. This was to allow a comparison to be made between different levels of catalysts. The samples were then well mixed before each subsample was taken for analysis.

In recording the TG and DTG curves, the weight of the coal only was used. This was accomplished by weighing the sample, calculating the weight of the metal in the sample and adding the weight of the metal to the sample pan weight already present on the tare dial on the TGS-2 apparatus. There will obviously be small errors in calculation of the weight, but it is believed that as five experiments are carried out for each sample, any very small errors will be eliminated or minimised.

8.2 THE EFFECT OF THE ADDITIVES UPON THE TG/DTG CURVES.

There are no noticeable differences between the curves for the coal samples themselves and the samples with the metals added. The temperature at which the maximum rate of weight loss occurs and the value of the maximum rate of weight loss do not change. This is illustrated in figures 8.1 and 8.2 which show comparisons between the TG curves for 301A and 501 with the curves for the coal with 5% and 10% Fe by weight. Compare these with the curves for the plain coals in figures 6.3(b) abd 6.3(d).

8.3 THE EFFECT UPON THE KINETIC RESULTS.

The metals do, however, cause changes in the apparent activation energies calculated as previously described. A full list of the activation energies can be found in Appendices B-E. Because it is uncertain which activation energies correspond to which type of reactions, and the extent to which the reactions overlap, only the first region of activation energy and the activation energy in operation at the temperature where the rate of weight loss is a maximum will be examined. Valuable comparisons between samples and additives may then be drawn.

% weight

0.067mg/min

Temperature (°C)

Initial weight = 11.7462 mg
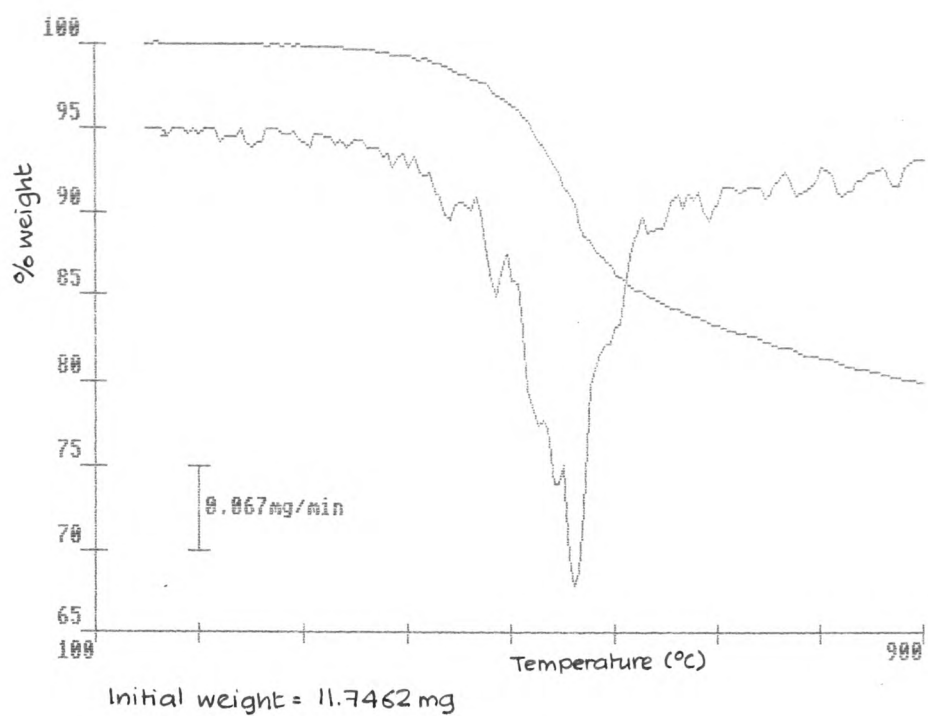
Figure 8.1a : 301A Cwm + 5%Fe at 20degC/min.

% weight

0.042mg/min

Temperature (°C)

Initial weight = 9.2184 mg
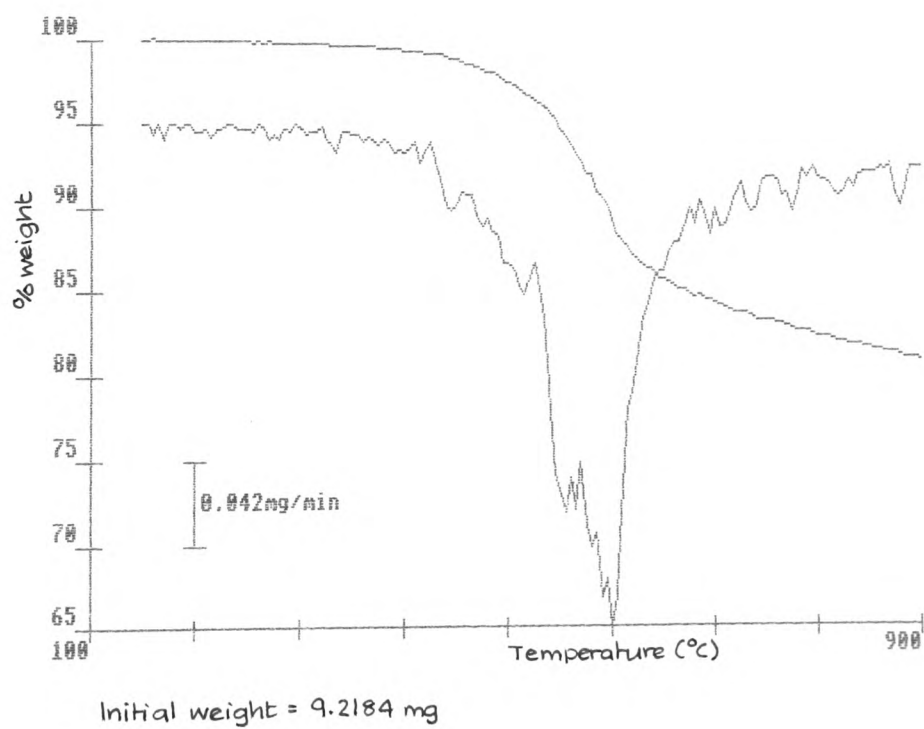
Figure 8.1b : 301A Cwm + 10%Fe at 20degC/min.

Initial weight = 11.8896mg
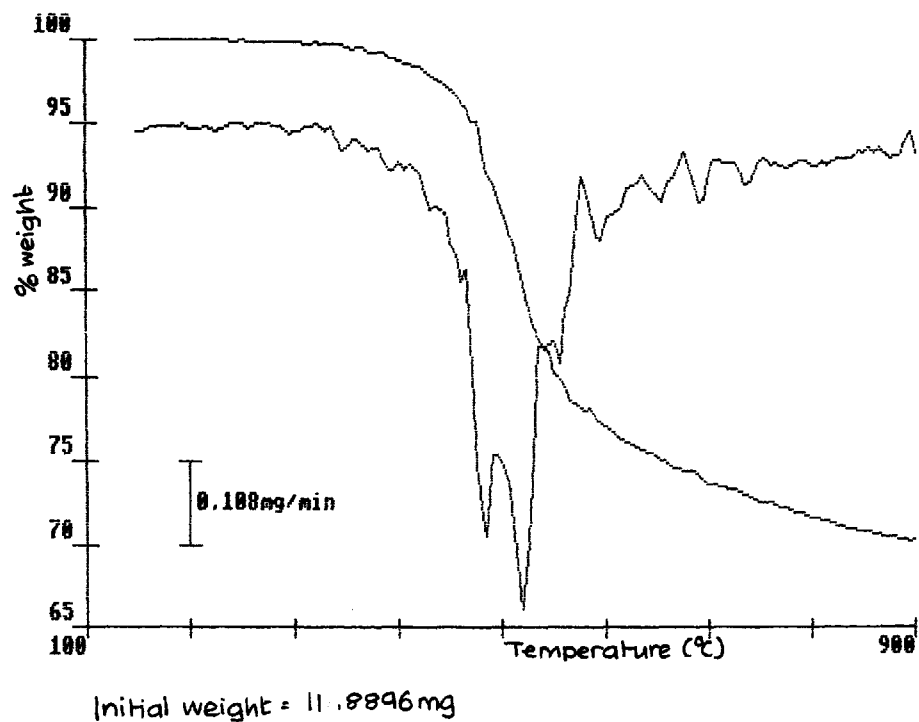
Figure 8.2b : 501 Llanharan + 5%Fe at 20degC/min.

Initial weight = 8.6437mg
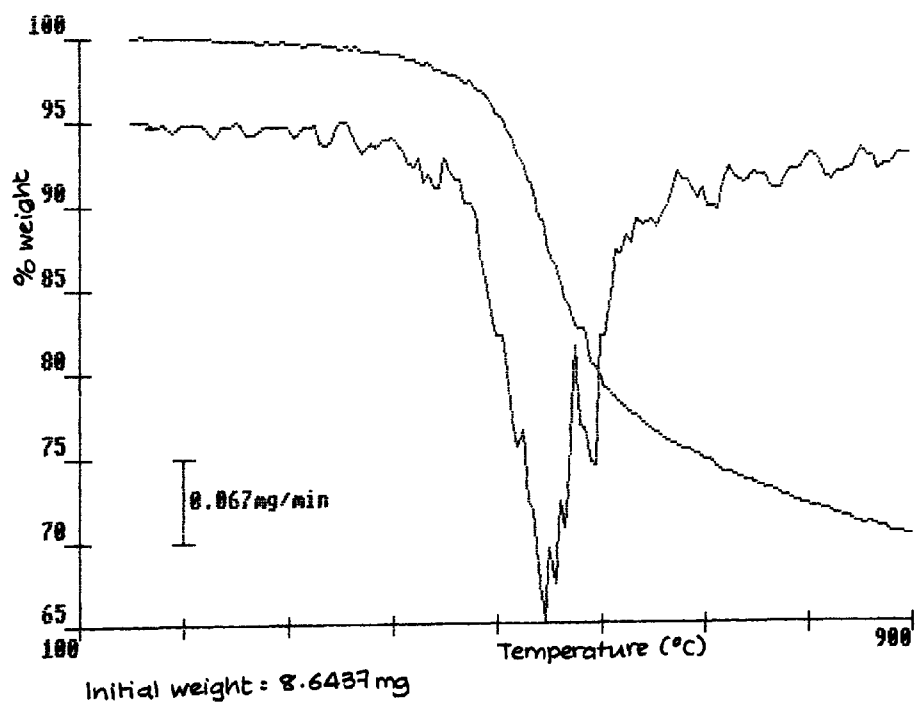
Figure 8.2b : 501 Llanharan + 10%Fe at 20degC/min.

8.4 THE EFFECT OF THE METALS UPON THE FIRST REGION OF ACTIVATION ENERGY.

A graph showing the effect of the metals upon the first region of activation energy - the distillation and diffusion of small organic molecules trapped in the small pores of the coal - for both 301A and 501 with both levels of addition of metals is shown in figure 8.3.

First, look at figure 8.3(a) which shows the effect of addition of 5% of the metals across period 4 of the periodic table. It can be seen that there is a similarity in the shape of the curves for the coals, the change in the value from that for the coal on its own being greater for 501.

Significant decreases in the apparent activation energies for 301A occur for 5% additions of Mn, Co, Ni, and Cu; ZnO causes a large increase in the activation energy. In the case of 501, the activation energy is increased in all cases, the greatest being for Cr where the activation energy was raised from around $4kJmol^{-1}$ to $22.5kJmol^{-1}$. Ti, V, Co and Cu barely affected the activation energy value.

A possible reason for these differences in behaviour is that 301A is likely to have a lower porosity that 501[62]. This is reinforced by the findings that for this region of gaseous diffusion, 501 has a lower apparent activation energy than 301A. Because the molecules diffusing out of 501 are likely to have a relatively easy time doing so, they are not likely to be helped by an additive to any great extent; indeed, it appears the diffusion process is hindered by addition of the transition metals to 501. Also, 501 has not matured as much as 301A, and the products from this first stage of pyrolysis are likely to be smaller than from 301A. The products produced by 301A during this region may need to be cracked to yield gaseous products which are easily liberated from the sample. It is in this function that the metals may aid the pyrolysis reaction.

Examination of figure 8.3(b) shows the effect of the addition of the transition metal elements of period 4 when added in 10% proportions. The apparent activation energy (E) for the diffusion of trapped gaseous molecules and smaller products of pyrolysis during this temperature region is decreased for 301A by the addition of Cr, Fe, and Co. Yet, relative to the addition of the metals in 5% proportions, the extent of change is not so great. Indeed, some metals have reversed their effects, Ni and Mn instead

of decreasing E have increased it, Fe has decreased E when added in 10% proportions rather than increasing it in 5% proportions. This suggests that for each metal there may be an optimum %addition at which their effects may be maximised. What these values may be will only be found by further work.

In the case of the 10% addition of metals to 501, the activation energies were all increased relative to the plain coal, but not to the same extent as for the 5% addition level. The activation energies have decreased for the addition of Cr, Fe, Ni and Zn in 10% portions relative to addition in 5% portions. The other metals have all increased their activation energies relative to the 5% addition level. Again, this suggests there may be an optimum amount of metal to add in order to gain maximum effects.

A discussion of the effects of addition of metals down the groups is necessary. Figures 8.3(c) and (d) show how the addition of 5% and 10% of the metals from groups IVB and VIB.
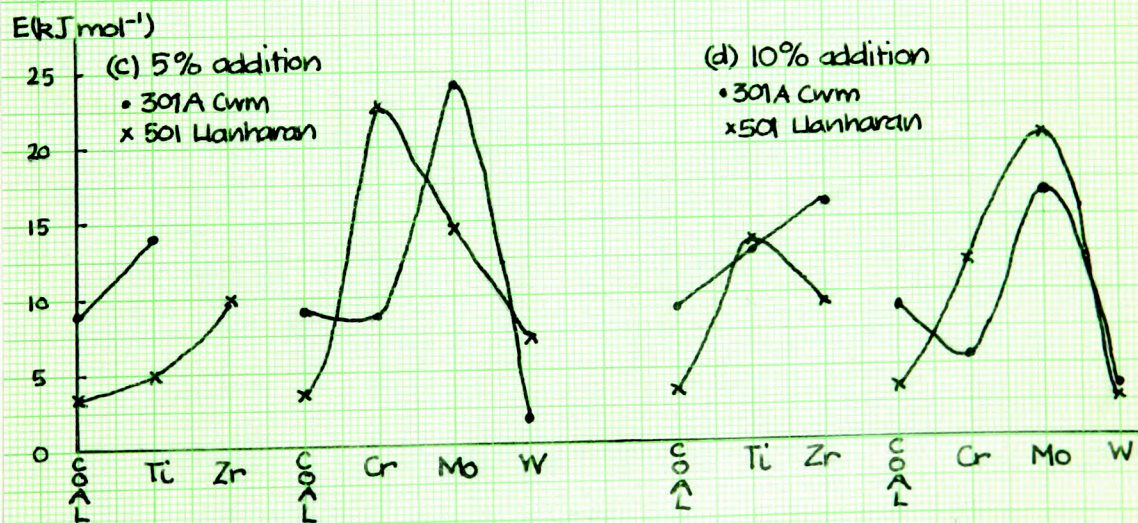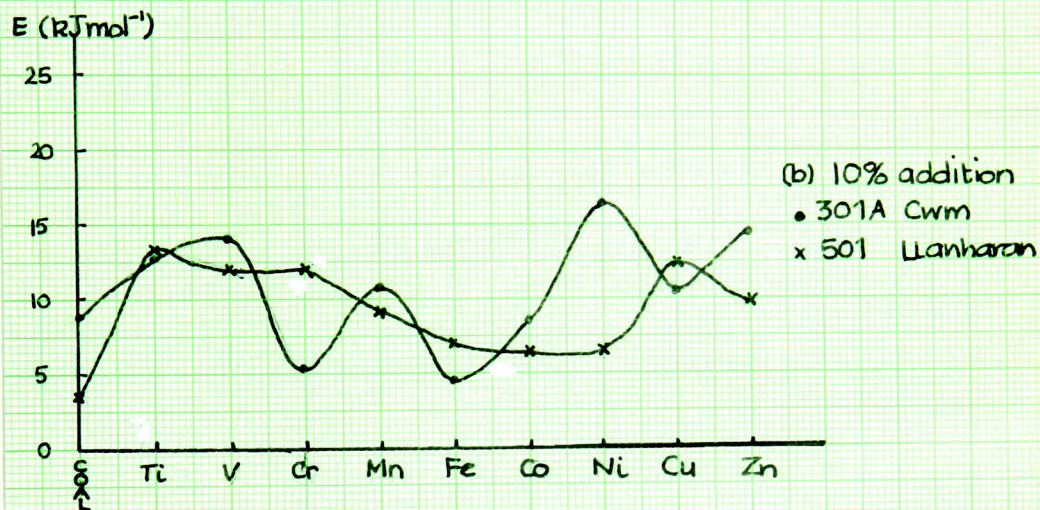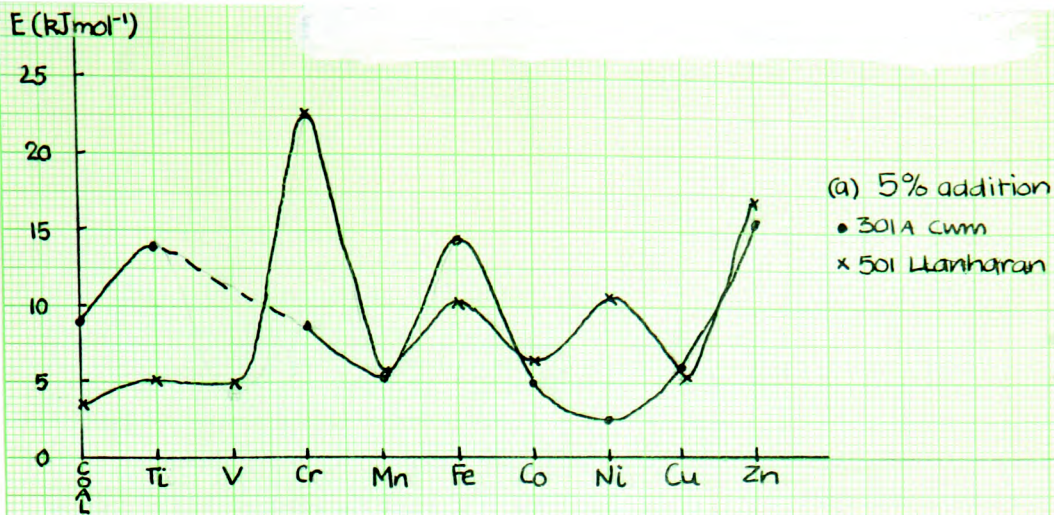
Figure 8.3 : The Effect of the Transition Metal Elements on the First Region of Activation Energy

Generally, the metals from group IVB (Ti and Zr) increase the activation energy for this first region of apparent activation energy to about the same level for both 5% and 10% additions relative to the plain coals. For the elements of group VIB (Cr, Mo, and W) the activation energy decreases for Cr, increases for Mo and decreases with W at both concentrations for 301A. For 501 the E increases to a maximum with Mo and decreases to a slightly smaller value than for the plain coal with W as the additive. This applies to both levels of addition.

8.5 EFFECT OF THE ADDITION OF METALS UPON E AT DTG$_{max}$

Examination of figure 8.4 shows the variation of the apparent activation energy at DTG$_{max}$ with the addition of the various transition metal elements.

It can be seen that for 301A and the metals at the two levels of addition that the shapes of the curves are similar, the greater effects occur for the 10% addition level, which is contrary to the effects of the metals upon the first region of activation energy. The metals which drastically reduce the apparent activation energy of this region are Mn, Mi and Zn, which reduce it from 120kJmol^{-1}

Figure 8.4 : Variation of the Activation Energy at the Point of Maximum Rate of Weight Loss for 301A CWM and the Addition of Transition metal Elements.

• 5% addition by weight
x 10% addition by weight
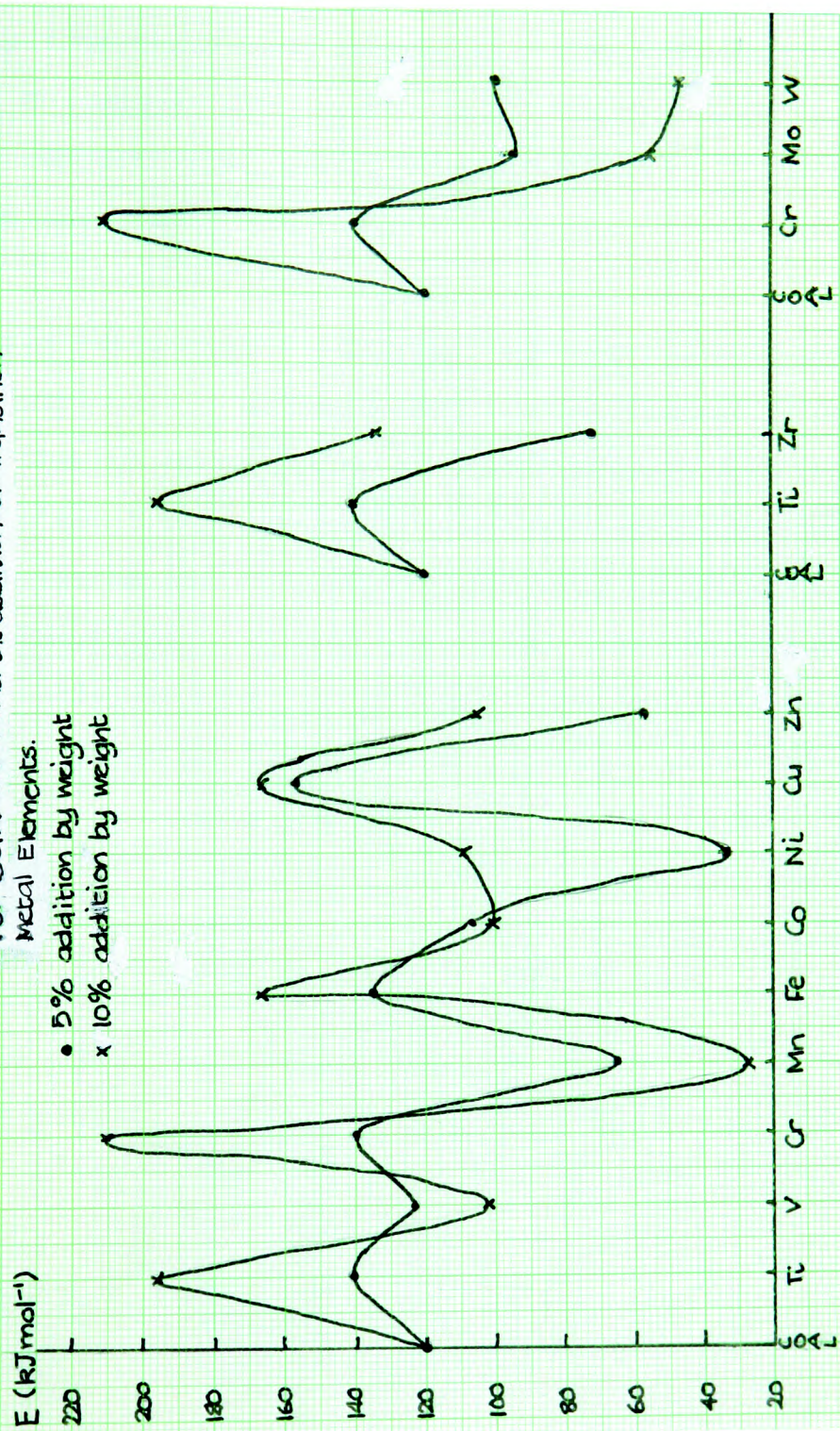
E (kJ mol⁻¹)

to 65,33, and 57kJmol^{-1} respectively for 5% additions, and to 27,109, and 105 kJmol^{-1} for 10% additions. Zr reduces the value from 120kJmol^{-1} to 72kJmol^{-1} for a 5% addition. Mo and W reduce the value to 55 and 47kJmol^{-1} for a 5% addition respectively, and to 93 and 100kJmol^{-1} respectively for a 10% addition.

The metals which greatly increase E for 301A are Ti, Cr, Fe and Cu, particularly at 5% additions; the increase is not so great at the 10% addition level. This suggests that Mn, Ni, Zn, Zr, Mo and W are particulary effective at promoting the reactions taking place in this temperature region when added in 5% proportions. These reactions are primarily the evolution of tar and the thermal degradation of the coal molecule by cracking of the bridging carbon bonds and the resultant dissociation of the aromatic ring units. It was also noted that Mo prevented the coal samples from coking, as did Ti, Ni, Mn and Cu. Also, the tar evolved from the sample with Ti added which condensed on the glass furnace cover was much more liquid and lighter in colour than for any other sample. These observations suggest that the addition of these metals affects the way in whicht the coal pyrolyses. It seems probable that Ti, at least, promotes the cracking of the tar into lower molecular weight compounds which are more readily released. Further

Figure 8.5 : Variation of the Activation Energy At the Point of Maximum Rate of Weight Loss for 5Ol Llaninaran and the Addition of Transition Metal Elements

• 5% addition by weight
x 10% addition by weight
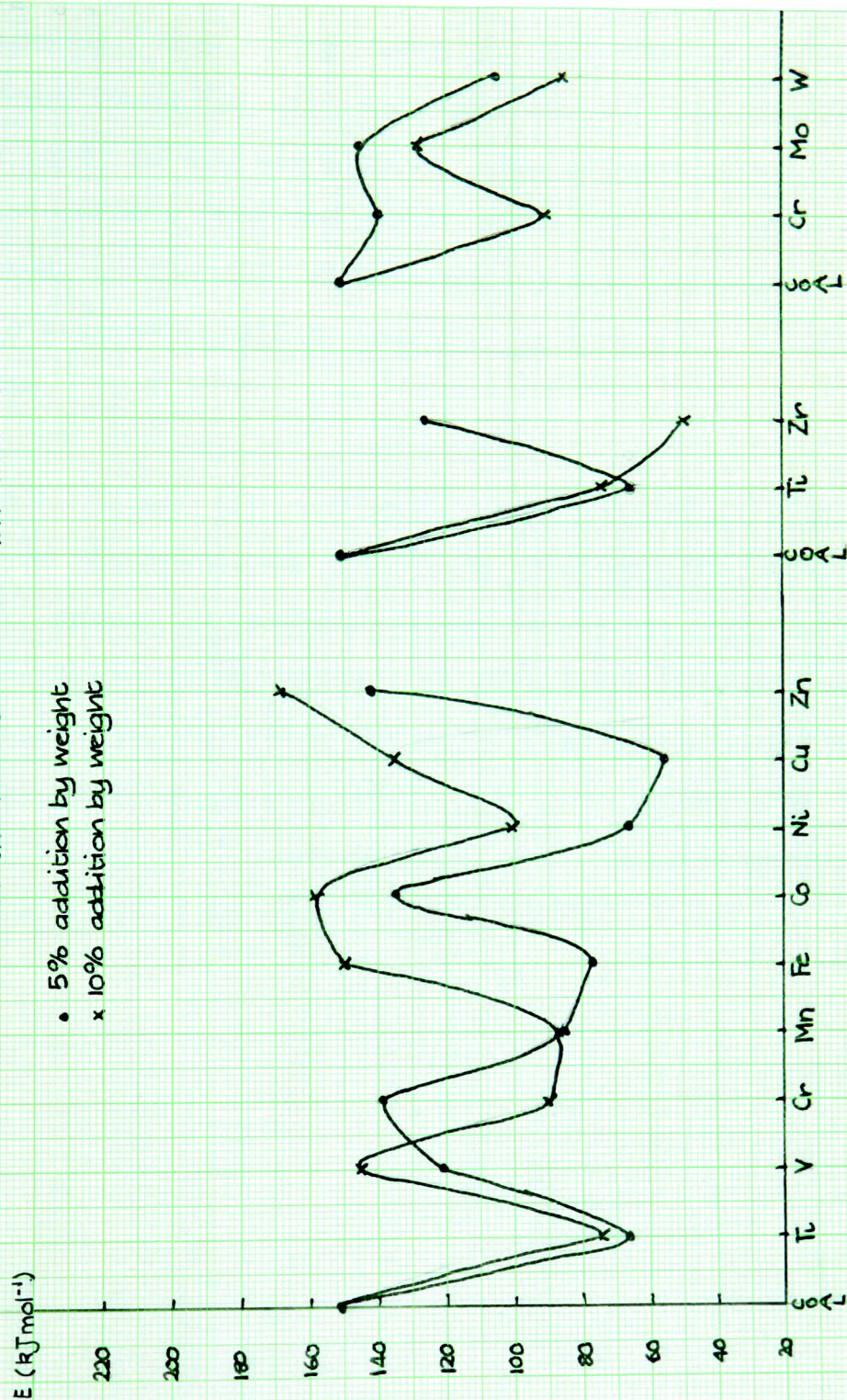
investigations, possibly by collecting the gaseous products and analysing them using mass spectrometry or infra-red spectroscopy could be utilised to see if the pyrolysis products are in any way altered. The prevention of coking certainly suggests that the way in which the coal pyrolyses is altered. There is no apparent correlation between the change in activation energy and the suppression of coking properties.

Figure 8.5 shows the variation in E at DTG_{max} with the addition of the metals to 501 at 5% and 10% addition levels. Again, a similar curve is seen for the two different levels of additives. In this case, however, the E is decreased in <u>all</u> cases except for 10% addition of ZnO. Generally, addition of the metals by 5%, except for the progression down the groups IVB and VIB, decreases the activation energy more than addition by 10%.

CHAPTER 9.

CONCLUSIONS AND RECOMMENDATIONS FOR FUTURE RESEARCH.

It is obvious that no "earth-shattering" discoveries would be made just by examining the aims presented in chapter 1. Yet, the thermogravimetric study of the coals at the different heating rates using the computer to record the data has revealed a wealth of fine peak structure on the rate of weight loss curve which previously has not been observed. Also, this fine structure is different for each coal sample, possibly unique for any given sample of coal. The implications of this have been touched upon in the suggestion of a method of fingerprinting the samples. The full implications of this finding have not yet been fully realized and further research into lots more samples is needed to fully appraise the value of this suggestion. Also, the identification of the reactions which take place throughout these curves may also help to increase the value of this method.

The hot-stage microscopy work has aided the understanding of the physical processes which take place during pyrolysis, but it obviously does not give enough information to enable the identification of the causes of each of the peaks except to suggest that they may be due, in part, to the formation of tar bubbles which trap volatile products. When these tar bubbles burst, they release the volatiles which results in a sudden release of weight and consequently a rate of weight loss peak. It also needs to be noted that these peaks continue long after the formation of these tar bubbles has ceased. Again, further work is necessary to elucidate the precise causes of these peaks.

The kinetic analysis of the thermogravimetric results has provided useful information about the possible number of different processes going on during pyrolysis. Yet, because of a lack of information about the type of processes which occur during each region of apparent activation energy, no more than a general interpretation of the processes taking place may be attempted. Further work could aid this process, especially if the use of infra-red spectroscopy of the effluent gas flow to monitor the formation of such gaseous products as CH_4, CO, CO_2, H_2O and H_2 was to be used.

The addition of the transition metal elements produced some unexpected results, mainly in the qualitative observations of the pyrolysis products and the tarry volatiles which condense on the glass furnace cover. The prevention of coking by some metals, notably Mo, Ti, Mn, Ni, and Cu suggests that the metals affect the way in which the coal pyrolyses. Also, the production of a pale yellow, low viscosity, tarry condensate upon the glass furnace cover when Ti had been added supports this view. It was also found that the addition of the metals in the 5% addition by weight proportion had a greater effect than addition by 10%.

This dissimilar pattern of kinetic results for the two samples investigated with the additives suggests that different types of reactions take place during pyrolysis of different coals, which is a reasonable conclusion in any case.

Some avenues for future research have already been outlined and include
1. the use of infra-red spectroscopy to monitor the effluent gas for various gaseous products.
2. mass spectroscopy of the tarry products.

Both of these techniques and suggestions could be used to further aid an understanding of the reactions and processes taking place during pyrolysis, particulary the effects of the additives. The results of these investigations could then aid the development of processes to more efficiently and effectively gain chemical feedstocks from coal. An investigation into the destructive distillation of coal could also prove fruitful, if a more suitable piece of thermogravimetic apparatus with a higher temperature range and the facility for high pressure work was to be used. The possibility of recovering the additives from the residue at the end of the process must also be examined closely, not least because of the high cost of these metals.

Other important areas of research could include:

1. the use of much faster and much slower heating rates in the thermogravimetric studies

2. the use of much higher temperatures

3. the investigation of further samples of different coals

4. the investigation of the addition of the transition metal elements in different ammounts

5. the observation of the samples with the additives using the hot stage microscope.

APPENDIX   A

TABULATED KINETIC RESULTS FOR COALS

AT 80, 40 & 20°C min^{-1} IN N$_2$ FLOWING AT 40cm^3 min^{-1}

AT ATMOSPHERIC PRESSURE

Coals heated at 80°C/min in N_2 flowing at $40 cm^3 min^{-1}$

Sample	Region	E (kJ/mol)	Temperature Range (°C)	$\frac{1}{T} \times 10^5 K^{-1}$	log k
101	E_1	8.08	205	2.90	-1.25
	E_2	53.76	620	1.12	-0.885
	E_3	159.22 TD	735	0.99	-0.52
				0.895	+0.27
201A	E_1	8.79	315 – 560	1.70	-1.37
	E_2	193.59 TD	560 – 630	1.20	-1.14
	E_3	21.88	630 – 655	1.11	-0.23
	E_4	-71.80	655 – 690	1.075	-0.19
	E_5	459.53	690 – 700	1.04	-0.34
	E_6	363.79	700 – 705	1.03	-0.10
	E_7	-19.15	705 – 735	1.02	-0.29
	E_8	121.26	735 – 800	0.99	-0.32
				0.93	+0.06
203	E_1	7.74	265 – 450	1.85	-1.82
	E_2	125.52 TD	450 – 590	1.38	-1.63
	E_3	41.77	590 – 635	1.155	-0.155
	E_4	-23.93	635 – 690	1.100	-0.035
	E_5	-54.25	690 – 745	1.04	-0.11
	E_6	138.45	745 – 820	0.98	-0.28
				0.915	+0.19
301A	E_1	10.68	215 – 365	2.04	-1.88
	E_2	41.88	365 – 440	1.565	-1.615
	E_3	84.79	440 – 495	1.405	-1.265
	E_4	47.87	495 – 535	1.30	-0.80
	E_5	149.35	535 – 565	1.24	-0.65
	E_6	224.98 TD	565 – 600	1.19	-0.26
	E_7	-95.73	600 – 660	1.15	+0.21
	E_8	88.08	660 – 705	1.07	-0.19
	E_9	-315.93	705 – 725	1.02	+0.04
	E_{10}	161.68	725 – 825	1.00	-0.29
				0.91	+0.47
301B	E_1	0.53	205 – 305	2.09	-2.01
	E_2	55.96	305 – 410	1.73	-2.0
	E_3	25.04	410 – 475	1.47	-1.24
	E_4	146.34	475 – 560	1.34	-1.07
	E_5	229.76 TD	580 – 595	1.17	0.0
	E_6	-268.06	595 – 610	1.15	+0.24
	E_7	-28.73	610 – 625	1.13	+0.04
	E_8	-54.44	625 – 660	1.11	-0.07
				1.07	-0.19

TD = temperature at which the rate of weight loss is greatest

A1

Coals heated at 80°C/min in N_2 flowing at 40cm³min⁻¹

Sample	Region	E (kJ/mol)	Temperature Range (°C)	$\frac{1}{T} \times 10^3 K^{-1}$	log k
501	E_1	10.10	265 - 400	1.85	-1.67
	E_2	71.80	400 - 435	1.49	-1.48
	E_3	14.73	435 - 460	1.41	-1.18
	E_4	130.20	460 - 555	1.36	-1.08
	E_5	60.18 TD	555 - 605	1.21	-0.06
	E_6	-402.09	605 - 610	1.14	+0.16
	E_7	-49.78	610 - 650	1.13	+0.05
	E_8	-127.65	650 - 680	1.08	-0.18
	E_9	73.95	680 - 830	1.05	-0.38
				0.905	+0.18
701	E_1	11.30	205 - 220	2.90	-1.95
		23.23	220 - 310	2.02	-1.77
	E_2	8.25	310 - 445	1.715	-1.40
	E_3	144.97	445 - 525	1.39	-1.26
	E_4	72.76 TD	525 - 595	1.25	-0.20
	E_5	-280.82	595 - 620	1.15	+0.18
	E_6	-14.89	620 - 695	1.12	-0.26
	E_7	82.06	620 - 695	1.03	-0.33
				0.89	+0.27

Coals heated at 40°C/min in N_2 flowing at 40cm³min⁻¹

Sample	Region	E (kJ/mol)	Temperature Range (°C)	$\frac{1}{T} \times 10^3 K^{-1}$	log k
201A	E_1	12.03	285 - 420	1.79	-2.07
	E_2	40.79	420 - 555	1.44	-1.85
	E_3	153.18	555 - 610	1.21	-1.36
	E_4	18.49 TD	610 - 740	1.13	-0.72
	E_5	78.06	740 - 810	0.985	-0.158
	E_6	139.78	810 - 875	0.92	-0.315
				0.87	+0.05
203	E_1	10.6	225 - 495	2.01	-1.94
	E_2	136.1 TD	495 - 585	1.305	-1.55
	E_3	-21.45	585 - 670	1.165	-0.555
	E_4	93.34	670 - 725	1.04	-0.695
	E_5	42.125	725 - 780	1.00	-0.50
	E_6	86.16	780 - 840	0.95	-0.39
	E_7	410.29	840 - 885	0.90	-0.165
				0.865	+0.585

Coals heated at 40°C/min in N_2 flowing at $40 cm^3 min^{-1}$

Sample	Region	E (kJ/mol)	Temperature Range (°C)	$\frac{1}{T} \times 10^3 K^{-1}$	log k
301A	E_1	28.80	245 - 460	1.93	-2.34
	E_2	156.66	460 - 495	1.365	-1.50
	E_3	42.12	495 - 520	1.31	-1.05
	E_4	162.75	520 - 545	1.26	-0.94
	E_5	111.94 TD	545 - 560	1.22	-0.6
	E_6	-123.39	560 - 625	1.155	-0.22
	E_7	-70.21	625 - 655	1.11	-0.51
	E_8	61.27	655 - 695	1.08	-0.62
	E_9	-39.91	695 - 725	1.03	-0.46
	E_{10}	55.70	725 - 850	1.00	-0.51
	E_{11}	268.06	850 - 890	0.89	-0.19
				0.86	+0.23
301B	E_1	7.60	250 - 360	1.91	-2.29
	E_2	195.57	360 - 395	1.57	-2.155
	E_3	5.11	395 - 465	1.50	-1.44
	E_4	394.65	465 - 485	1.35	-1.40
	E_5	61.27	485 - 515	1.32	-0.86
	E_6	186.64 TD	515 - 545	1.27	-0.70
	E_7	-10.31	545 - 595	1.22	-0.21
	E_8	-229.77	595 - 610	1.155	-0.245
	E_9	-20.74	610 - 660	1.13	-0.545
	E_{10}	12.76	660 - 745	1.07	-0.61
	E_{11}	96.93	745 - 840	0.98	-0.55
	E_{12}	315.11	840 - 885	0.90	-0.145
				0.865	+0.43
501	E_1	11.62	210 - 335	7.07	-2.365
	E_2	55.31	335 - 370	1.65	-2.11
	E_3	81.09	370 - 405	1.56	-1.85
	E_4	11.49	405 - 430	1.475	-1.49
	E_5	70.21	430 - 465	1.425	-1.46
	E_6	228.17	465 - 500	1.35	-1.185
	E_7	55.05 TD	500 - 555	1.29	-0.47
	E_8	-78.84	555 - 615	1.21	-0.24
	E_9	-14.89	615 - 650	1.125	-0.59
	E_{10}	15.56	650 - 725	1.08	-0.625
	E_{11}	47.87	725 - 770	1.00	-0.56
	E_{12}	118.71	770 - 825	0.96	-0.46
	E_{13}	172.34	825 - 875	0.91	-0.15
				0.87	+0.21
701	E_1	22.45	370 - 450	1.555	-1.60
	E_2	199.85	450 - 495	1.38	-1.39
	E_3	62.76 TD	495 - 555	1.30	-0.555
	E_4	-122.54	555 - 590	1.21	-0.26
	E_5	-4.77	590 - 690	1.16	-0.58
	E_6	51.06	690 - 815	1.04	-0.29
	E_7	244.13	815 - 890	0.92	-0.29
				0.86	+0.475

Coals heated at 20°C/min in N_2 flowing at $40 cm^3 min^{-1}$

Sample	Region	E (kJ/mol)	Temperature Range (°C)	$\frac{1}{T} \times 10^3 K^{-1}$	log k
203	E_1	16.08	210 - 485	2.07	-2.39
	E_2	125.82	485 - 525	1.32	-1.76
	E_3	148.39	525 - 555	1.25	-1.30
	E_4	82.33 TD	555 - 595	1.25	-0.99
	E_5	-91.48	595 - 670	1.15	-0.56
	E_6	157.96	670 - 705	1.06	-0.99
	E_7	-229.77	705 - 725	1.02	-0.66
	E_8	74.34	725 - 820	1.00	-0.90
	E_9	267.57	820 - 875	0.915	-0.57
				0.87	+0.08
301B	E_1	17.44	210 - 365	2.07	-2.96
	E_2	210.62	365 - 375	1.565	-2.23
	E_3	41.49	375 - 415	1.54	-1.955
	E_4	19.15	415 - 450	1.45	-1.76
	E_5	177.79	450 - 490	1.38	-1.69
	E_6	118.07 TD	490 - 525	1.31	-1.04
	E_7	32.55	525 - 595	1.25	-0.67
	E_8	-670.15	595 - 600	1.15	-0.50
	E_9	-21.27	600 - 640	1.14	-0.85
	E_{10}	15.04	640 - 775	1.095	-0.90
	E_{11}	161.24	775 - 890	0.995	-0.79
				0.86	+0.01
301A	E_1	8.78	230 - 395	1.98	-2.39
	E_2	68.21	395 - 475	1.5	-2.17
	E_3	143.60	475 - 495	1.34	-1.60
	E_4	110.10	495 - 545	1.30	-1.30
	E_5	120.35 TD	545 - 595	1.22	-0.84
	E_6	- 220.19	595 - 630	1.15	-0.40
	E_7	-27.35	630 - 660	1.11	-0.86
	E_8	8.84	660 - 715	1.075	-0.91
	E_9	71.37	715 - 840	1.01	-0.88
	E_{10}	357.41	840 - 875	0.90	-0.47
				0.87	+0.09
501	E_1	3.51	255 - 350	1.90	-2.55
	E_2	94.26	350 - 405	1.60	-2.50
	E_3	4.79	405 - 445	1.47	-1.86
	E_4	150.62 TD	445 - 535	1.39	-1.84
	E_5	-11.49	535 - 570	1.245	-0.66
	E_6	70.21	570 - 590	1.19	-0.69
	E_7	- 217.00	590 - 610	1.16	-0.58
	E_8	1.91	610 - 700	1.13	-0.92
	E_9	38.29	700 - 810	1.03	-0.91
	E_{10}	247.44	810 - 890	0.925	-0.70
				0.86	+0.14

Coals heated at 20°C/min in N_2 flowing at $40cm^3min^{-1}$

Sample	Region	E (kJ/mol)	Temperature Range (°C)	$\frac{1}{T} \times 10^3 K^{-1}$	log k
701	E_1	12.18	200 – 370	2.11	-2.50
	E_2	80.42	370 – 390	1.56	-2.15
	E_3	5.47	390 – 420	1.51	-1.94
	E_4	80.84	420 – 445	1.44	-1.92
	E_5	146.52	445 – 510	1.395	-1.73
	E_6	85.10 TD	510 – 535	1.28	-0.85
	E_7	-37.78	535 – 680	1.235	-0.65
	E_8	77.23	680 – 840	1.05	-1.015
	E_9	229.77	840 – 890	0.90	-0.41
				0.86	+0.07

APPENDIX B

TABULATED KINETIC RESULTS FOR 301A CWM + 5% CATALYSTS

AT 20°C min^{-1} AND 40°cm^3 N$_2$ min^{-1}

301A CWM in 5% CATALYSTS at 20°C/min

Sample	Region	Temperature Range (°C)	E (kJ/mol)	$\frac{1}{T} \times 10^5 \mathrm{K}^{-1}$	log k
ZnO	E_1	235 – 330	15.64	1.96	-2.56
	E_2	330 – 395	37.7	1.66	-2.35
	E_3	395 – 430	107.7	1.50	-2.04
	E_4	430 – 465	22.34	1.42	-1.59
	E_5	465 – 545	125.8	1.36	-1.52
	E_6	545 – 570 TD	57.4	1.22	-0.60
	E_7	570 – 580	-306.35	1.19	-0.51
	E_8	580 – 595	220.2	1.17	-0.83
				1.15	-0.60
Fe	E_1	200 – 235	14.47	2.11	-2.67
	E_2	235 – 375	60.6	1.66	-2.33
	E_3	375 – 415	13.2	1.54	-1.95
	E_4	415 – 430	191.5	1.45	-1.89
	E_5	430 – 455	7.7	1.42	-1.54
	E_6	455 – 495	73.6	1.37	-1.52
	E_7	495 – 560 TD	134.9	1.30	-1.27
	E_8	560 – 625	-54.7	1.20	-0.53
	E_9	625 – 725	-18.1	1.09	-0.83
	E_{10}	725 – 855	111.5	1.00	-0.92
	E_{11}	855 – 885	436.5	0.88	-0.25
				0.86	+0.32
Cr	E_1	225 – 335	8.7	2.00	-2.50
	E_2	335 – 450	55.3	1.65	-2.34
	E_3	450 – 515	120.1	1.38	-1.56
	E_4	515 – 540	76.6	1.27	-0.87
	E_5	540 – 560 TD	140.4	1.23	-0.71
	E_6	560 – 605	-67.0	1.20	-0.49
	E_7	605 – 640	-129.2	1.14	-0.70
	E_8	640 – 780	30.6	1.10	-0.97
	E_9	780 – 825	110.1	0.95	-0.73
	E_{10}	825 – 880	354.2	0.91	-0.50
				0.87	+0.24
Mn	E_1	210 – 340	5.2	2.07	-2.66
	E_2	340 – 435	82.7	1.63	-2.54
	E_3	435 – 455	23.93	1.41	-1.59
	E_4	455 – 505	93.3	1.37	-1.54
	E_5	505 – 515	392.5	1.29	-1.15
	E_6	515 – 535	70.2	1.27	-0.75
	E_7	535 – 550	-140.4	1.24	-0.64
	E_8	550 – 590 TD	64.8	1.22	-0.75
	E_9	590 – 620	-181.9	1.16	-0.53
	E_{10}	620 – 725	285.6	1.12	-0.91
	E_{11}	725 – 845	70.8	1.00	-0.88
	E_{12}	845 – 880	357.4	0.90	-0.51
				0.87	+0.05

301A CWM in 5% CATALYSTS at 20°C/min

Sample	E Region	Temperature Range (°C)	E (kJ/mol)	$\frac{1}{T}$ x 10^3K^{-1}	log k
Mo	E_1	200 – 395	24.2	2.11	-2.90
	E_2	395 – 430	104.2	1.51	-2.14
	E_3	430 – 465	28.7	1.42	-1.65
	E_4	465 – 475	19.1	1.36	-1.56
	E_5	475 – 495	157.9	1.34	-1.54
	E_6	495 – 515	172.3	1.30	-1.21
	E_7	515 – 565 TD	94.5	1.27	-0.94
	E_8	565 – 675	-56.8	+1.19	-0.57
	E_9	675 – 730	47.87	1.05	-1.00
	E_{10}	730 – 850	112.5	0.97	-0.80
	E_{11}	850 – 885	293.6	0.89	-0.33
				0.86	+0.13
Ti	E_1	205 – 330	14.1	2.09	-2.70
	E_2	330 – 400	36.1	1.695	-2.38
	E_3	400 – 440	98.1	1.48	-2.05
	E_4	440 – 475	28.7	1.40	-1.64
	E_5	475 – 510	150.0	1.34	-1.55
	E_6	510 – 560 TD	141.2	1.28	-1.08
	E_7	560 – 720	-57.4	1.20	-0.49
	E_8	720 – 755	38.3	1.05	-0.94
	E_9	755 – 835	76.6	0.97	-0.78
	E_{10}	835 – 875	383.0	0.90	-0.50
				0.87	+0.10
W	E_1	230 – 330	1.7	+1.99	-2.55
	E_2	330	53.2	1.66	-2.52
	E_3	400	126.4	1.48	-2.02
	E_4	425	19.1	1.43	-1.69
	E_5	470	220.2	1.35	-1.61
	E_6	490 TD	99.2	1.31	-1.15
	E_7	560	-45.9	1.20	-0.58
	E_8	620	-124.5	1.125	-0.76
	E_9	650	39.9	1.085	-1.02
	E_{10}	755	76.6	0.97	-0.78
	E_{11}	845 – 875	390.6	0.895	-0.48
				0.87	+0.03
Zr	E_1	255 – 285	153.2	1.89	-3.41
	E_2	285	42.4	1.79	-2.61
	E_3	370	6.4	1.55	-2.09
	E_4	410	126.7	1.46	-2.06
	E_5	440	61.3	1.40	-1.63
	E_6	515	163.6	1.27	-1.25
	E_7	555 TD	71.8	1.22	-0.78
	E_8	575	-31.2	1.18	-0.63
	E_9	730	82.9	0.99	-0.94
	E_{10}	835 – 885	335.1	0.9	-0.55
				0.86	+0.15

301A CWM in 5% CATALYSTS at 20°C/min

Sample	E Region	Temperature Range (°C)	E (kJ/mol)	$\frac{1}{T} \times 10^3 K^{-1}$	log k
NiO	E_1	205 - 285	2.5	2.09	-2.66
	E_2	285	27.5	1.79	-2.62
	E_3	385	95.7	1.525	-2.24
	E_4	430	48.5	1.425	-1.74
	E_5	470	95.7	1.35	-1.55
	E_6	505	143.6	1.29	-1.25
	E_7	540　TD	33.5	1.23	-0.8
	E_8	600	-53.6	1.15	-0.66
	E_9	680	15.3	1.05	-0.94
	E_{10}	780 - 885	161.7	0.95	-0.86
				0.86	+0.10
Cu	E_1	210	6.0	2.07	-2.57
	E_2	345	59.3	1.625	-2.43
	E_3	405	111.0	1.47	-1.95
	E_4	430	56.5	1.42	-1.66
	E_5	490　TD	157.4	1.315	-1.35
	E_6	545	-34.8	1.225	-0.61
	E_7	725	113.1	1.005	-1.01
	E_8	845 - 875	352.3	0.895	-0.36
				0.87	+0.10
Co	E_1	200	5.0	2.11	-2.97
	E_2	260	41.7	1.88	-2.91
	E_3	375	86.5	1.54	-2.17
	E_4	440	5.9	1.40	-1.56
	E_5	475	196.3	1.34	-1.54
	E_6	495　TD	107.2	1.30	-1.13
	E_7	560	-62.5	1.20	-0.57
	E_8	635	20.1	1.10	-0.88
	E_9	725	52.4	1.00	-0.77
	E_{10}	835 - 885	462.0	0.90	-0.51
				0.86	+0.38
V	E_1	305	35.6	1.73	-2.54
	E_2	415	134.0	1.45	-2.02
	E_3	435	17.4	1.41	-1.74
	E_4	470	144.7	1.35	-1.69
	E_5	490	38.3	1.31	-1.35
	E_6	520　TD	123.6	1.26	-1.25
	E_7	600	-87.5	1.15	-0.54
	E_8	625	-27.3	1.11	-0.70
	E_9	755	109.2	0.97	-0.9
	E_{10}	835 - 885	366.5	0.90	-0.48
				0.86	+0.19

APPENDIX   C

TABULATED KINETIC RESULTS FOR 501 LLANHARAN AND 5% CATALYSTS

AT 20°C min^{-1} AND 40cm^3 N$_2$ min^{-1}

Sample	Region	Temperature Range (°C)		E (kJ/mol)	$\frac{1}{T} \times 10^5 K^{-1}$	log k
ZnO	E$_1$	220		17.1	2.03	-2.77
	E$_2$	315		48.5	1.705	-2.48
	E$_3$	410		96.97	1.46	-1.86
	E$_4$	455	TD	142.0	1.37	-1.43
	E$_5$	525		-54.7	1.25	-0.54
	E$_6$	655		15.9	1.08	-1.04
	E$_7$	710		70.25	1.02	-0.99
	E$_8$	835 - 875		414.8	0.90	-0.55
					0.87	+0.10
Fe	E$_1$	210		10.26	2.07	-2.76
	E$_2$	285		45.8	1.79	-2.61
	E$_3$	390		70.0	1.56	-2.06
	E$_4$	435		111.9	1.41	-1.53
	E$_5$	470		164.9	1.35	-1.15
	E$_6$	510	TD	76.6	1.28	-0.59
	E$_7$	525		-60.2	1.25	-0.47
	E$_8$	655		55.3	1.08	-1.02
	E$_9$	835 - 875		414.8	0.90	-0.50
					0.87	+0.50
Cr	E$_1$	220		22.9	2.03	-2.80
	E$_2$	355		118.4	1.59	-2.28
	E$_3$	375		31.9	1.54	-1.94
	E$_4$	415		110.4	1.45	-1.79
	E$_5$	460	TD	139.2	1.36	-1.30
	E$_6$	525		-63.8	1.25	-0.50
	E$_7$	620		22.9	1.12	-0.95
	E$_8$	740		103.6	0.98	-0.79
	E$_9$	835 - 875		38.3	0.90	-0.33
					0.87	+0.27
Mn	E$_1$	210		5.3	2.07	-2.71
	E$_2$	300		58.2	1.75	-2.62
	E$_3$	400		14.7	1.48	-1.83
	E$_4$	430		181.9	1.42	-1.78
	E$_5$	485	TD	84.8	1.32	-0.83
	E$_6$	525		-54.1	1.25	-0.52
	E$_7$	655		56.8	1.08	-1.00
	E$_8$	810 - 870		237.4	0.92	-0.54
					0.87	+0.04
Mo	E$_1$	205		14.6	2.08	-2.90
	E$_2$	300		54.4	1.74	-2.64
	E$_3$	400		94.3	1.45	-1.83
	E$_4$	445	TD	145.0	1.39	-1.51
	E$_5$	530		-79.7	1.25	-0.45
	E$_6$	620		15.3	1.12	-0.97
	E$_7$	725		86.2	1.00	-0.87
	E$_8$	835 - 885		317.3	0.90	-0.42
					0.86	+0.16

C1

501 LLANHARAN in 5% CATALYSTS at 20°C/min, 40cm^3/min N_2

Sample	Region	Temperature Range (°C)	E (kJ/mol)	$\frac{1}{T}$ x 10^5K^{-1}	log k
Ti	E_1	215	5.0	2.05	-2.68
	E_2	315	65.4	1.70	-2.59
	E_3	395	15.3	1.50	-1.89
	E_4	415	159.6	1.45	-1.85
	E_5	430	61.3	1.42	-1.6
	E_6	455	178.1	1.37	-1.44
	E_7	515	-40.1	1.27	-0.51
	E_8	675 TD	66.0	1.05	-0.96
	E_9	825 - 870	317.3	0.91	-0.46
				0.87	+0.12
W	E_1	200	7.0	2.11	-2.67
	E_2	290	27.0	1.78	-2.55
	E_3	390	80.7	1.56	-2.24
	E_4	430	51.1	1.42	-1.65
	E_5	465	215.4	1.36	-1.49
	E_6	485 TD	105.9	1.32	-1.04
	E_7	540	-46.6	1.23	-0.57
	E_8	680	65.1	1.05	-1.02
	E_9	835 - 875	268.1	0.9	-0.51
				0.87	+0.09
Zr	E_1	225	10.0	2.01	-2.73
	E_2	295	39.0	1.76	-2.60
	E_3	400	84.8	1.49	-2.05
	E_4	470	153.2	1.35	-1.43
	E_5	505 TD	125.8	1.29	-0.95
	E_6	550	-63.0	1.22	-0.49
	E_7	670	42.5	1.06	-1.00
	E_8	755	79.1	0.97	-0.80
	E_9	835 - 875	229.8	0.90	-0.49
				0.87	+0.13
NiO	E_1	205	10.8	2.09	-2.75
	E_2	335	61.6	1.64	-2.50
	E_3	420	111.4	1.44	-1.84
	E_4	480	242.5	1.33	-1.20
	E_5	495 TD	66.4	1.30	-0.82
	E_6	545	-81.7	1.22	-0.56
	E_7	600	-34.5	1.15	-0.88
	E_8	640	35.7	1.10	-0.97
	E_9	780	91.9	0.95	-0.69
	E_{10}	835 - 885	404.8	0.90	-0.45
				0.86	+0.29

501 LLANHARAN in 5% CATALYSTS at 20°C/min, 40cm³/min N_2

Sample	Region	Temperature Range (°C)	E (kJ/mol)	$\frac{1}{T}$ x 10^5K^{-1}	log k
Cu	E_1	200	5.3	2.10	-2.75
	E_2	290	42.4	1.77	-2.66
	E_3	375	83.6	1.54	-2.14
	E_4	470	253.7	1.35	-1.31
	E_5	490 TD	56.3	1.31	-0.78
	E_6	550	-80.1	1.22	-0.52
	E_7	630	34.0	1.11	-0.98
	E_8	755	67.8	0.97	-0.74
	E_9	825 - 885	314.9	0.91	-0.51
				0.86	+0.23
Co	E_1	215	6.4	2.05	-2.75
	E_2	250	36.6	1.90	-2.70
	E_3	325	29.5	1.67	-2.27
	E_4	380	64.6	1.53	-2.12
	E_5	455 TD	134.6	1.37	-1.58
	E_6	550	-50.4	1.22	-0.49
	E_7	715	101.1	1.01	-1.03
	E_8	850 - 885	478.8	0.89	-0.37
				0.86	+0.25
V	E_1	205	4.7	2.09	-2.73
	E_2	295	23.0	1.76	-2.65
	E_3	375	94.2	1.54	-2.38
	E_4	470	196.9	1.35	-1.47
	E_5	485 TD	120.6	1.32	-1.11
	E_6	550	-61.9	1.22	-0.48
	E_7	645	18.3	1.09	-0.90
	E_8	755	83.6	0.97	-0.79
	E_9	810 - 885	206.8	0.92	-0.55
				0.87	-0.01

APPENDIX   D

TABULATED KINETIC RESULTS FOR 301A CWM AND 10% CATALYSTS

AT 20°C min^{-1} AND 40cm^3 N$_2$ min^{-1}

301 CWM in 10% CATALYSTS at 20°C/min, 40cm³/min N_2

Sample	Region	Temperature Range (°C)		E (kJ/mol)	$\frac{1}{T} \times 10^5 K^{-1}$	log k
ZnO	E_1	200		14.5	2.11	-2.81
	E_2	290		26.4	1.78	-2.56
	E_3	365		51.17	1.57	-2.27
	E_4	415		93.3	1.45	-1.95
	E_5	455			1.37	-1.56
	E_6	470	TD	105.3	1.35	-1.56
	E_7	565		-54.35	1.19	-0.68
	E_8	665		135.8	1.07	-1.02
	E_9	815		454.7	0.91	-0.72
		880			0.87	+0.23
Zn	E_1	200		16.0	2.11	-2.93
	E_2	280		47.9	1.81	-2.68
	E_3	355		12.8	1.39	-2.13
	E_4	395		111.1	1.50	-2.07
	E_5	440		61.7	1.40	-1.49
	E_6	490	TD	134.0	1.31	-1.20
	E_7	555		-69.6	1.21	-0.50
	E_8	640		12.8	1.10	-0.90
	E_9	745		142.4	0.98	-0.82
		875			0.87	+0.002
Ti	E_1	205		12.9	2.09	-2.69
	E_2	340		48.9	1.63	-2.38
	E_3	415		134.0	1.45	-1.92
	E_4	440		19.1	1.40	-1.57
	E_5	470		108.5	1.35	-1.52
	E_6	520	TD	196.3	1.26	-1.01
	E_7	550		2.7	1.22	-0.60
	E_8	600		-118.7	1.15	-0.59
	E_9	640		19.1	1.10	-0.90
	E_{10}	780		268.1	0.95	-0.75
		880			0.87	+0.32
W	E_1	200		3.6	2.11	-2.48
	E_2	285		16.9	1.79	-2.42
	E_3	380		92.87	1.53	-2.19
	E_4	440		61.9	1.40	-1.56
	E_5	515		181.9	1.27	-1.14
	E_6	540	TD	40.7	1.23	-0.76
	E_7	600		-86.25	1.15	-0.59
	E_8	665		33.5	1.07	-0.95
	E_9	780		181.9	0.95	-0.74
		875			0.87	+0.02

301 CWM in 10% CATALYSTS at 20°C/min, 40cm^3/min N$_2$

Sample	Region	Temperature Range (°C)		E (kJ/mol)	$\frac{1}{T}$ x 10^{5}K^{-1}	log k
Mn	E$_1$	205		10.8	2.09	-2.77
	E$_2$	290		36.4	1.77	-2.59
	E$_3$	410		124.5	1.46	-2.00
	E$_4$	440		79.5	1.40	-1.61
	E$_5$	515		201.0	1.27	-1.07
	E$_6$	540	TD	27.4	1.23	-0.65
	E$_7$	590		-95.7	1.16	-0.55
	E$_8$	655		45.5	1.08	-0.95
	E$_9$	815		256.6	0.92	-0.57
		875			0.87	+0.10
Cr	E$_1$	220		5.4	2.03	-2.59
	E$_2$	290		29.5	1.78	-2.52
	E$_3$	375		108.5	1.54	-2.15
	E$_4$	415		130.2	1.45	-1.96
	E$_5$	440		66.3	1.40	-1.62
	E$_6$	515	TD	210.6	1.27	-1.17
	E$_7$	540		31.9	1.23	-0.73
	E$_8$	560		-44.2	1.17	-0.63
	E$_9$	685		36.4	1.04	-0.93
	E$_{10}$	795		270.8	0.94	-0.74
		880			0.87	+0.25
Mo	E$_1$	200		16.8	2.11	-2.70
	E$_2$	375		72.5	1.54	-2.20
	E$_3$	440		69.27	1.40	-1.67
	E$_4$	515		191.5	1.27	-1.20
	E$_5$	540	TD	55.0	1.23	-0.80
	E$_6$	600		-82.3	1.15	-0.57
	E$_7$	680		159.35	1.05	-1.00
	E$_8$	810		291.0	0.92	-0.63
		880			0.87	+0.13
NiO	E$_1$	200		16.5	2.11	-2.60
	E$_2$	405		106.7	1.47	-2.05
	E$_3$	440		34.5	1.40	-1.66
	E$_4$	470		197.9	1.35	-1.57
	E$_5$	485		27.4	1.32	-1.26
	E$_6$	530	TD	109.1	1.25	-1.16
	E$_7$	600		-76.6	1.15	-0.59
	E$_8$	675		56.2	1.05	-0.99
	E$_9$	835		510.6	0.90	-0.55
		875			0.87	+0.25

Sample	Region	Temperature Range (°C)		E (kJ/mol)	$\frac{1}{T} \times 10^5 K^{-1}$	log k
V	E_1	205		14.1	2.09	-2.69
	E_2	385		86.8	1.52	-2.27
	E_3	535	TD	102.1	1.24	-1.00
	E_4	600		-107.2	1.15	-0.52
	E_5	680		57.4	1.05	-1.08
	E_6	830		450.0	0.91	-0.66
		875			0.87	+0.28
Co	E_1	200		8.5	2.11	-2.72
	E_2	800		34.0	1.75	-2.56
	E_3	400		102.1	1.48	-2.08
	E_4	430		50.3	1.42	-1.76
	E_5	475	TD	101.8	1.34	-1.55
	E_6	600		-122.5	1.15	-0.54
	E_7	675		59.4	1.05	-1.18
	E_8	780		220.2	0.95	-0.87
		875			0.87	+0.05
Cu	E_1	230		10.6	1.99	-2.60
	E_2	395		143.6	1.50	-2.33
	E_3	440		31.1	1.40	-1.58
	E_4	485		72.5	1.32	-1.45
	E_5	575	TD	167.5	1.18	-0.92
	E_6	605		-191.5	1.14	-0.57
	E_7	655		98.1	1.08	-1.17
		815			0.92	-0.35
Fe	E_1	205		4.5	2.09	-2.72
	E_2	250		29.2	1.92	-2.68
	E_3	305			1.71	-2.36
	E_4	410		220.2	1.46	-2.36
	E_5	440		67.0	1.40	-1.67
	E_6	510	TD	166.9	1.28	-1.25
	E_7	595		30.1	1.21	-0.64
	E_8	605		-118.1	1.14	-0.53
	E_9	655		24.3	1.08	-0.90
	E_{10}	805		245.7	0.93	-0.71
		875			0.87	+0.06

APPENDIX   E

TABULATED KINETIC RESULTS FOR 501 LLANHARAN AND 10% CATALYSTS

AT 20°C min^{-1} AND 40cm^3 N$_2$ min^{-1}

Sample	Region	Temperature Range (°C)		E (kJ/mol)	$\frac{1}{T} \times 10^5 K^{-1}$	log k
ZnO	E_1	200		9.9	2.11	-2.82
	E_2	270		26.9	1.84	-2.68
	E_3	365		126.4	1.57	-2.30
	E_4	385		28.7	1.52	-1.97
	E_5	410		85.1	1.46	-1.88
	E_6	455		196.9	1.37	-1.48
	E_7	495	TD	38.3	1.30	-0.76
	E_8	535		-53.3	7.24	-0.64
	E_9	640		30.8	1.10	-1.03
	E_{10}	810		233.6	0.92	-0.74
		875			0.87	-0.13
Zr	E_1	200		9.3	2.11	-2.84
	E_2	315		98.9	1.70	-2.64
	E_3	335		34.7	1.64	-2.33
	E_4	400		137.2	1.48	-2.04
	E_5	430		67.0	1.42	-1.61
	E_6	460		207.4	1.36	-1.40
	E_7	495	TD	48.9	1.30	-0.75
	E_8	555		-84.2	1.21	-0.52
	E_9	630		41.3	1.11	-0.96
	E_{10}	810		329.3	0.92	-0.55
		880			0.87	+0.31
Ti	E_1	205		13.0	2.09	-2.67
	E_2	370		191.5	1.56	-2.31
	E_3	375		56.2	1.54	-2.11
	E_4	445		174.5	1.39	-1.67
	E_5	495	TD	74.2	1.30	-0.85
	E_6	545		-45.1	1.22	-0.54
	E_7	675		60.0	1.05	-0.94
	E_8	835		357.4	0.90	-0.47
		880			0.87	+0.09
W	E_1	200		2.8	2.11	-2.48
	E_2	315		31.1	1.70	-2.42
	E_3	410		129.2	1.46	-2.03
	E_4	430		57.4	1.42	-1.76
	E_5	460		202.4	1.36	-1.58
	E_6	505	TD	84.8	1.29	-0.84
	E_7	550		-63.8	1.22	-0.53
	E_8	635		20.6	1.10	-0.93
	E_9	755		82.1	0.97	-0.79
	E_{10}	835		338.3	0.90	-0.49
		875			0.87	+0.04

501 LLANHARAN in 10% CATALYSTS at 20°C min^{-1} N$_2$-40cm^3 min^{-1}

Sample	Region	Temperature Range (°C)		E (kJ/mol)	$\frac{1}{T}$ x 10^{5}K^{-1}	log k
Mn	E$_1$	245		9.3	1.93	-2.47
	E$_2$	345		43.4	1.62	-2.32
	E$_3$	405		90.5	1.47	-1.98
	E$_4$	460		268.1	1.36	-1.46
	E$_5$	485	TD	86.2	1.32	-0.90
	E$_6$	550		-58.7	1.22	-0.45
	E$_7$	660		49.8	1.07	-0.91
	E$_8$	810		218.3	0.92	-0.52
		875			0.87	+0.05
Cr	E$_1$	205		12.0	2.09	-2.82
	E$_2$	320		29.6	1.69	-2.57
	E$_3$	360		81.1	1.58	-2.40
	E$_4$	435		38.3	1.41	-1.68
	E$_5$	455		117.6	1.37	-1.60
	E$_6$	495	TD	90.3	1.30	-0.87
	E$_7$	540		52.7	1.23	-0.54
	E$_8$	665		46.0	1.07	-0.98
	E$_9$	810		294.9	0.92	-0.62
		875			0.87	+0.15
Mo	E$_1$	200		20.4	2.11	-3.07
	E$_2$	325		88.8	1.65	-2.58
	E$_3$	375		8.2	1.54	-2.07
	E$_4$	405		105.3	1.47	-2.04
	E$_5$	470	TD	128.1	1.35	-1.38
	E$_6$	550		-60.4	1.22	-0.51
	E$_7$	645		27.4	1.09	-0.92
	E$_8$	775		19.1	0.95	-0.72
	E$_9$	835		491.4	0.90	-0.48
		875			0.87	+0.29
NiO	E$_1$	225		6.6	2.01	-2.60
	E$_2$	395		148.7	1.49	-2.42
	E$_3$	485	TD	101.5	1.32	-1.10
	E$_4$	550		-54.9	1.22	-0.57
	E$_5$	665		44.7	1.07	-1.00
	E$_6$	810		367.6	0.92	-0.65
		875			0.87	+0.31
V	E$_1$	210		12.2	2.07	-2.86
	E$_2$	340		106.4	1.63	-2.58
	E$_3$	375		14.9	1.54	-2.08
	E$_4$	415		90.9	1.45	-2.01
	E$_5$	455	TD	145.5	1.37	-1.63
	E$_6$	550		-60.4	1.22	-0.49
	E$_7$	645		19.1	1.09	-0.90
	E$_8$	780		203.4	0.95	-0.76
		875			0.87	+0.09

501 LLANHARAN in 10% CATALYSTS at $20°C$ min^{-1} N_2-$40cm^3$ min^{-1}

Sample	Region	Temperature Range (°C)		E (kJ/mol)	$\frac{1}{T} \times 10^5 K^{-1}$	log k
Co	E_1	200		6.5	2.11	-2.59
	E_2	320		42.8	1.67	-2.44
	E_3	395		111.1	1.50	-2.06
	E_4	415		44.0	1.45	-1.77
	E_5	470	TD	159.6	1.35	-1.54
	E_6	545		-54.7	1.23	-0.54
	E_7	645		33.5	1.09	-0.94
	E_8	800		325.5	0.93	-0.66
		880			0.87	+0.36
Cu	E_1	200		12.6	2.11	-2.76
	E_2	350		73.9	1.61	-2.43
	E_3	440		30.6	1.40	-1.62
	E_4	470	TD	135.3	1.35	-1.54
	E_5	560		-65.8	1.20	-0.48
	E_6	685		26.8	1.04	-1.03
	E_7	730		268.1	0.99	-0.96
		785			0.95	-0.40
Fe	E_1	200		7.1	2.11	-2.80
	E_2	315		63.2	1.68	-2.64
	E_3	470	TD	150.2	1.35	-1.55
	E_4	550		-57.4	1.22	-0.53
	E_5	655		29.3	1.08	-0.95
	E_6	825		450.0	0.91	-0.69
		880			0.87	+0.25

E3

APPENDIX F

A Sample Calculation showing the use of the Serageldin and Pan Method of Kinetic Analysis

The final equation obtained by Serageldin and Pan[44] is

$$\left[\log\ -\left[\frac{dm/dt.}{m_i - m_f}\right]\right]\cdot\left[\frac{m_i - m_f}{m - m_f}\right] = \log A \quad - \frac{E}{2.3T}$$

where $-$ dm/dt = rate of mass change at time t ($mg\,min^{-1}$)

m_i = initial mass of sample (mg)

m_f = final mass of sample at the end of the experiment (mg)

m = mass of sample at time t (mg)

E = activation energy ($kJ\,mol^{-1}$)

R = universal gas constant

T = temperature (K)

A = pre-exponential factor (s^{-1})

At a temperature of 350°C (623K) the sample 501 Llanharan with 10% ZnO added by weight has the following values for these parameters

dm/dt = -0.0201 $mg\,min^{-1}$

m_i = 12.9679 mg

m_f = 8.9124 mg

m = 99.5% of 12.9679

T = 623K

As A and E are not known a graph needs to be drawn of the left hand side of the equation vs. 1/T. The left hand side of the equation is equivalent to logK.

$$\log k = \left[\log \left[\frac{-dm/dt}{m_i - m_f}\right]\right] \cdot \left[\frac{m_i - m_f}{m - m_f}\right]$$

$$= \left[\log \left[\frac{+ \, 0.0201}{12.9679 - 8.9124}\right]\right] \cdot \left[\frac{12.9679 - 8.9124}{12.9031 - 8.9124}\right]$$

$$= \log \quad 5.0367 \times 10^{-3}$$

?

$$= \underline{\underline{-2.29}}$$

In order to find E (and A if required) a series of calculations at different temperatures must be performed. A graph must then be plotted of log k against I/T, where the gradient of the straight line is equal to E/2.3R and the intercept on the y-axis is equal to log A.

REFERENCES

1. EVAN, T and PHELPS, T.H.C. Proc. S.Wales Inst. Engrs. 54 (1938) 169

2. BURGESS, M.J. and WHEELER, R.V. J.Chem.Soc. 97(1910) 1911, 1917.

3. BURGESS, M.J. and WHEELER, R.V. J.Chem.Soc.99 (1914) 649

4. BURGESS, M.J. and WHEELER, R.V. J.Chem.Soc.105(1920) 131

5. HOLROYD, R. and WHEELER, R.V. J.Inst. Fuel 9 (1930),40,76,104

6. AUDIBERT, E. Rev.Ind.Minerate (1926) 115-36

7. HONDA, K. Sci.Rep. Totoku Univ. Scr 1, 4 (1915) 97

8. THEVENIN, R. Bull.Soc.Hist. Nat.Toulouse 85 (1950) 383-8

9. VAN KREVELEN, D.W., VAN HEERDEN, C. and HUNTJENS, F.J. Fuel 30 (1951) 253-59

10. BOYER, A.F. Compt. Rend.Congr.Ind. Gaz 69th Congr. 1952, 653-650, 668-671.

11. TANNO, H.J. Coal Research Inst. Japan 3 (1952) 43

12. Bracia Goyanes, C. Inform. Quim. Anal (Madrid) 9 (1955)159-174

13. VAN KREVELEN, D.W. HUNTJENS, F.J. and DORMANS, H.N.M. Fuel 35 (1956) 462-475.

14. CHERMIN, H.A.G. and VAN KREVELEN, D.W. Fuel 36 (1957)85-104

15. VAN KREVELEN, D.W. and SCHUYER, J. "Coal Science", Elsevior 1957.

16. FROLICH, P.K. and FULTON, S.C. "The Science of Petroleum" vol.3, pg 2099, Oxford Univ. Press 1928.

17. D'ALELIO, C.F. "Fundamental Principles of Polymerization" Wiley 1952.

18. SCHLIYER, J. Brennst.Chemie 37 (1956) 74

19. BROWN, H.R. Fuel 30 (1957) 157-159.

20. WATERS, P.L. Nature 178 (1956) 324

21. WATERS, P.S. Coke and Gas 20 (1958), 252, 289, 341

22. DRYDEN, I.G.C. Fuel 36 (1957) 156

23. BERKOWITZ, N. Fuel 39 (1960) 47-58

24. VERAA M.J. and BELL, A.T. Fuel 57 (1978) 194-200

25. TAYLOR, H.S. and NEVILLE, H. J.Am.Chem.Soc.43 (1921) 2055

26. DENT, F.J., BLACKBURN, W.H. and MILLET H.C. Trans. Inst. Gas Engrs. 88 (1938) 150.

27. WELLER, S. and PELIPETZ, M.C. Ind. Eng.Chem. 43 (1951) 243.

28. WALKER, P.L., SHELEF, M. and ANDERSON, R.A. "Catalysis of Carbon Gasification", Chemistry and Physics of Carbon 4 (1968) 287.

29. HAYNES, WP, GASIOR, S. and FORNEY, A.J., A.C.S. Div. Fuel Chem. Proc. 18(2) (1973) 1.

30. WILSON, W.G., SEALOCK, L.J., HOODMAKER, F.C., HOFFMAN, R.W., COX, J.L., AND STINSON, D.L., A.C.S. Div. Fuel Chem. Proc. 18(2) (1973) 29.

31. GARDNER, N.C., SAMUELS, WE. and WILKS, K.A. "Coal Gasification" td L. Masset, A.C.S. Advances in Chemistry Series 131 (1974) 213.

32. WILKS K.A., GARDNER, N.C. and ANGUS, J.C., A.C.S. Div. Fuel Chem. Proc. 20(3) (1975) 52.

33. WISER, W.N., ANDERSON, L.L., QADER, S.A. and HILL, G.R. J. Appl. Biotechnol. 21. (1971) 82.

34. RAI.C. AND TRAN, D.Q. Fuel 58 (1979) 603-608.

35. CIURYLA, V.T., WEIMER, R.F., BIVANS, D.A. and MOTIKA, S.A. Fuel 58 (1979) 748-754.

36. SMITH, S.E., NEAVEL, R.C., HIPPO, E.J. and MILLER, R.N. Fuel 60 (1981) 458-462.

37. ROSENVOLD, R.J, DUBOW, J.B. and RAJESHWAR, K. Thermochim. Acta 53 (1982) 321-332.

38. CUMMING, J.W. and McLAUGHLIN, J, Thermochim.Acta 57 (1982) 253-272.

39. WAGONER, C.L. and DUZY, A.F. "Burning Profiles of Solid Fuels" ASME Paper 67-WA/FU-4 (1976).

40. WAGONER, C.L. and WINEGARTER, E.C. J.Eng.Power 95 (1973) 119.

41. VECCI, S.J., WAGONER, C.L. and OLSON, G.B. Proc. AM Power Conf. Vol.40 (1978) 850-864.

42. CUMMING, J.W. Fuel 63 (1984) 1436-1440).

43. SERAGELDIN, M.A. and PAN, W. THERMOCHIM. ACTA 71 (1983) 1-14.

44. SERAGELDIN, M.A. and PAN, W. THERMOCHIM.ACTA 76 (1984) 145-160

45. VAN KREVELEN, O.W. "Coal" Elsevier 1961.

46. JUNTGEN, H. and VAN.HEEK, K.H. Fuel 62 (1983) 534.

47. EVANS, M.G. and POLANYL, M. Trans. Faraday Soc.34 (1984) 11.

48. MERRICK, D. Fuel 62 (1983) 534-539.

49. MERRICK, D. Fuel 62 (1983) 540-546.

50. MERRICK, D. Fuel 62 (1983) 547-552.

51. JUNTGEN, H. Fuel 63 (1984) 731-737.

52. ELDER, J.P. and HARRIS, M.B. Fuel 63 (1984) 262-267.

53. GHETTI, P., De.ROBERTIS, U., D'ANTONE, S, VILLANI, M. and CHIELLINI, E. Fuel 64 (1985) 950-955.

54. GHETTI, P. Fuel 65 (1986) 636-639.

55. VARGAS, J.M. and PERLMUTTER, D.D. Ind. Eng. Chem. Process Des. Dev. 25 (1986) 49-54.

56. SUUBERT, E.M., PETERS, W.A. and HOWARD, J.B. Ind.Eng. Chem.Process Des.Dev. 17 (1978) 37.

57. WEAST, R.C. in "Handbook of Chemistry and Physics" 54th Edition. CRC. Press 1973.

58. FRANCIS, W. "Coal: its Formation and Structure" - E. Arnold and Sons 1954.

59. PITT, G.J. and MILLWARD, G.R. "Coal and Modern Coal Processing: An Introduction" Academic Press 1979.

60. HARKER, J. and BACKHURST, J.R. "Fuel and Energy" Academic Press 1981.

61. FRANCIS, W. and PETERS, M.C. "Fuel and Fuel Technology" Pergamon 1980.

62. BERKOMITZ, N. "An Introduction to Coal Technology" Academic Press 1979.

63. STOPES, M.C. and WHEELER, R.V. "Monograph on the Constitution of Coal" H.M.S.O. 1918.

64. HILT, C. STIZBER, Aach.Bez. Ver. V.D.I. H4 (1873)

65. RENTON, J.J. in "Coal Structure" Ed. R.A. Meyers Academic Press 1982.

66. GLUSKOTER, H.J. Adv.Chem.Ser. 141 (1975) 1-22.

67. MACKOWSKY, M.T. in "Coal and Coal Bearing Strata" Eds. D. Murchison and T.S. Westroll Elsevier (1968) pp 309-321.

68. National Enviromental Research Council, Inst. Geol.Sci. "British Regional Geology-South Wales" 3rd Edition, HMSO,1982.

69. TROTTER, F.M. Quar.J.Geol.Soc. 104 (1948) 387-437.

70. TROTTER, F.M. Geol.Mag. 87 (1950) 196-208.

71. TROTTER, F.M. Proc.Yorks. Geol.Soc. _29_ (1954) 267-303.

72. LAURENDEAU, N.M. Proj.Energy Combust. Sci._4_ (1978) 231-270.

73. BRUNAUER, S., EMMETT, P.H. and TELLER, E.J. AmChem.Soc.
     _60_ (1938) 309-319.

74. DUBININ, M.M. in "Chemistry and Physics of Carbon"
     Ed. P.L. Walker Jr. Edward Arnold 1966.

75. WILLIAMS, P. (ed) "Programming the BBC Micro" Newnes
     Microcomputer Books, Butterworth and Co. 1963.

76. FREEMAN, R. "Step by Step Basic" BBC Micro/Electron Edn.
     Lifelong Learning Ltd. 1983.

77. MARSH, H. and SIEMIENIEWSKA, T. Fuel _44_ (1965) 355.

78. MARSH, H. Fuel _44_ (1965) 253.

79. WALKER P.L. and KINI, K.A. Fuel _44_ (1965) 453

80. WALKER, P.L. and PATEL, R.L. Fuel _49_ (1970) 99.

81. LARSEN, J.W. "Coal Structure" in "Chemistry and Physics"
     of Coal Utilization", Eds. B.R. Cooper and L. Petrakis,
     AM.INST. Physics, 1980.

82. HARRIS, L.R. and YUST, C.S. Fuel _55_ (1976) 233.

83. GAN, H., NANDI, S.P. and WALKER P.L. Fuel _51_ (1972) 272.

84. SWIETERING, P. and VAN KREVELEN, D.W. Fuel _33_ (1954) 331.

85. HIRSCH, P.B. Proc. Royal Soc. (London) _A226_ (1954) 143-169.

86. HIRSCH, P.B. Proc. Royal Soc. (London) _A252_ (1960) 68.

87. MAHAJAN, O.P. and WALKER, P.L. in "Analytical Methods
     for Coal and Coal Products, Volume 1". Ed. C.Karr Jr.
     Academic Press 1978.

88. GIVEN, P.H., BIMER, J. and RAJ, S. "Oxidative Study
     of the structure of Vitrinites". Presented at Fuel
     Division Chicago ACS Meeting August 1977.

89. WINANS, R.E., HAYATSU, R. SCOTT, R.G., MOORE, L.P. and
     STUDIER, M.H. "Examination and Comparison of Structure,
     Lignite, Bituminous and Anthracite Coal". Presented at
     SRI Coal Chemistry Workshop, Menlo Park, California,
     August, 1976.

90. CHAKRABARTTY, S.K. and BERKOWITZ, N. Fuel _53_ (1974) 240.

91. ERGUN, S. and TIENSUU, V. Nature _183_ (1959) 1668.

92. ERGUN, S. and TIENSUU, V. Acta Cryst. 12 (1959) 1050.

93. FRIEDEL, R.A., and QUEISER, J.A. Fuel 38 (1959) 369.

94. GIVEN, P.H. and PEOVER, M.E. Fuel 39 (1960).

95. BLOM. L., EDELHAUSEN, L. and VAN KREVELEN, D.W. Fuel 36 (1957).

96. GIVEN, P.H., WALKER, P.L., SPACKMAN, W., DAVIS, A., and LOVELL, H.L., "The Relation of Coal Characteristics to Coal Liquefaction Behaviour" Report 4 from Pensylvania State Univ. submitted to National Science Foundation, Dec. 1st 1975, pg. 13.

97. SCHAFER, H.N.S. Fuel 49 (1970) 197

98. RUBERTO, R.G. "Oxygen and Oxygen Functional Groups in Coal and Coal Liquids". Presented at EPRI Contractors Conference, Palo Alto, California, May 1977.

99. CRONAUER, D.C. and RUBERTO, R.G. An investigation of Mechanisms of Reactors involving oxygen containing compounds in coal Hydrogenation" EPRI AF-442 Jan. 1977.

100. WHITEHURST, D.D., MITCHELL, TO., and FARCASIU, M. "Coal Liquafaction". Academic Press 1980.

101. GIVEN, P.H. Fuel 31 (1960) 147.

102. FUCHS, W. and SANDHOFF, A.G. Ind.Eng.Chem. 34 (1942) 567-71.

103. LOWRY, H.H. Fuel 10 (1937) 291-301.

104. WISER, W.H. "Research in Coal Technology – The University's Role". OCR/NSF-RANN Workshop Proceedings, Buffalo, New York, October 1974.

105. MAZUMDAR, B.K. GANGULY, S., SANYAL, P.K., and LAHIRI, A. "Aliphatic Structures in Coal" Coal Science Adv. in Chemistry Series No. 55 (1966) 475. AmChem.Soc.

106. MOOKHERJEA, S.K. and MAZUMDAR, B.K. Fuel 48 (1969) 277.

107. HAYATSU, R., WINANS, R.E., SCOTT, R.G. MOORE, L.P. and STUDIER, M.H. Fuel 57 (1978) 541.

108. WENDER, I., HEREDY, L.A., NEUWORTH, M.B. and DRYDEN, I.G.C. "Chemical Reactions and the Constitution of Coal" in "Chemistry of Coal Utilization, 2nd Supplementary Volume", Ed. H.H. Lowry Wiley, New York, 1981.

109. HOWARD, H.C. "Pyrolytic Reactions of Coal" in "Chemistry of Coal Utilization Supplementary Volume" Ed. H.H. Lowry Wiley 1963.

110. NEAVEL, R.C. "Coal Plasticity Mechanism" in Coal Science" "Volume 1". Eds. M.L. Gorbaty, J.W. Larsen & I. Wender. Academic Press 1982.

111. ORECHKIN, D.B. Chem.Abs. 50 (1956) 7425.

112. LOWRY, H.H. Soc.Chem.Ind. (1950) 619-25.

113. NADZIAKIEWICKS, J. Fuel Abstr. 22 (1957) 38.

114. RILEY, H.L.J.Inst. Fuel War Time Bull. (1945) 117.

115. HIRST, W. Proc.of Conference on Ultrafine Structure of Coals and Coke, pg. 35, B.C.U.R.A. London 1944.

116. LAHIRI, A. Fuel 30 (1951) 241.

117. BERKOWITZ, N. Fuel 28 (1949) 97.

118. BERKOWITZ, N. Fuel 29 (1950) 138.

119. OELE, A.P. Brennst. Chemie. 33 (1953) 231.

120. SOLOMON, P.R. and COLKET, M.B. Fuel 57 (1978) 749-755.

121. ANGELOVA, G. and LAZAROV, L. Brennst.Chem. 46 (1965) 204.

122. MRAZIKOVA, J., SINDLER, S., VEVERKA. L. and MACAK, J. Fuel 65 (1986) 342-345.

123. WENDLANDT, W.W. "Thermal Methods of Analysis" 2nd Ed.Wiley 1974.

124. DANIELS, T. "Thermal Analysis" Kogan Page 1973.

125. BLAZEK, A. "Thermal Analysis" Van Nostrand 1973.

126. KEATTCH, C.J. and DOLLIMORE, D. "An Introduction to Thermogravimetry" 2nd Ed. Heyden 1975.

127. LAIDLER, K.J. "Chemical Kinetics" Tara McGraw-Hill 1976.

128. ARRHENIUS, S. Z.Physik Chem. 4 (1889) 226.

129. SERAGELDIN, M.A. and PAN, W. 185th National A.C.S. Meeting, Seattle, W.A. 1983.

130. GOLDFARB, I.J., McCUCHAN, R. and MEEKS, A.C. Tech. Rep. AFML-TR-68-181 Part II, 1968.

131. SATTERFIELD, C.N. "Heterogeneous Catalysis in Practice" McGraw-Hill 1980.

132. TAYLOR, H.S. Adv. Catal. 1 (1948) 1.

133. HAYS, D., PATRICK, J.W. and WALKER, A. Fuel 55 (1976) 297-302.

134. WALKER, P.L. Phil.Trans. R.Soc.London A300 (1981) 65-81.

135. DAVIES, C., PORTER, A.I. and REES, G.J. Fuel 65 (1986) 753.

136. JAMES, M. "The BBC Micro An Expert Guide" Granada Publishing 1983.